LIQUID FUEL PRODUCTION FROM CATALYTIC PYROLYSIS OF MUNICIPAL PLASTIC WASTE USING SYNTHESIZED ZEOLITE FROM KAOLIN

By

Olusegun Ayodeji Olagunju

BEng, MEng (Chemical Engineering)

A thesis submitted in fulfilment of the academic requirements for the award of the degree of

DOCTOR OF ENGINEERING (DEng)

Department of Chemical Engineering,

Faculty of Engineering and the Built Environment,

Durban University of Technology, South Africa

Supervisor

Prof. Sammy Lewis Kiambi

November 2022

DECLARATION

I, Olusegun Ayodeji Olagunju, hereby declare that the content presented in this thesis entitled "***Liquid Fuel Production from Catalytic Pyrolysis of Municipal Plastic Waste using Synthesized Zeolite from Kaolin"*** is my scientific study. To the best extent possible, it doesn't contain any content that has been published or authored by someone else before or anything that has been used significantly to award a degree to someone else at DUT or another university. Furthermore, I affirm that no copyright has been violated in the content contained in this thesis because all cited sources have been listed at the end of the document, along with a complete list of in-text citations for each one.

Author: Olusegun Ayodeji Olagunju

Signature: Date: 29/11/2022

Supervisor: Prof Sammy Lewis Kiambi

Signature: Date: 29/11/2022

ACKNOWLEDGEMENT

I want to express my gratitude to the Almighty God for His mercy throughout my academic journey to this level and for enabling me to complete this Doctoral program successfully.

I would like to express my gratitude to my supervisor, Prof. Sammy Lewis Kiambi, for his unwavering support and inspiration and for directing this entire project. It is really appreciated that he made effort to provide the necessary tools and materials, sponsor the analysis, organize meetings and workshops to provide guidance, carefully examine the article, and make significant contributions.

Additionally, I would like to express my gratitude to Dr Farai Dziike for his encouragement and assistance, in addition to his detailed assessment of the manuscript and helpful suggestions at each level of this study's advancement.

Special thanks go out to the HOD and his secretary (Ms Khanyisile Ntuli) and the entire technical team, especially Jaf Bux, for his support during the design and development of the reactor utilized in this study, Vishnu, for his aid in processing requisitions and acquiring all the equipment and supplies used in this work, and all other individuals whose names are not stated.

The Durban University of Technology and the National Research Foundation (NRF) South Africa for their financial support during this research project.

I want to thank all of the postgraduate students in the chemical engineering department at DUT for their highly welcoming environment and the valuable conversations and social engagement that have helped me stay focused on my studies.

Finally, my humble gratitude goes to my family for their thoughtful support. Thank you to my beautiful wife (my Babie), Anu Christianah Olagunju, and my children, Daniella Oluwatomisin Olagunju and Diana Oluwafikayomi Olagunju, for their unwavering support and encouragement throughout my doctoral studies. I owe my success to my loving father, Mr Soladoye Samuel Olagunju, whose love and encouragement of my education have propelled me this far.

To my dear mother, Chief (Mrs.) Folusho Mary Olagunju, I would like to express my gratitude for her wonderful encouragement and support during my academic endeavours. Thank you to each and every one of my siblings for their encouragement and emotional support along this journey. I sincerely appreciate all of you.

DEDICATION

I dedicate this thesis to God the Father, Son, and the Holy Spirit. Also, to my wife and children.

PUBLICATIONS

The research outputs that emerged out of this thesis are as follows: They have been published or are undergoing review in ISI, Scopus, and DHET- accredited journals:

Olagunju, O.A. and Kiambi, S.L. 2022. Impact of life cycle assessment for municipal plastic waste treatment in South Africa. Biofuels, Bioproducts, and Biorefining – **under review**

Olagunju, O.A. and Kiambi, S.L. 2022. Catalytic Depolymerization of Municipal plastic wastes using commercial and synthesized ZSM-5. Sustainability, MDPI. - **under review**

Olagunju, O.A., Musonge, P., Kiambi, S.L., 2022. Production and Optimization of Biodiesel in a Membrane Reactor, Using a Solid Base Catalyst. *Membranes* 12, 674. https://doi.org/10.3390/membranes12070674

Accredited Conferences

Olagunju, O.A. and Kiambi, S.L. 2021. Catalytic Pyrolysis of Municipal Solid Waste: Effect of South African synthesized zeolite on Polyethylene plastic waste. Proceedings of the South African Chemical Engineering Congress 2021. South Africa, 20 – 22 September 2021. ISBN 978-1-991213-99-0. - **(Oral presentation)**

Olagunju, O.A. and Kiambi, S.L. 2021. Application of synthesized selected South African kaolin deposit on catalytic pyrolysis of municipal plastic waste. E-proceeding of the International Conference on Green Technologies for Sustainable Development, Dharmsinh Desai University Nadiad, Gujarat, India, 09 – 11 March 2021. ISBN: 978-93-5457-142-8. - **(Oral presentation)**

Olagunju, O.A. Musonge, P., and Kiambi, S.L. 2021. Influence of operating parameters on Biodiesel optimisation process using a heterogeneous catalyst in a membrane reactor. E-proceeding of the International Conference on Green Technologies for Sustainable Development, Dharmsinh Desai University Nadiad, Gujarat, India, 09 – 11 March 2021. ISBN: 978-93-5457-142-8. - **(Oral presentation)**

Olagunju, O.A., and Kiambi, S.L. 2021. Effect of synthesized zeolite from South African Kaolin on catalytic pyrolysis of Polystyrene plastics. Global Conference on Catalysis & Applied Chemical Engineering, Crowne Plaza Dubai - Deira, Dubai, UAE. - **(Oral presentation)**

Commercialization and Innovation engagement:

Olagunju, O.A., and Kiambi, S.L. 2021. Liquid fuel production from catalytic pyrolysis of municipal plastic waste using synthesized zeolite from kaolin. DUT Research, Innovation and Entrepreneurship Day, 28th April 2021. – **Prize winner**

Olagunju, O.A., and Kiambi, S.L. 2022. Recycling plastic wastes to Biofuels. Entrepreneurship Development in Higher Education (EDHE), Entrepreneurship Intervarsity 2022. – **Regional round finalist**

ABSTRACT

Municipal Plastic wastes are potential sources of alternative energy owing to their long-chain hydrocarbon with high heating values. Plastic waste (PW) is the major constituent of municipal solid waste (MSW) and it is becoming one of the largest MSWs in developing countries. The accumulation of plastic wastes over a length of time in conjunction with the improper and conventional waste management strategies has led to major health and environmental hazards such as greenhouse gas emissions, groundwater pollution, and several other human health and aquatic inhabitant problems. To address the environmental problem associated with municipal plastic waste, it is necessary to explore the catalytic pyrolysis recycling method of plastic waste which is a promising method of Municipal plastic waste management.

In this research four major used Municipal Plastic Wastes (MPW) namely Polystyrene (PS), Polypropylene (PP), Polyethylene (PE), and polyethylene terephthalate (PET) were investigated for the liquid-oil production individually and at mixed ratios.

Three different samples of kaolin (G1, G3, and G10) obtained from Grahamstown, South Africa were used as the raw materials in the synthesis of ZSM-5 zeolite used as the catalyst. In the preparation of the kaolin-based ZSM-5, the required amount of G&W metakaolin and sodium hydroxide were dissolved in deionized (DI) water, and tetrapropylammonium bromide (TPABr) were also mixed separately with the required amount of DI water. The solution of NaOH/Kaolin and sodium silicate solution were added simultaneously to the solution of the TPABr while stirring. Nitric acid was used to control the pH until the solution mixture is homogenous. The synthesized gel was transferred to stainless steel Teflon-lined autoclave cup and was hydrothermally treated at 180 ℃ for two days. The resulting product was washed with DI until the pH is less than 8. The sample was dried overnight at 80 ℃ and calcined for 5 hours at 550 ℃. The resulting synthesized zeolites (G1/ZSM-5, G3/ZSM-5, and G10/ZSM-5) were then characterized using Fourier transforms infrared (FT-IR), X-ray diffraction (XRD), and scanning electron microscopy (SEM). The catalysts produced were applied in the production of liquid fuel from Municipal waste plastics such as Polystyrene (PS), Polypropylene (PP), Polyethylene (PE), and polyethylene terephthalate (PET) under an optimized catalytic

pyrolysis reaction process. The operating parameters considered were catalyst loading, reaction time, and the temperature was investigated and optimized using response surface methodology (RSM) to obtain the best operating condition for the maximum yields. The optimized conditions established from the liquid fuels produced were used as a standard for the catalytic pyrolysis process condition for the single and mixed ratios.

The catalytic pyrolysis of mixed plastic wastes in different ratios was conducted with the synthesized G1/ZSM-5, G3/ZSM-5, and G10/ZSM-5 zeolite catalysts separately. All the mixtures of PP and PE produced higher liquid oil yields than the single PP or PE feedstock. Also, the highest liquid oil yield was obtained from PS/PE/PP sample with G10/ZSM-5 zeolite, and the lowest yield was from PP/PE sample with G1/ZSM-5 zeolite catalysts. The highest gases and char yields were from PP/PE and PS/PE with G1/ZSM-5 zeolite catalysts.

The quality, quantity, and chemical composition of the products were analyzed. The liquid oils, produced from the selected types of plastic wastes using synthesized and commercial catalysts, mainly consisted of aromatic hydrocarbons such as styrene, ethylbenzene, benzene, azulene, naphthalene, and toluene with a few aliphatic hydrocarbon compounds as confirmed by GC–MS and FT-IR analysis. The analysis showed that the liquid oils produced had high HHV (30.6–45 MJ/kg), similar to conventional diesel. The physicochemical properties of the oil produced were also compared with South African (SANS) and International standards (ASTM).

The synthesis of ZSM-5 zeolite was successfully carried out from locally sourced kaolin. The characterization results revealed that the patterns of G3/ZSM-5 and G10/ZSM-5 exhibit sharp reflections (2θ 7.8, 8.8, 23.1, 23.3, 23.7, and 24.3^{o}) with high intensity, which shows that the synthesized zeolite are solid crystals owing to their high Si/Al ratio. These catalysts were found to be effective and active in the oil conversion of both single and mixed feedstock ratios. The process of mixing the plastic wastes was found to be a very effective approach in the catalytic pyrolysis production process as it eliminates the need for sorting these wastes. Optimizing the process also helps in establishing operating parameters that produce optimum yield. The hydrocarbon properties obtained were within the international and South African standard specifications.

TABLE OF CONTENT

LIST OF FIGURES

LIST OF TABLES

LIST OF ABBREVIATIONS

PE - Polyethylene

PP - Polypropylene

PS - Polystyrene

PET - Polyethylene terephthalate

PVC - Polyvinyl chloride

ZSM-5 - Zeolite Socony Mobil–5

CO_2 - Carbon dioxide

NaOH - Sodium hydroxide

DUT - Durban University of Technology

OFAT - One factor at a time

RSM - Response Surface Methodology

CCD - Central Composite Design

DOE - Design of Experiment

ASTM - American Society for Testing Materials

SANS - The South African Bureau of Standards

TiO_2/Al_2O_3 - Titanium dioxide/Aluminium Oxide

ANOVA - Analysis of Variance

LOF - Lack of Fit

CHAPTER 1: INTRODUCTION

1.1 Background and research motivation

The rate of plastic waste production and consumption rate has increased in the last five decades due to the increase in human population, continuous urbanisation, rapid economic growth, and modern lifestyle (Miandad *et al*., 2016a). Furthermore, the daily generation of plastic garbage is accelerated by the short life span of plastic. Approximately 300 million tons of plastic are produced worldwide each year, and this number continues to increase (Ratnasari et al., 2017). Plastics are designed and produced from petrochemical hydrocarbons and contain chemicals like retardants, oxidants, and flame stabilizers, that prevent them from decomposing in natural environments (Ma et al., 2017).

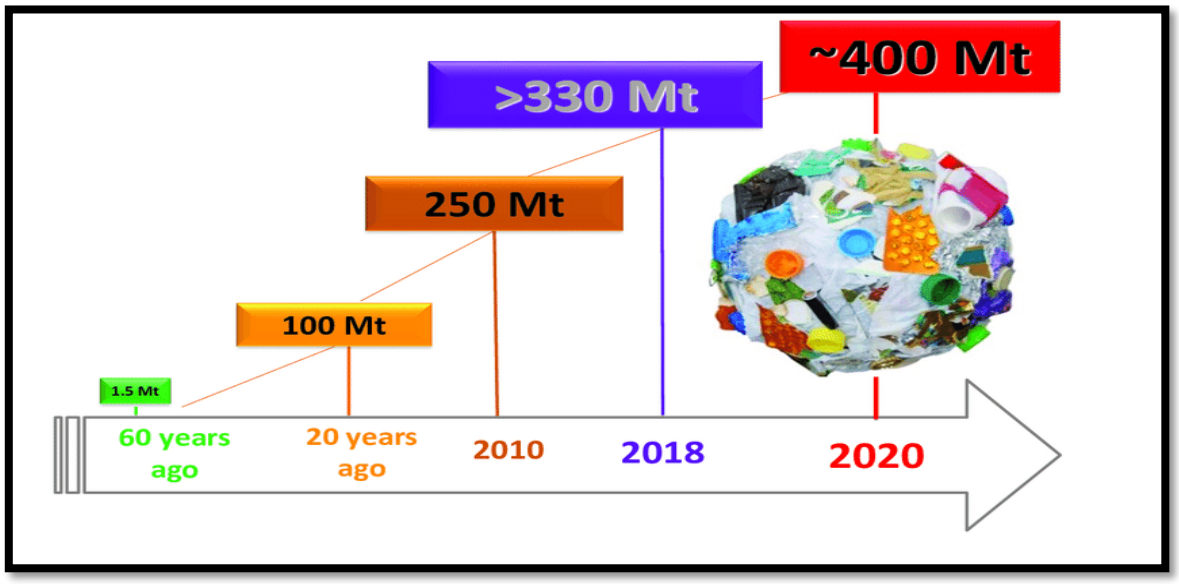

Figure 1.1: The increasing plastic generation worldwide (Koller and Raunegg, 2018)

Thermoplastics and thermosetting plastics are the two main categories of plastic waste. Thermoplastics, which may be reprocessed, are made of polyolefins such polyethylene terephthalate (PET), polyethylene terephthalate (LDPE), polypropylene (PP), polystyrene (PS), and polyvinyl chloride (PVC).

Polyurethanes and epoxy resins make up the majority of thermosetting plastics, which are not recyclable (Sarker et al., 2012).

Figure 1.2: Different types of plastics (Plastics For Change, 2021)

Over the past century, South Africa has become a significant plastics producer. In 1966, the government of South Africa provided financial assistance to stimulate development in the plastic manufacturing sector, to which Sasol contributed significantly. Polypropylene manufacturing in South Africa began in 1991 with an initial capacity of 120,000 metric tons per year. Ten years later, the plastic facility increased its annual production output to 220,000 tons (Babayemi et al., 2019).

Like many developing nations, plastic usage has increased in South Africa due to economic development and rapid urbanisation. Consequently, this significant consumption has led to disposal issues and impacted the environment negatively.

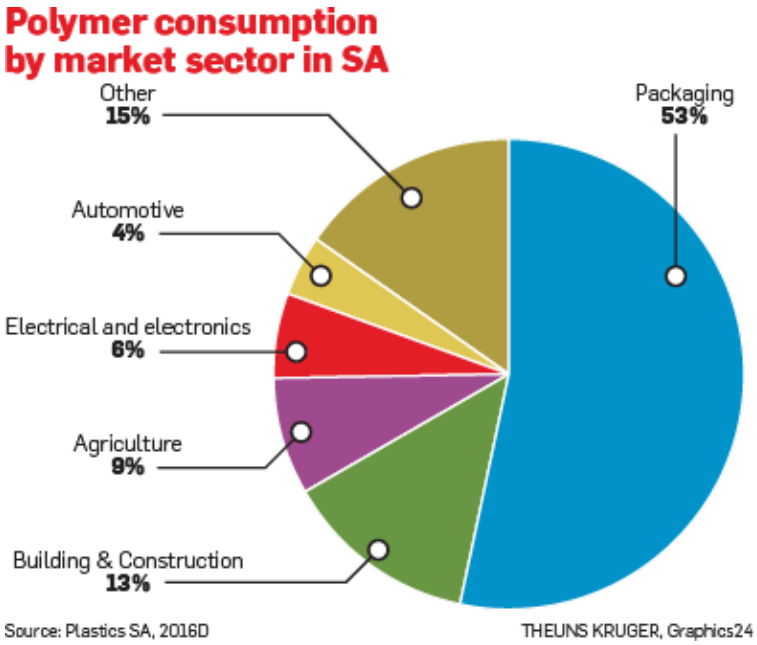

Figure 1.3: Plastic usage by different sectors of the economy in South Africa (Lange, 2019)

According to the survey, recycling rates in South Africa are comparable to those in Europe, with just approximately 30 per cent of plastic in the country being recyclable. For instance, the plastic emanating from electronic wastes are still present in landfill after the extraction of the metals. Also, plastics from automobile components are extremely challenging to recycle due to the complexity of different plastic-type formations. One of the most significant contributors to the problem is packaging, which accounts for 53 per cent of all plastics produced in South Africa (Lange, 2019).

1.2 Plastics waste Origin

Wastes originating from the use of plastics can be classified into two main groups, namely, municipal and industrial. A more significant portion of municipal solid waste is from plastics; faulty plastic products and by-products form majorities of plastic waste from industrial plastic waste.

1.3 Disposing of plastic wastes

Plastic wastes are categorised as solid waste. Therefore, the disposal method for these types of waste is already known, even though there are several ways of disposing of solid organic wastes. However, due to the non-degradable nature of plastic wastes, the most suitable method of managing them are; landfilling, incineration, and recycling.

1.3.1 Land Filling

Landfilling is the most conventional method used in managing plastic waste. However, it is not a suitable option for the disposal of these wastes because it provides a habitat for insects and rodents, which may cause different diseases (Alexandra, 2012), and landfill sites are exhausted. Furthermore, transportation, labour, and maintenance costs may increase the cost of recycling projects (Gandidi *et al*., 2018).

1.3.2 Incineration

This method is considered a Waste-to-Energy (WtE) technology for recovering energy from combustible resources, including plastics. However, using incinerators stimulates the growing emission of harmful greenhouse gases, such as; NOx, SOx, and Cox, into the air, which causes environmental pollution.

1.3.3 Chemical recycling

Chemical recycling converts polymer waste into monomers or other valuable products that can be used as a starting material for various secondary products. The recycling method can serve as an alternative solution to minimise environmental impact and convert these wastes into biodegradable fuels (solid, liquid, and gaseous fuels).

There are numerous recycling methods, including gasification, hydrolysis, and pyrolysis, and so on. Among them, pyrolysis stands out as the most promising method. (Ratnasari et al., 2017).

1.3.4 Pyrolysis

By definition, pyrolysis is the thermal degradation of plastic waste at temperatures ranging between 300 – 900 °C, in the absence of oxygen, to produce liquid fuel (Rehan et al., 2017). This process can be categorised into low, medium, and high-temperature regions, as shown in Figure 1.1.

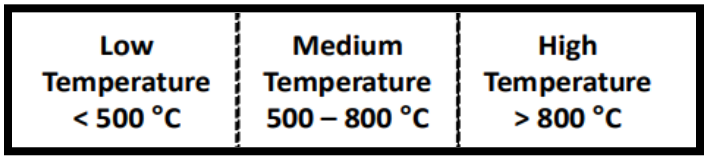

Figure 1.4: Classification of temperature ranges for pyrolysis (Suresh et al., 2021)

Using pyrolysis to manage waste has enormous potential and can add value to the economy with the revenue from the sales of products derived from the process.

1.4 Plastic degradation via Thermal method

The process of thermal degradation of plastic wastes involves two reaction steps, which occur simultaneously in the reaction medium. The first reaction involves a random scission of chemical bonds, causing a molecular weight reduction of the polymer compound. The second is a chain end scission of C-C bonds, producing volatile products. The composition and type of pyrolysis give helpful information about thermal degradation mechanisms (Murata, 2002). Thermal degradation of the polymers follows either chain end degradation (unzipping route) or random degradation route (Singh and Sharma 2008).

Chain end degradation or unzipping route

$M^*_n \rightarrow M^*_{n-1} + M$

$M^*_{n-1} \rightarrow M^*_{n-2} + M$

Random degradation route

$M^*_n \rightarrow M_x + M_y$

Chain-end degradation involves the continuous release of monomer units from the chain ends, known as a depolymerisation reaction. The reaction occurs through free radical mechanisms and is the opposite of the propagation step in addition to polymerisation. The molecular weights of the polymer decrease slowly and simultaneously, and many monomers are liberated. Thus, in general, chain end degradation occurs when the backbone bonds are weaker than the bonds of the side groups and only with polymer molecules carrying active chain ends with a free radical, cation, anion, and so on. (Murata, 2002).

Despite the potentiality of thermal pyrolysis to address the problem of plastic waste disposal, the process is temperature dependent, and the liquid fuel contains a lot of impurities and residues. Therefore, catalytic pyrolysis is more suitable for overcoming this challenge.

1.5 Catalysis

Catalysis is a general term used to describe a process in which a substance (i.e. catalyst) is used to promote a reaction in which the substance itself is not taking part in the reaction. The catalyst speeds up the reaction rate by order of magnitude and at a lower temperature and pressure (Singh and Sharma 2008). There are two types of catalysts, namely, homogenous and heterogeneous.

Homogenous catalysis means the reactants and the catalyst are in the same phase, while the reactants and the catalyst are in different phases in heterogeneous catalysis.

The use of catalysts in pyrolysis has numerous advantages, such as critically promoting process efficiency and reducing process temperature and time (Serrano et al., 2012; Ratnasari et al., 2017). Another added advantage is that in thermal pyrolysis, a wide variety of products are formed by breaking the polymeric chain. In contrast, the product distribution will be much narrower in catalytic degradation, with a peak at lighter hydrocarbons (Rehan et al., 2017). Due to these reasons, this method is adopted in the present work to synthesize liquid oil from plastic waste. Different types of catalysts have been used to improve the pyrolysis process of plastic waste, but the most extensively used catalysts are HZSM-5, zeolite, Y-zeolite, FCC, and MCM-41 (Ratnasari et al., 2017). The catalytic reaction during the pyrolysis of plastic waste on solid acid catalysts may include cracking, oligomerization, cyclization, aromatization, and isomerization reactions (Serrano et al., 2012).

Several studies have reported using microporous and mesoporous catalysts to convert plastic waste into liquid oil and char. Uemichi et al. (1998) carried out catalytic pyrolysis of polyethylene (PE) with HZSM-5 catalysts. The use of HZSM-5 increased liquid oil production with the composition of aromatics and isoalkanes compounds. Gaca et al. (2008) performed pyrolysis of plastic waste with modified MCM-41 and HZSM-5 and reported that using HZSM-5 produced lighter hydrocarbons (C_3–C_4) with maximum aromatic compounds. Lin et al. (2004) used different kinds of catalysts and reported that even mixing HZSM-5 with mesoporous SiO_2-Al_2O_3 or MCM-41 led to the maximum production of liquid oil with minimal gas production. Aguado et al. (1997) reported that the production of aromatics and aliphatic compounds from the catalytic pyrolysis of PE with HZSM-5 while using mesoporous MCM-41 decreased the aromatic compounds produced due to its low acid catalytic activity.

Using commercial synthetic catalysts enhanced the overall pyrolysis process and improved the quality of produced liquid oil. However, this type of catalyst is costly, and using it, increases the cost of the pyrolysis process.

1.6 Zeolites

Zeolites are classified as oxides having microporous crystalline aluminosilicates properties and exist in both natural and synthesized forms. This catalyst can be used to overcome the economic challenges of catalytic pyrolysis, which comes with the use of expensive catalysts. The application of zeolite can be in its natural or synthesized form. However, synthesized zeolites are majorly used in the petroleum and petrochemical industries. The utilization of clay as a source of silica and alumina for synthesizing zeolites offers numerous advantages such as cost-effectiveness, abundance of raw material, and the ability to produce high-quality zeolites with tailored properties. (Chandrasekhar and Pramada 1998; Liu et al. 2003). Durisol clay in South Africa was found to have a cost advantage of 25% over the commercial chemical in zeolite synthesis. This kaolin clay is abundant in many parts of South Africa, and previous work has shown that it is a rich alternative source for obtaining aluminosilicate (Martin 2010).

There have been several published articles on the catalytic degradation of PE plastics, particularly the LDPE. For example, Neves et al. (2007) undertook the catalytic pyrolysis of polyethylene using zeolite. Almeida and Marques (2015) also investigated the thermal and catalytic pyrolysis of PW and obtained products with a high added value, such as fuel oils and feedstock, for new products. Kunwar et al. (2016) investigated the catalytic and thermal depolymerization of low-value post-consumer high-density polyethylene plastic. Adeoye et al. (2016) synthesized zeolite Y from Arobieye clay in Nigeria and further tested its catalytic effect on cyclohexane. Most of these studies focused more on a single plastic waste type as feedstock than a mixture of different kinds of plastic waste.

This research seeks to investigate and evaluate the activity of zeolite synthesized from South African kaolin as the catalyst in the pyrolysis process of municipal plastic waste mixture of PET, PE, PP, and PS at a different ratio to liquid fuel. The success of this work will enhance the effectiveness of plastic waste processing to valuable products in South Africa and Africa in general in an economically affordable manner and hence reduce the environmental hazard posed by their indiscriminate dumping.

1.7 Aims and Objectives

This research seeks to demonstrate that an effective catalyst for thermochemical conversion of plastic waste can be obtained through transformation of the kaolin. Thus, the research study focused on addressing two aspects associated with the plastic waste pyrolysis process under the following aims.

- To investigate the synthesizing and characterization of zeolite from locally sourced kaolin. This is because the naturally occurring kaolin is abundantly available and is cost effective as a material resource for the synthesis of the zeolites of interest. The locally available kaolin will be valorised in this research as a material that may be commercially utilized as a mineral resource for industrial applications. The use of the material will have long term effect including job creation and rural industrial development in areas where it naturally occurs.
- To perform catalytic pyrolysis experiments of different plastic waste types and pyrolysis process modelling.

To achieve the aims mentioned above, the following specific objectives were set:

- To synthesize and characterize zeolite from locally selected kaolin.
- To investigate the effect of different catalysts on feedstock ratios and temperature on the maximum pyrolysis product yields and then characterize the product fuels.
- To simulate the Municipal plastic waste pyrolysis process with appropriate tools.

- To explore the interaction of parameters, via response surface methodology, during the catalytic pyrolysis process of mixed plastic waste.

- To model and optimize the catalytic pyrolysis process of different plastic waste.

1.8 Project scope

Catalytic pyrolysis of municipal plastic waste is a method of converting this waste into useful and valuable products. The scope of this study focused on a selected mixture of plastic scraps such as PET, PE, PP, and PS as these constitute the more significant part of municipal plastic wastes found in Durban, South Africa metropolis.

1.9 Thesis layout

The thesis is divided into seven chapters, chapters 1 to 3 are written in the traditional thesis format while chapters 4,5, and 6 are result sections, written in the format of journal publication manuscripts.

Chapter 1 - Introduction

This section introduces the research title, provides the background of the study, and highlights the study's problem statement, objectives, and scope.

Chapter 2 - Literature review

This section is a survey of existing studies and findings on this topic. It provides knowledge of the problem-solving strategies and shortcomings encountered by other researchers.

Chapter 3: Methodology

The methodology section details the means and approaches to achieve the research aim and objectives. The techniques and strategies used for the synthesis of the

catalyst. Also, this section outlined the method and procedure used in carrying out the catalytic pyrolysis of individual and mixed municipal plastic wastes, as well as data collection and analysis of results obtained. Experiments were carried out using the response surface methodology based on a central composite design.

Chapters 4 and 5: Results and discussion

This section details the experimental findings and the interpretation of the results. The results generated from the experiments were compared to the findings in the literature and were checked against the developed model for validation and reliability.

Chapter 6: Modelling and optimization studies

This section presented the modelling results, including model fitting and diagnosis, model analysis, model diagnostic plots, influence statistics, perturbation and interaction plots, response surface plots, and optimization—study results.

Chapter 7: Conclusions and recommendations

This section summarizes the research findings according to the objectives set and demonstrates whether the researcher has met the targets set at the commencement of the study. It also provides recommendations for further research in light of the result obtained and shortcomings encountered.

CHAPTER 2: LITERATURE REVIEW

2.1 Introduction

Plastics continue to provide countless advantages to society and have become an essential component of our everyday lives. The effects of plastics on the planet, society, and economy have been hotly debated in recent years. People's opinions about plastic materials were investigated in research carried out by the American Chemistry Council. One in three respondents to the study had unfavorable opinions about how plastics affect the environment, including how they pollute, contaminate water sources, are not compostable nor recyclable, and litter the environment (Orzolek, 2017). Plastics do, however, enhance human civilization in several ways. The current focus has been on the potential health and safety risks of particular plastic products. While the polymers are generally benign, many monomers and additives could raise safety concerns.

Plastics are criticized for contributing to litter because of their persistent nature in natural environments where they are disposed of. In recent years, the accumulation of plastic garbage and its pieces in the environment and marine water has come under closer investigation. Furthermore, plastic pollution of the air, water, and land is a critical issue that, if not addressed, might have detrimental effects on the environment and generations to come (Shrivastava, 2018).

The two main types of plastics available are thermoplastics and thermosetting plastics. Thermoplastic materials are those that, once moulded or created, can be softened by applying heat and may be moulded again until it loses their original features. Polypropylene (PP), polystyrene (PS), polyethylene (PE) and are just a few examples of these types of materials. Plastics classified as thermosetting are those that, once moulded or produced, cannot be modified by heat. It is a polymer consisting of a cross-linked structure or heavily branched molecules, and the material burns off with excessive heat.

Examples include thermosetting polyester, melamine formaldehyde, urea formaldehyde, and phenol-formaldehyde. The structures of both thermoplastic and thermosetting plastics are displayed in Figure 2.1.

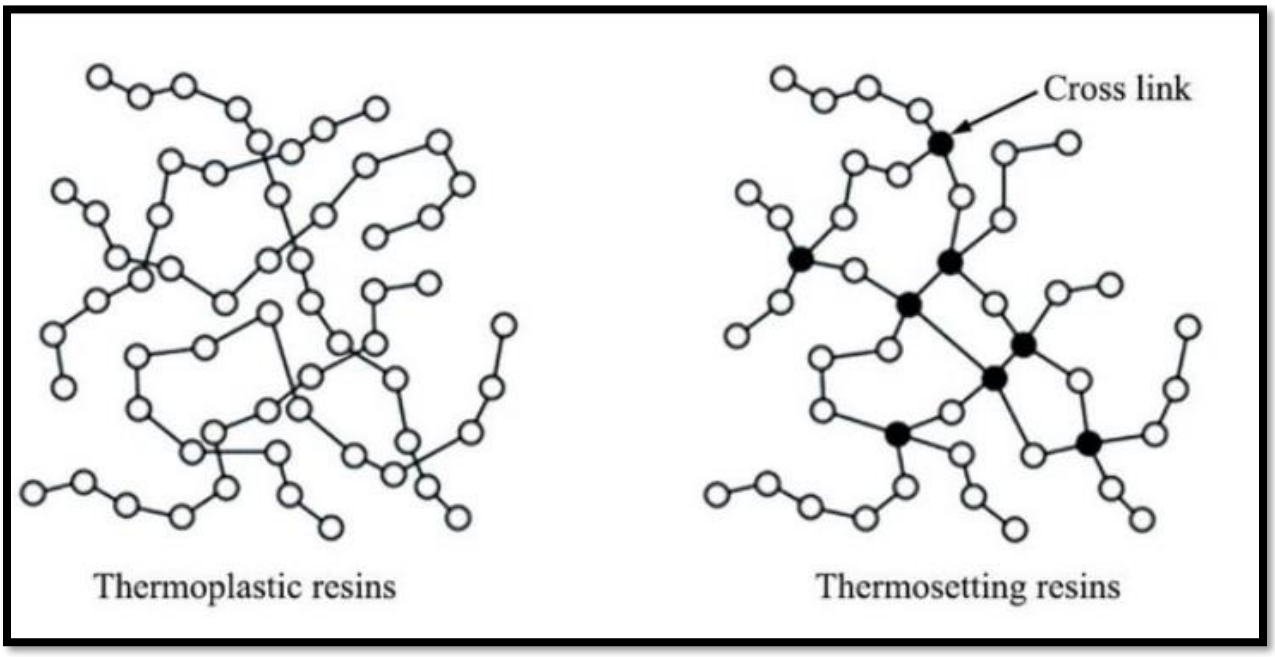

Figure 2.1: Structure of Thermoplastic and Thermosetting polymers

Thermoplastics generally provide high strength and flexibility and are resistant to shrinkage, depending on the type of resin (the polymer in melted liquid form). They are versatile materials that can be used for anything from plastic carrier bags to high-stress bearings and precision mechanical parts. In contrast, thermosets generally yield higher chemical and heat resistance and a more robust structure that does not deform easily. The most significant source for fuel production, whether in liquid or solid form, is thermoplastics made of carbon and hydrogen. PE, PP, and PS thermoplastics are preferred as feedstock in synthesising hydrocarbon fuels, as illustrated in Table 2.1. The pace and yield of liquid products are decreased when thermosetting polymers, wood, and paper are added to the feedstock because they cause the production of carbon-containing compounds.

Table 2.1: Suitable and non-suitable feedstock for liquid hydrocarbon synthesis

Type of plastics	As a feedstock of liquid fuel
Polyethylene (PE) Polypropylene (PP) Polystyrene (PS) Polymethyl metacrylate (PMMA)	Allowed. Allowed. Allowed. Allowed.
Acrylonitrile-Butadiene-Styrene copolymer (ABS)	Allowed. But not suitable. Nitrogen-containing fuel is obtained. Special attention required to cyanide in oil.
Polyvinyl alcohol (PVA) Polyoxymethylene (POM)	Not suitable. Formation of water and alcohol. Not suitable. Formation of formaldehyde.
Polyethylene terephthalate (PET)	Not suitable. Formation of terephthalic acid and benzoic acid.
Polyurethane (PUR) Phenol resin (PF)	Not suitable. Not suitable.
Polyvinyl chloride (PVC) Polyvinylidene chloride (PVDC)	Not allowed. Not allowed.

2.2 Statistics of plastics usage and plastics waste production

Global plastic waste was quantified and found to be 368 million metric tons in 2019, and a dramatic increase of 20% in the production of plastic waste was reported in the last five years (Soni et al., 2021). In another report by the World Economic Forum, the plastics industry will have a 20% share of global petroleum consumption with a 15% contribution to annual carbon emissions by 2050 (World Economic Forum, 2016). Presently, these wastes are causing issues for both the environment and people worldwide, but notably in the continent of Africa, where a substantial proportion of waste plastics are treated inappropriately, and there are no advanced and innovative recycling technologies in place (Jambeck et al., 2018).

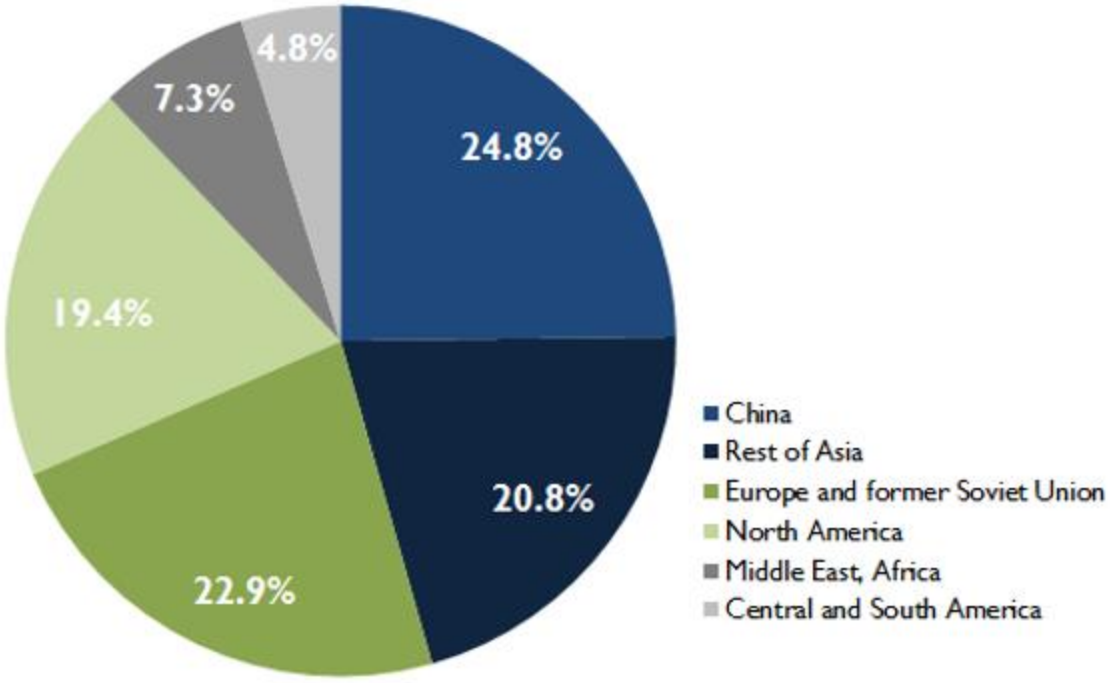

Figure 2.2: Production of polymetric materials by nations

The weight of the environmental implications carried by the communities from these plastic products increases as more and more diverse polymers with varying additives flow into society in terms of production and distribution of plastic waste generated as depicted in Figure 2.2; China leads the way with a 24.8 % share of global production volume. Europe follows it with 22.9 %. The rest of Asia is responsible for 19.4 %, and Middle East / Africa produces 7.3 %. Ecosystems, biodiversity, and human health are all impacted by the ever-increasing volume of plastic waste infiltrating the land, and ocean (Wright et al., 2013). As a result of their polymer accumulation structure (Chen et al., 2019), plastic wastes are notoriously difficult to break down, which increases the environmental impact of carelessly disposing of the materials (Shen et al., 2020).

In a research conducted by Jambeck et al. (2018), South Africa ranks 11th in the world for the amount of plastic waste generated each year. Over 630,000 tons are projected to be produced each year. This amount represents 2% of all plastic wastes improperly disposed of globally, and it is more than the contributions made by nations with higher populations, such as Brazil (1.5%) and the United States of America (USA) (0.9%).

Due to their inability to degrade, plastics have become a serious problem. As a result of indiscriminate dumping, other issues arise, such as drainage problems and animal health issues. Since no efficient end-of-life treatment of plastic waste is established in South Africa, their presence in the waste stream creates a severe concern. In the last five years, the massive littering of plastics on the landscape of South Africa has garnered much attention in the country. Plastic waste is causing environmental problems mostly because of the disposable lifestyle it promotes and the absence of an effective waste management infrastructure.

2.3 Plastic waste generation systems

Plastic wastes are generated from different applications, including industrial or municipal sources. These plastic wastes have distinct features and properties and are subject to various environmental management procedures (Faraca and Astrup 2019). Plastic wastes account for a sizeable portion of municipal trash; in addition, enormous quantities of plastic waste are produced in industry and agriculture as a by-product or as a result of defective products (Rajmohan et al., 2019; Tejaswini et al., 2022). More than 80 per cent of all plastic waste comprises thermoplastics, while the remaining 20 per cent is thermosets (Phanisankar et al., 2020). Thermoplastics are reusable and recyclable materials made of polyolefins such as polyethylene, polypropylene, polystyrene, and polyvinyl chloride, among others (Evode et al., 2021). On the other hand, thermosets are mainly composed of epoxy resins and polyurethanes and, therefore, cannot be recycled (Liu et al., 2021).

2.4 Municipal plastic waste (MPW)

Municipal plastic wastes (MPW) are often included in municipal solid wastes (MSW) since they are typically disposed of and collected as home refuse. Household items such as food tubs, plastic wraps, disposable utensils, and many more are among the numerous sources of MPW.

Consequently, the plastic waste produced from municipal solid waste is a mixture of polyethylene, polypropylene, polystyrene, and so on. The proportion of plastics in municipal solid waste has grown substantially (Lebreton and Andrady., 2019).

To recycle MPW, plastic materials must be separated from other types of home trash. Mechanical separation machinery for mixed polymers is accessible (Idumah and Nwuzor., 2019). Plastic mixtures may be divided into two categories using a wet separation technique: plastics having a density greater than water, including PS, PET, and plastics less dense than water, such as PE and PP. The second group is significantly larger than the first. Therefore, recycling municipal plastic wastes should involve plastic combinations of polyethylene, polypropylene, and polystyrene, provided the aforementioned separation techniques are followed. Despite substantial research into MSW separation methods, it is still not practicable to sort MSW mechanically and generate marketable fractions. Therefore, waste sorting at the home level is preferable, with wastes being segregated into three categories: combustible materials, incombustible, and plastics.

2.5 Industrial plastic waste (IPW)

Industrial plastic wastes are derived from large-scale plastics production, processing, and packaging industries. Industrial waste plastic consists primarily of plastics from the construction industries (PVC pipes and valves), electronic and electrical factories (electrical appliances, wiring sheaths, television sets), and automobiles (seat covers, battery containers, and front grills). The vast majority of industrial plastic waste has reasonably acceptable physical properties, i.e., it is adequately clean and contaminant-free and readily available in a substantial quantity. It has been subjected to high temperatures throughout the production process, which may have reduced its qualities, although it has not been deployed for commercial use.

While industrial plastic wastes are homogenous in nature, MPW are heterogeneous and complex. Repelletization and reshaping are quick and efficient methods of recycling homogenous plastic waste.

However, heterogeneous plastic wastes made up of many resins are not appropriate for recycling. In this situation, chemical recycling—also known as thermal cracking into hydrocarbons—might be an appropriate method of recycling (Dogu et al., 2021).

2.6 Municipal Plastic Waste

The demand for plastic materials has constantly grown in the past four decades due to the rising population. Plastic materials' life cycles stop at waste disposal sites since they cannot readily be recycled into the natural carbon state due to their non-biodegradability (Law and Narayan, 2022). Municipal and industrial plastic waste can be disposed of using various techniques, including landfilling, incineration, and chemical regeneration (Khan et al., 2022). One of the most critical issues in waste management is how to properly handle plastic waste, which is significant from an energy, environmental, economic, and political standpoint (Chen et al., 2021). Sanitary landfill (67–70%) and incineration (20–25%) have been the primary methods used to dispose of plastic waste in the last 20 years, and only 10% of waste gets recycled (d'Ambrières., 2019). Figure 2.3 depicts the various approaches explored for the handling of plastic waste.

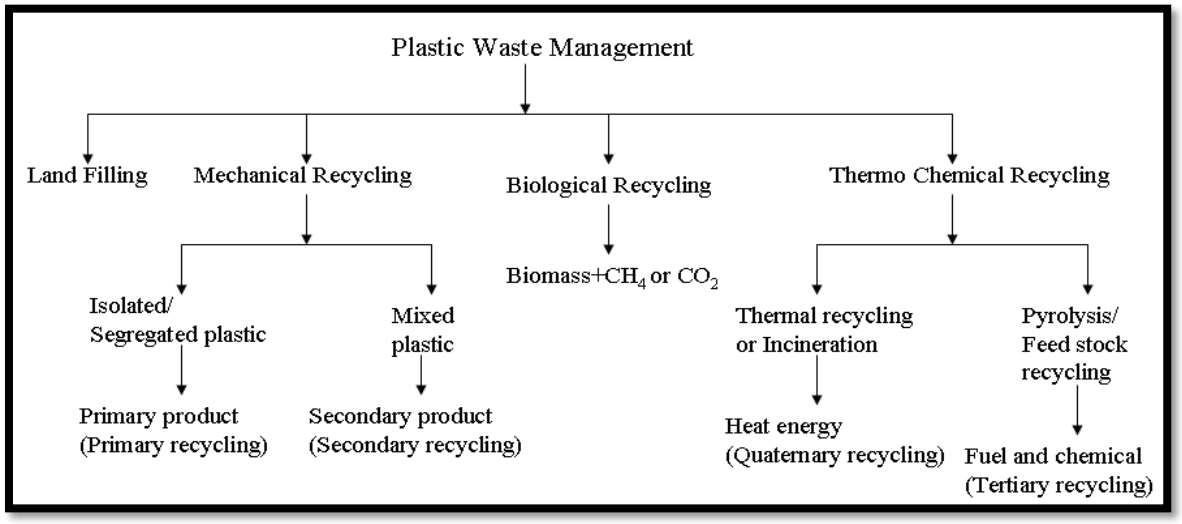

Figure 2.3: Diverse plastic waste management strategies

Most solid wastes, particularly plastics, have been disposed of in landfills. However, owing to governmental pressure, increased costs, harmful greenhouse gas emissions, and the non-biodegradability of frequently post-used plastics, discarding waste to landfills has become unappealing (Khan et al., 2022). The Environmental Protection Agency of SA has enhanced federal laws for landfill disposal in response to these risks by standardizing the use of lining in the dump site and conducting groundwater leakage detection tests. Nevertheless, because plastic wastes have a high volume-to-weight ratio, suitable landfills have become scarce and costly. Therefore, the other techniques described in Figure 2.3 should be considered as an alternative to landfilling for waste management.

Recycling by mechanical means involves refining discarded plastics to make new ones that are functionally equivalent to the originals. This is a sort of specific plastic regeneration in which homogenous waste polymers are processed into a product with virtually the same or lower quality than the previous product. Various technologies, such as X-ray luminescence, infrared electron microscopy, and electromagnetism, are being developed to enable the autonomous sorting of polymers. However, the economic sustainability and applicability of such a procedure in industrial settings are not feasible (Bai et al., 2020). There are environmental advantages to developing specialized machinery to transform mixed MPW into concrete alternatives for construction and building purposes. Significant academic attention has surrounded the use of hybrid composites to improve the working efficiency of mixed polymers poly blends; however, this is a costly and energy-intensive process that cannot be justified for household mixed MPWs (Bai et al., 2020; Alwai, 2021). In this way, it becomes clear that mechanical recycling, despite being commonly used, is not an appropriate technology when the reliability of the secondary product and environmental factors are considered. This has led to the investigation of other techniques, such as the biological recycling method (Ellis et al., 2021).

Plastic materials such as is-poly (isoprene) are used to create industrial goods (like tires), and both natural and synthetic isoprene become extremely resistant to bio-degradation, which is a direct result of the addition of highly potent antioxidants during their manufacturing (Andler-Osorio, 2020).

This has prompted considerable research in industry and academia to produce biodegradable polymers that meet user needs and can be recycled into the natural (biological) cycle after using them. This led to the creation of biodegradable plastics that can be converted back to organic matter in a reasonable amount of time (Luyt and Malik, 2019; Wojnowska-Baryła et al., 2020; Ali et al., 2022). In several nations, biodegradable polymers are currently utilized with great effectiveness. The food services business is where they are commonly used since they photodegrade within a couple of weeks. There is also the possibility of employing these polymers for non-packaging purposes, such as a computer or automobile parts. Nevertheless, there are several problems with the usage of biodegradable polymers. First, these plastics will only disintegrate under the proper disposal parameters. For instance, a photodegradable type of polymer that is placed in a dump site where there is no sunlight will not decompose. Furthermore, they may increase emissions of the greenhouse gas methane, as methane is emitted during anaerobic decomposition. Also, combining biodegradable and non - biodegradable polymers may confound screening methods for polymers. Last but not least, if individuals think that trashed plastic will just vanish, then their usage may result in more plastic pollution (Bai et al., 2020). Due to itemized issues, biodegradable polymers might not replace conventional polymers in all applications. Further investigation to find alternative means of resolving plastic management issues has led to critically examining the incineration technique.

In theory, reclaimed waste plastics may be used to generate energy by burning the waste since carbonaceous polymeric materials can substitute non-renewable resources (petroleum), thereby lessening carbon dioxide's environmental impact. According to Table 2.2, PE has a heating value that is comparable to fuel oil and produces heat energy at a rate equivalent to what is required for its production. Since money is being made from selling used plastics as fuel, incinerating waste is the municipal governments' favored energy conversion method (Li et al., 2021). Since polymers have a significant heating value and can increase MSW's heating rate and make incineration more effective whilst still recovering some of its energy, it is possible that co-incineration of waste plastic with other MSWs will become more common.

Nonetheless, the potential of waste-to-energy technology is still limited in many of these industrialized nations due to public mistrust of incineration, which emits greenhouse gases and certain extremely harmful pollutants, including polychlorinated dibenzo para dioxins (PCDD) and polychlorinated dibenzofurans (PCDF). It has been hypothesized that the chlorine concentration in PVC and other polymers is connected to the development of dioxins. Still, the possible connection between polymeric materials loaded into an incinerator and the release of dioxins into the atmosphere remains unknown (Bhat et al., 2022). For this reason, the plastic recycling method through chemical technique is worth considering.

Table 2.2: Comparing the heating value ratings of plastics to traditional fossil fuels (Bhat et al., 2022)

Fuel	Calorific value (MJ/kg)
Methane	53
Gasoline	46
Fuel oil	43
Coal	30
Polyethylene (PE)	43
Mixed plastics	30-40
Municipal solid waste	10

The goal of the most advanced feedstock recycling processes, often referred to as chemical recycling or tertiary recycling, is to transform waste polymers into their primary constituents or any other useful compounds. These compounds can be used as fuel for vehicles or raw materials for various industrial operations that occur further down the production chain. Cracking (which could be thermal or catalytic), depolymerization, and partial oxidation are the three primary methods that can be used.

2.7 Depolymerization

Reversible synthesized processes allow for the depolymerization of condensed plastics, encompassing substances like polyamides, polyesters, nylons, and polyethylene terephthalate, to their original diacids, diols, or diamines. Alcoholysis, glycolysis, and hydrolysis are standard depolymerization processes that convert these wastes into substantial amounts of their base constituents. Nevertheless, addition polymers, like polyolefins, which generally account for 60–70% of MPWs, cannot be readily depolymerized into the initial constituents through a reversed synthesized process.

2.8 Partial oxidation (Incomplete combustion)

The direct burning of plastic waste, which has a high heating value, may be bad for the environment since it produces dangerous compounds such as light hydrocarbons, nitrogen oxides, sulfur dioxide, and dioxins. In contrast, incomplete combustion (with oxygen or steam) might result in the production of synthesis gas (CO and H_2) and a mixture of hydrocarbons, the quality, and quantity of which would be significantly influenced by the kind of polymers used. A cutting-edge waste gasification and smelting system that employs metallic materials and steelworks technology to produce a dioxin-free, high-calorie purified gas has been shown by Oballim (2021). A two-stage pyrolysis and partial oxidation process are said to be capable of generating 60–70% hydrogen from polymer waste. It has also been shown that the co-gasification of biomass and polymer waste may increase the amount of hydrogen produced while lowering the CO content. By employing oxidation methods with nitrogen oxide or air, it is possible to create bulk chemicals from polyolefins, such as acetic acid.

2.9 Pyrolysis

Pyrolysis is the process of heating a material in the absence of air. The process of converting long-chain polymers into oligomers, and occasionally monomeric components, is known as plastic pyrolysis. These compounds ultimately decompose under the influence of several variables, including temperature, residence time, catalysts, and other process variables. A catalyst is not necessary for the pyrolysis process to take place.

Pyrolysis is a dependable and environmentally friendly method for achieving a twin goal of reducing waste plastic and augmenting rising energy needs from the petroleum sectors (Rajendran et al., 2020). Oil, gas, and solid residue are the main derivatives of the pyrolysis process. A variety of plastic feedstock may be processed using the adaptable method of pyrolysis, which can also be adjusted for high yields of certain products for desired uses. Thermal degradation of waste plastics yields liquid oil for furnaces, irrigation pumping machines, generators, boilers, and more without the need for extra processing (Miandad et al., 2019). Interestingly, the pyrolysis plant's energy needs may be met by the combustion of gaseous byproducts. Commercially, the pyrolysis process may be tuned to generate up to 85 wt% of liquid fuel or more at a temperature greater than 450 °C using excellent-grade plastic feedstock. MPWs may be pyrolyzed using three distinct processes: thermal pyrolysis, hydrocracking, and catalyzed pyrolysis.

2.9.1 Hydro-cracking

The hydro-cracking of the waste polymer generally comprises a reaction with hydrogen in the presence of a catalyst in a stirring batch autoclave at moderate temperatures and pressures (normally in the range of 150– 400 ^{o}C and 30–100 bars of hydrogen). The major goal of the study described is to create high-quality gasoline starting from a variety of feedstock. Polyethylene, polyethylene terephthalate, polystyrene, and polyvinyl chloride, from MSW and other sources, co-mixing of plastics with coal, co-mixing of plastics with various petrochemicals like vacuum gas–oil, and waste tires alone or co-processed with coal are typical the feedstock.

Solvents such as 1-methyl naphthalene, tetralin, and decalin have moderately effectively facilitated mixing and reaction. Numerous precursors (catalysts) have been employed in hydrocracking processes. These include transition metals (e.g., Pt, Ni, Mo, Fe) supported on acid solids (e.g., alumina, amorphous silica-alumina zeolites, and sulphated zirconia). Although streams of a variety of petroleum products have been produced, these precursors combine hydrogenation and cracking processes. However, very little information is available on the impact of metal and catalyst, porous structure, Silica-Alumina ratios, or susceptibility to degradation.

2.9.2 Thermal pyrolysis

Thermal pyrolysis, also known as thermal decomposition, is the process of breaking down polymers by the application of heat in the absence of oxygen. A carbonaceous residue (solid char) and highly combustible hydrocarbons are produced due to this process, typically carried out at a temperature range of 300 °C to 850 °C (Wu et al., 2022). The combustible fractions may then be divided into condensable liquid fuels made up of saturated hydrocarbons and non-condensable gas. The type of waste polymeric materials and the processing parameters used significantly impact the proportion of each component and its specific chemical characteristics (Al-Rumaihi et al., 2022). Due to the type and intensity of the process, which is largely influenced by temperature and residence time in the reaction chamber. High temperatures are necessary for the thermal breakdown of long-chain polymeric materials into short-chain compounds. This process has the significant drawback of yielding a very wide spectrum of products. The process of catalytic pyrolysis gives a solution to these issues.

2.9.3 Catalytic Pyrolysis

An appropriate catalyst is employed in this methodology to drive the cracking process. The influence of a precursor decreases the temperature and duration of a reaction process.

In addition, catalytic pyrolysis occurs at a lower temperature and culminates in a significantly narrowed distribution of the carbon chains in the final product, with a peak at lighter hydrocarbons. From an economic standpoint, additional cost reduction will make this procedure a more desirable alternative. This method can be enhanced by reusing catalysts and employing efficient catalysts in smaller amounts. This approach appears to have the best chance of being developed into a practical commercial polymer recycling process to address the urgent environmental issue of plastic waste disposal.

The use of a catalyst improves the quality of the liquid oil produced as well as the conversion. Catalytic conditions reduce degradation temperature and reaction time (Ong et al., 2019), which increases conversion rates for a wide variety of polymers (Fortman et al., 2018; Nemani et al., 2018). It also restricts and improves control over the distribution of hydrocarbon products in Low-density polyethylene (LDPE) (Lin et al., 2020; Zeng et al., 2022), High-density polyethylene (HDPE), polypropylene (Cheng et al., 2021), and polystyrene (Maafa, 2021) pyrolysis. While thermal pyrolysis produces a wide range of hydrocarbons from C_5 to C_{28} (Idumah, 2022), the existence of catalysts greatly improves the selection of hydrocarbons in the gasoline range (C_5–C_{12}) (Olivera et al., 2020; Nasution et al., 2022). Again, oils derived from catalytic pyrolysis include fewer olefins and a greater proportion of branched hydrocarbons and aromatic compounds (Liu et al., 2020; Wang et al., 2022). Furthermore, the presence of a catalyst increases a much greater gaseous product yield for polyethylene at comparable temperatures and reaction periods (Dai et al., 2022).

Catalyzed breakdown of polymers has profoundly impacted the field of catalysis and polymer degradation research. Thus, it is determined that the catalytic degradation of polymers has the best potential for commercialization (Hou et al., 2021). Table 2.3 compares the various characteristics of the fuel generated from plastics wastes to those of conventional gasoline. It is evident from the table that the oil generated by this technique is identical to conventional gasoline in all aspects and is believed to provide superior fuel economy than regular gasoline. In addition, production costs are believed to be quite low (Budsaereechai et al., 2019).

Table 2.3: Comparing gasoline with waste plastic fuel (Budsaereechai et al., 2019)

Properties	Regular gasoline	Plastic waste fuel
Colour, visual	Orange	Pale yellow
Specific gravity at 28 °C	0.7423	0.7254
Specific gravity at15 °C	0.7528	0.7365
Gross calorific value	11210	11262
Net calorific value	10460	10498
API gravity	56.46	60.65
Sulphur content(by mass)	0.1	<0.002
Flash point (Abel) °C	23	22
Pour point °C	<-20	<-20
Cloud point	<-20	<-20

2.10 Plastic Pyrolysis Feedstock

Plastic wastes are widely divided into post-consumer and post-industrial categories depending on the type of waste streams (Horodytska et al., 2019). Consumer plastic waste is unclean and polluted with other elements, such as biomass, organic waste, metals and. In contrast, post-industrial plastic waste is often clean, indicating constant standard and known content. Although synthetic plastics are seldom biodegradable in natural environments, some chemical reactions, such as thermal and photochemical degradation of polymer resins, partial hydrolysis of certain polymers, and aerobic oxidation, are largely determined by the composition of the material. Post-consumer waste must be thoroughly cleaned, separated, and sorted since it is unsuitable for mechanical recycling. Contrarily, pyrolysis of polymers enables the valorization of these waste materials into useful oligomers, monomeric units, and other compounds with a wider range of feedstock types (Al-Salem et al., 2017; Maisarah et al., 2018; Dwivedi et al., 2019). The pyrolysis method requires less presorting since it can tolerate much larger concentrations of impurities in the feedstock.

Figure 2.4 illustrates how the framework and functional groups of various resins determine their selectivity and distribution of products. During pyrolysis, high yields of pyrolytic oil are caused by the plastic waste's high volatile percentage and low amount of ash (Kalem, 2022). Functional groups encourage depolymerization to yield monomers, as in the examples of PET and PS, when they are present in polymeric chains (Chen et al., 2021). However, polymers like PP and PE produce oligomeric or high-molecular-weight compounds under normal pyrolysis processes (Patel et al., 2020).

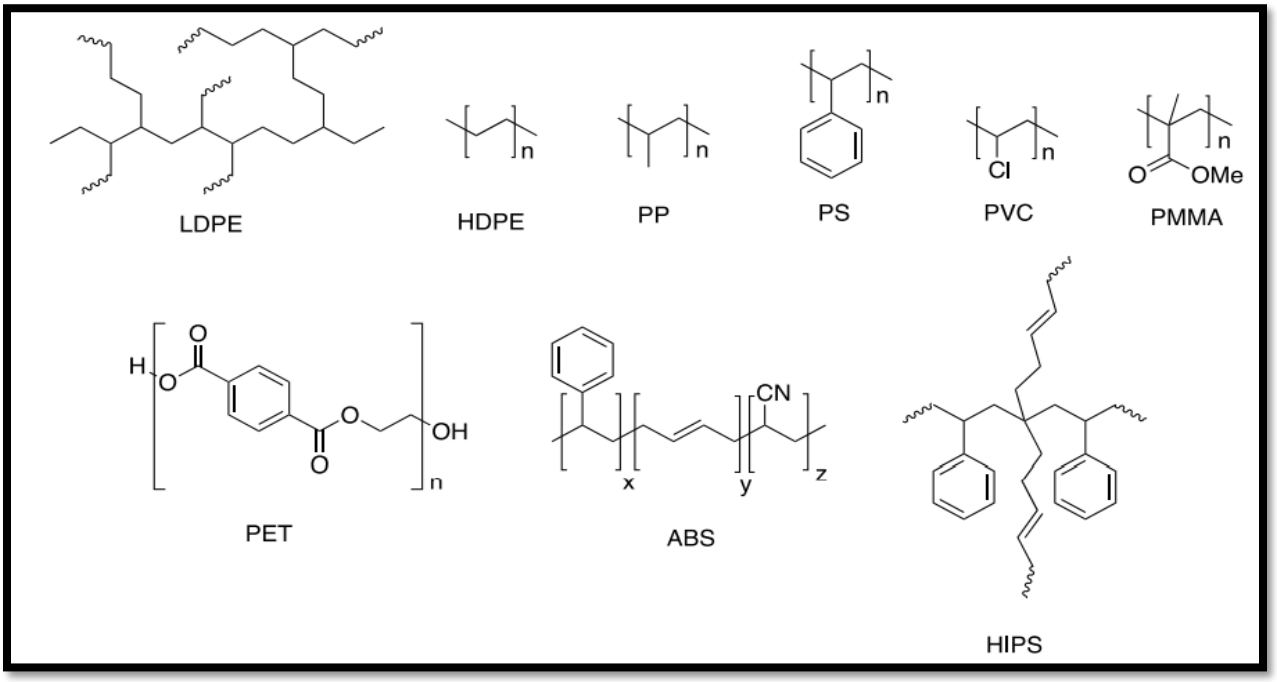

Figure 2.4: Chemical Structures of Synthetic Polymers

2.10.1 Polyethylene (PE)

Polyethylene has a strong crystalline structure due to the existence of long linear chains with little branching; as a result, it is frequently used in containers, toys, and reusable bottles and ranks third in the world among plastics made from waste. PE is suitable for high liquid productivity since it lacks aromatic compounds and other heteroatom substituents. Good crystalline structure, or strong intermolecular interactions and high-

molecular-weight linear formations, make high temperatures (over 500 °C) necessary for successful PE pyrolysis. High waxes are produced by thermal pyrolysis between 450 and 550 °C, whereas higher temperatures increase selectivity toward gaseous products. By causing the secondary breaking of PE waxes, an increase in residence time enhances the liquid fraction's quality. Additionally, even at relatively low temperatures, the existence of a catalyst allows for high conversion and simultaneous wax upcycling.

2.10.2 Polypropylene (PP)

The oppositely charged, partly polycrystalline polymeric category of plastics includes polypropylene, a valuable resource material. While Polypropylene and polyethylene (LDPE and HDPE) have many characteristics, Polypropylene is tougher and more heat resistant due to its higher melting temperature. The most extensively manufactured raw material plastic is polypropylene, trailed by polyethylene (LDPE and HDPE), both of which make up a significant portion of discarded plastics. Since there is a growing need for this plastic, its recycling has become a major problem. The difference in reactivity between Polypropylene and other Polyethylenes is caused by the presence of a tertiary carbon in its structure due to the methyl group present. Figure 2.5 illustrates the polyolefins' framework.

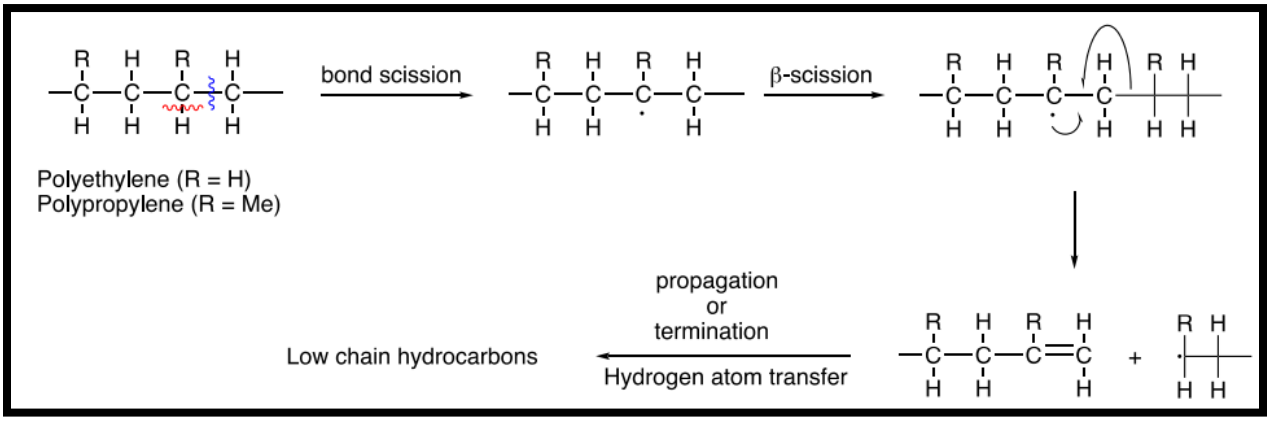

Figure 2.5: Polyolefins pyrolysis mechanism (Yan et al., 2015)

While the presence of a catalytic promotes C-H activation, thermal pyrolysis occurs via C-C bond homolysis and subsequent free-radical production. A catalyst's acidic/basic sites encourage the development of ionic intermediate species. Additionally, it is thought that degradation is mostly caused by flaws in polymer networks (Miskolczi., 2006). Inter/intramolecular hydrogen transfer and β-scission pathways are more prominently affected by reaction temperature than other routes because they have lower activation energies. At elevated temperatures, monomer yields rise because of the greater energy barrier for β-scission (Kumar et al., 2011).

2.10.3 Polystyrene (PS)

Phenyl groups are found in long hydrocarbon chains' substitute to carbons in the Polystrene, which is made of styrene monomers. Polystyrene is often translucent, rigid, and fragile. Polystrene may be used to create foams, which are light materials with density values of 11–32 kg/m^3, with transformation temperature exceeding 100 °C. Numerous construction components, such as concrete forms and panel systems, incorporate styrofoam as insulators. Polystrene resin has several uses in packaging material, boxes, caps, cartons, and so on since it is lightweight, strong, and affordable per unit of weight.

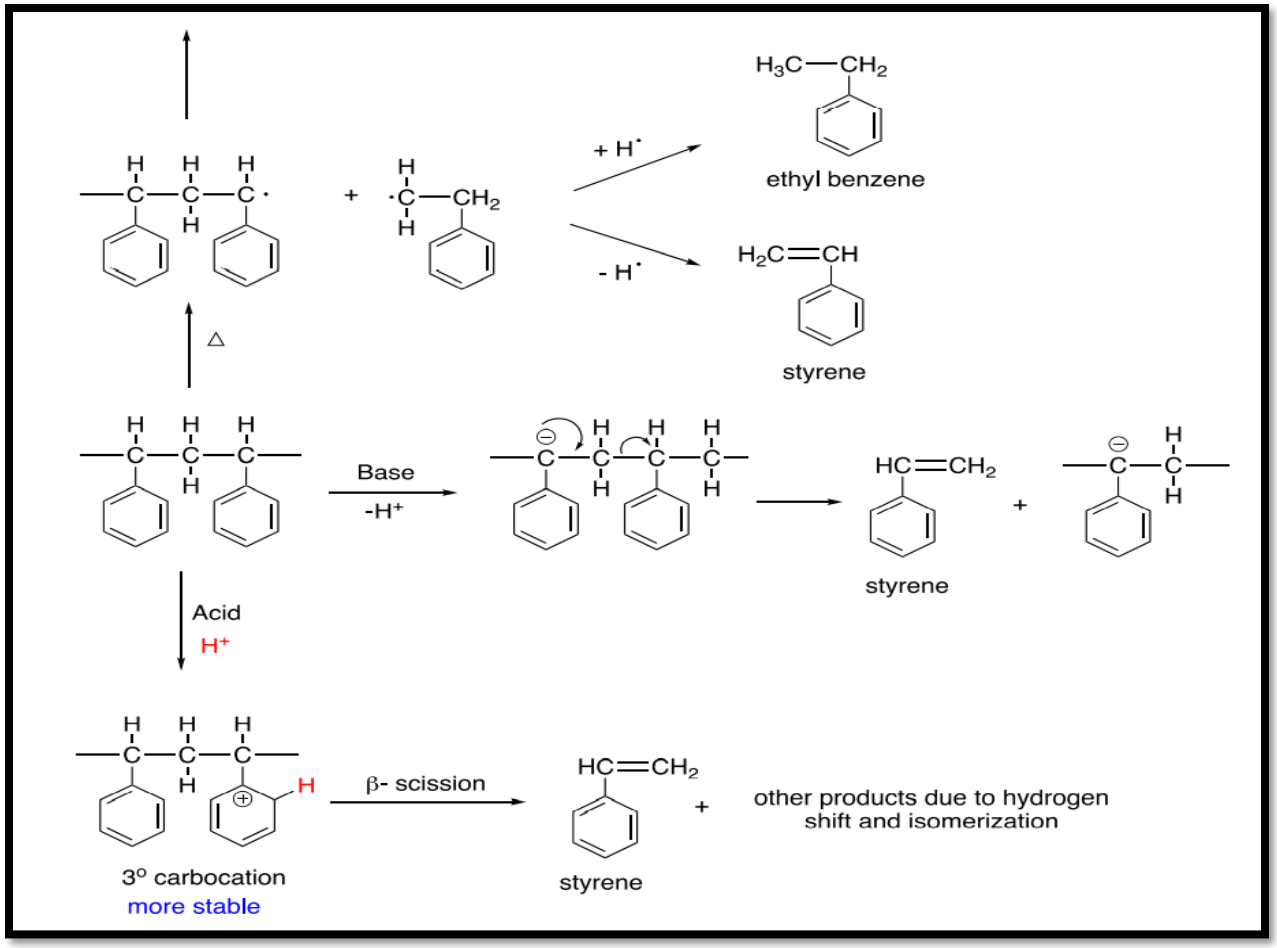

Figure 2.6: Polystyrene pyrolysis mechanism (Ke et al., 2005)

Figure 2.6 depicts the processes of PS pyrolysis (Park et al., 2003; Ke et al., 2005). Current findings revealed that base-catalyzed degradation is more selective for the synthesis of styrene. In contrast, acid catalysts are found to produce significantly greater quantities of benzene, toluene, xylene, and ethylbenzene (Ukei et al., 2000). Thermal homolysis of C-C bonds leads to the generation of polymeric radicals; thus, the bond energies of C-C and C-H bonds next to radical centers decrease by three times their actual bond energies, i.e. 346.9 and 406.8 kJ/mol, respectively. Styrene monomer is created by carefully unzipping polymeric chains, whereas benzene, toluene, and other alkylated aromatics are created via processes such as H abstraction, -decomposition, and radical radical couplings (Ke et al., 2005).

Styrene is produced naturally by the spontaneous migration of bonding electrons following the base-catalyzed removal of protons from polymeric chains.

In conclusion, PS pyrolysis has the potential to generate the largest liquid yields (up to 99 wt%) when carried out under ideal circumstances, i.e., temperatures lower than 500 °C (Chai et al., 2020). Styrene is produced as the main product under thermal or catalytic settings, followed by ethylbenzene, from the perspective of product distribution (Zhu et al., 2021)

2.10.4 Polyethylene Terephthalate (PET)

Polyethylene Terephthalate (PET) ranks fourth in terms of global polymer output, making up around 18% of all polymer production. PET plastic waste has accumulated as a result of its broad use in the electronics industry, including magnetic tapes, insulation, printing sheets, and printmaking, as well as synthetic fibres, food containers, and other packaging materials. Several studies explored the pyrolysis of PET, where the proportion of gaseous products generated was larger than the proportion of liquid fractions. The product analysis also showed that benzoic acid was formed as a significant liquid product. The corrosive nature of benzoic acid and its propensity to sublime, resulting in blocked heat exchangers and pipes, might harm the reactor. Because benzoic acid and its derivatives increase the fuel's total acid number (TAN), they are undesirable components. However, a catalyst can encourage decarboxylation, significantly decreasing the TAN number and raising monoaromatic yields.

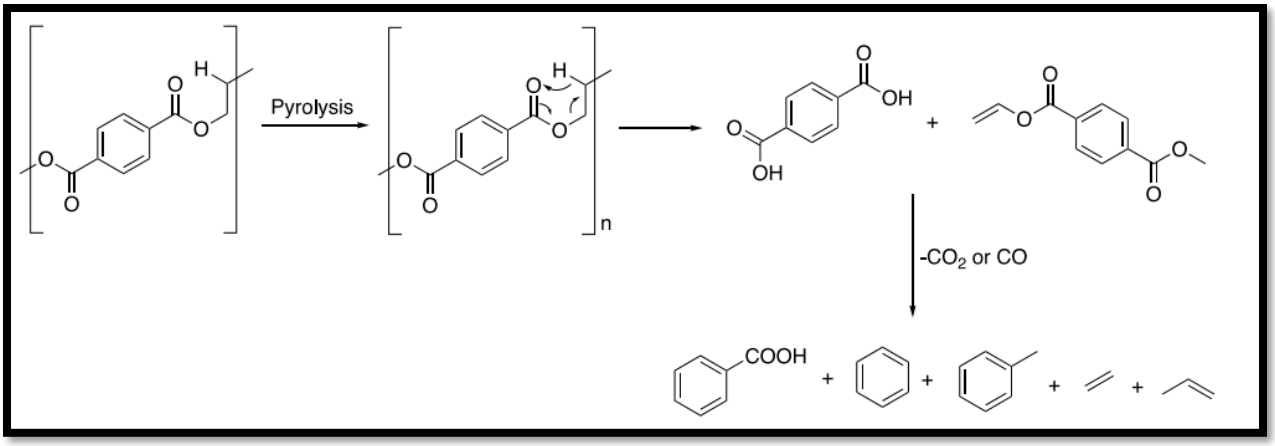

Figure 2.7: Polyethylene Terephthalate pyrolysis mechanism (Du et al., 2016)

Figure 2.7 depicts the PET heat breakdown pathway (Du et al., 2016; Kumagai et al., 2015). Phthalic acid and its vinyl ester derivatives are formed more easily because hydrogen is present at the carbon's α-position and the C-O bond has a lower bond dissociation energy. Benzoic acid, benzene, and toluene are three of the main liquid products produced by the decarboxylation and decarbonylation of carboxyl groups.

2.11 Organic and synthesized zeolites

Natural zeolites may be found in various geographical regions, including ash ponds, alkaline landscapes, and oceanic deposits at moderate temperatures. Synthesized zeolites are the result of chemical processes. They are made in a more consistent and precise condition than the natural zeolites concerning lattice topologies and porosity within their structures. Silica and alumina-rich compounds are the primary source constituents for synthesized zeolites (Jha and Singh, 2016). Compared to natural zeolites, synthesized zeolites have several benefits. These qualities include, but are not limited to, purity, uniform pore size distribution, and ion-exchange capabilities. (Von-kiti, 2012).

Scientific research in the fields of engineering and nanomaterial have recently made much progress with synthesizing and creating new zeolites from raw material such as kaolin.

The impressive results attained and the objectives met in these procedures are unquestionably correlated with advancements in another engineering (chemical) areas, like polymers and polymer-based materials. The expression $x_2/bO.yl_2O_3.aSiO_2.bH_2O_2.O$ is used to determine the identity of zeolites. In this expression, x is an interchangeable cation with valence y that belongs to either group I or group II ions,. At the same time, a and b indicate the stoichiometric coefficients of Alumina and Silica in the instance of the tetragonal structure (Von-kiti, 2012).

In addition to physical and chemical features, zeolites are distinguished by their adsorption and ion-exchange capabilities; their mineralogical and morphological characteristics; their thermal properties; their crystal structure; their acidic medium characteristics; and the surface properties of their crystals (Singh, 2016).

2.12 The categorization of zeolites

The chemical makeup of zeolites determines their classification. They can be classified as low, moderate, and high, with relative Si/Al ratios of 1.5–4, 4–20, 20–200, and infinite. The size of the particles, and chemical content, are one of the primary classification criteria for zeolite, as shown in Figure 2.8. In general, all zeolites with tiny pore sizes are composed of an eight-membered ring with a nominal width of approximately 0.30 to 0.45 nm. Zeolite comes in three different pore sizes: intermediate pore size has 10 membered bands with a free width that ranges from 0.45 to 0.60 nm; wide pore size has 12 membered bands with a free diameter that ranges from 060 to 0.80 nm; and extended porosity has 14 membered bands (Flanigen, Broach and Wilson, 2010).

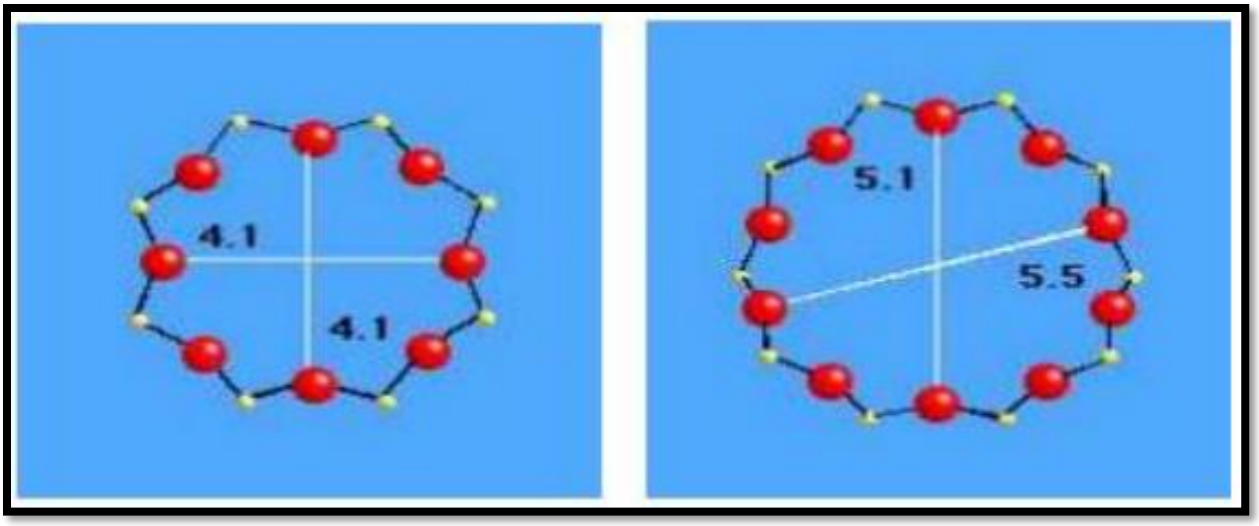

Figure 2.8: The 8 and 12-band pore framework segments of zeolite A and ZSM-5 zeolite

2.13 Zeolite structure

Zeolites are known as molecular sieves owing to the consistent size of their holes. Zeolites' pore diameter is comparable to the sizes at which bigger molecules cannot pass and are adsorbed, while smaller molecules may pass or are completely adsorbed. Molecular sieve in zeolites refers to zeolites having a porosity between 0.3 nm and 2 nm that can be used to screen molecules (Sánchez and Garca-Martnez, 2011). Porous materials such as activated carbon and inorganic gel are categorized as disordered sieve structures, whereas zeolites and zeotypes are categorized as ordered sieve structure materials (Sánchez and Garca-Martnez, 2011).

Zeolites are molecular sieves because particles with a kinetic diameter larger than the zeolite pores cannot enter the canal system, but smaller particles may. Dehydration and heat may impact the quality of molecular sieves because heating can alter the lattice and increase the void volume of the channels, whilst dehydration induces cation exchange and charge diffusion in the structure. The spatial arrangement of the tetrahedral structure caused by the continual vibration of the molecule controls the pore diameter in a zeolite framework at ambient temperature. If the molecular vibration temperature increases, the form and size of the framework's porosity are flexible.

Due to their different architectures, zeolites are vital to chemical industries. Due to their distinct framework and pore topologies, zeolites can be utilized in catalysis, adsorption, and ion exchange. Therefore, understanding the structural framework properties of zeolites is essential for research concerning their use (Fig. 2.9). Zeolites consist of tetrahedral AlO_4 and SiO_4 particles held together by an oxygen atom and a porous cation structure (Shabani, 2016).

Typically, the structure of zeolites is described by their geometry, pore size, or pore space connectivity, which is translated as their framework. The pore size that restricts molecule entry into the pore space is determined based on the size of the limiting ring (Lijalem, 2016). Consistently, zeolites are separated into substances with small, medium, large, and moderately large pores. Zeolites with small pores, such as zeolite A, have a pore space aperture surrounded by eight 4.2-diameter TO_4 tetrahedra. MFI is a moderately porous zeolite with 10 ring-shaped pore apertures and a 5.5 diameter. Faujasite and Mordenite have a pore aperture of 12 and a diameter of around 7.5. Any zeolite with an aperture larger than 12 T atoms is categorized as having big pores. The most common zeolites have eight or ten rings. Figures 2.9 and 2.10 depict the first two classes' most common zeolite pore structures.

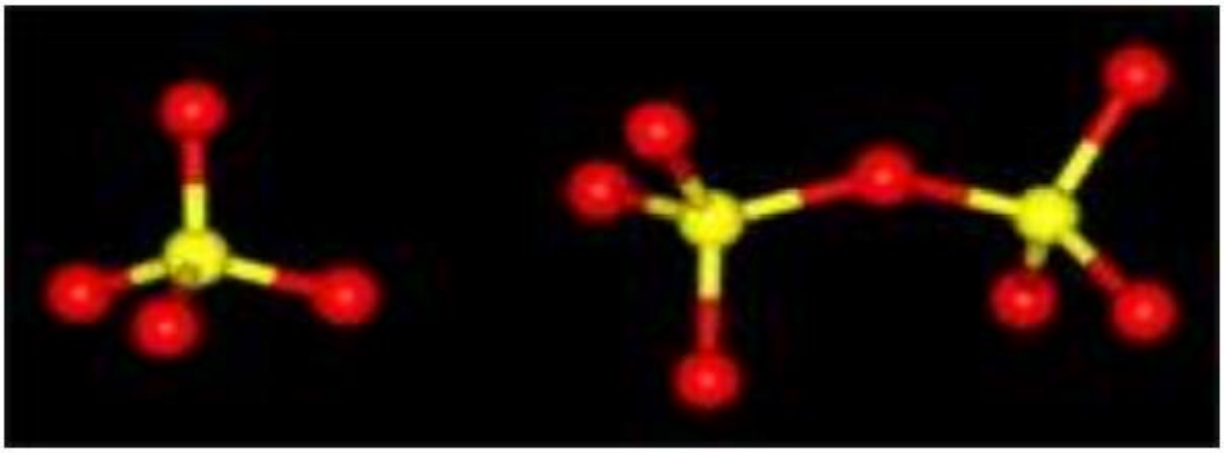

Figure 2.9: Main building component unit and the two connected to demonstrate how they worked together to make a bigger configuration (Ayele et al., 2016)

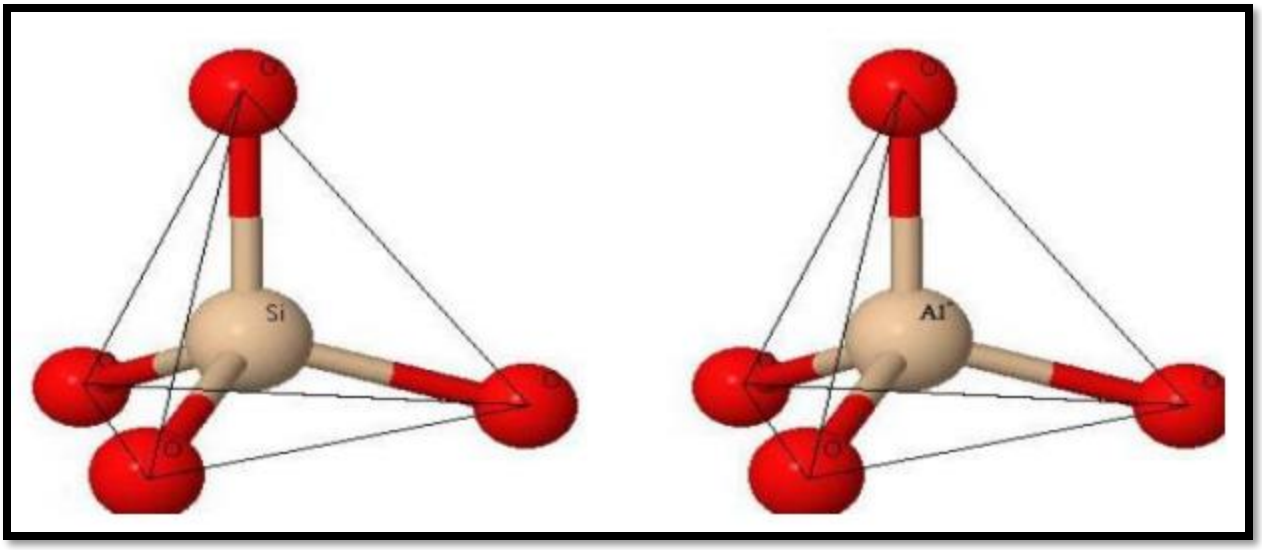

Figure 2.10: A schematic illustration of the framework of zeolite, showing the tetragonal configuration of either SiO_4-4 or AlO_4-5 (Ayele et al., 2016)

Aluminosilicate minerals, such as zeolites, are divided into more than 50 different subgroups. ZSM-5 was examined in this study. The fundamental zeolite unit is a [TO_4] tetrahedral composed of major and minor units. The main building unit (MBU) creates an infinite lattice of identical building pieces known as supplementary building units (SBU). The supplementary building unit establishes the structure of the zeolite but eliminates the moisture and cation inside the framework. Figure 2.11 depicts the structure of every identified zeolite. Zeolites are made from the aforementioned SBUs and frequently from combinations of SBUs.

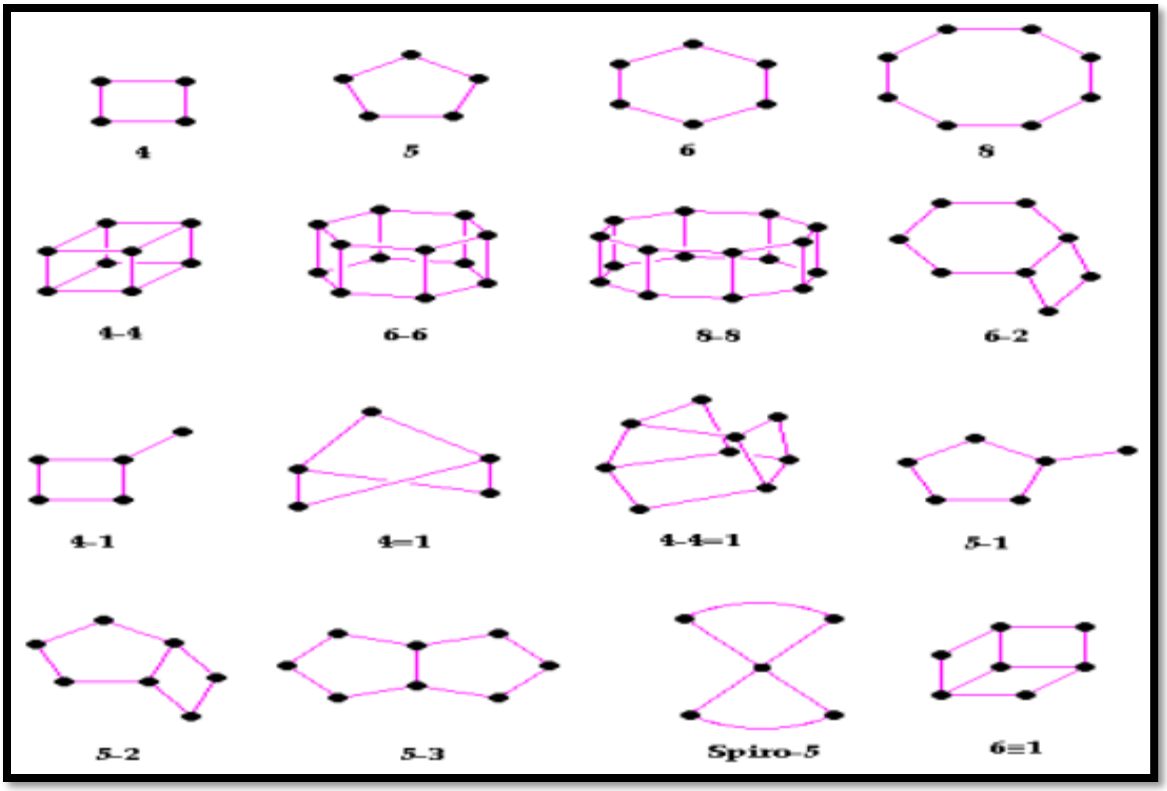

Figure 2.11: Zeolite configuration additional structural components (Lijalem, 2016)

2.13.1 ZSM-5 Zeolite

Aluminosilicate crystals ZSM-5 have a pore shape that can adsorb particles as large as cyclohexane (fig 2.12). ZSM-5 is composed of the interconnectivity of tetragonal SiO_4 and AlO_4, which produce pores, and cages with non-identical geometries. This structure allows certain compounds to permeate across the pores (Gre et al., 2010).

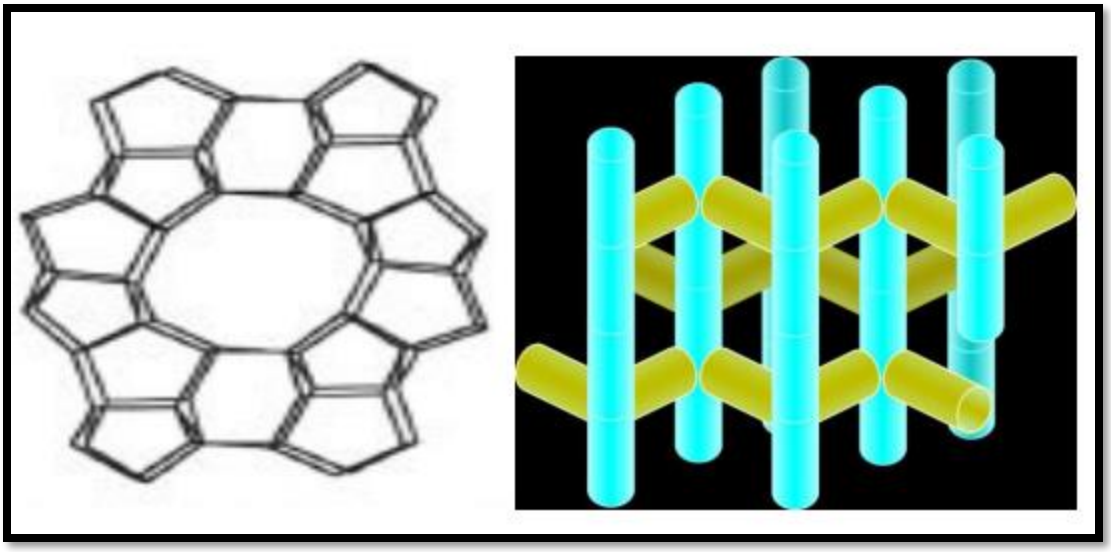

Figure 2.12: ZSM-5 Structure

2.13.2 Synthesis of Zeolite

Zeolite can be produced synthetically or naturally. Natural zeolite is generated by volcanic eruption ashes, while laboratory-created synthetic zeolite is developed in the laboratory (Aliyu, 2021).

Typically, the hydrothermal technique is utilized for zeolite synthesis. Salvo-thermal, iono-thermal, and hydrothermal processes are being used to separate the synthesis process. Ionic liquids are used as the solvent and template (the agent that directs the structure) in the ionothermal method, which has been used to create zeolites and organic-inorganic hybrids such as organic-metal structures (Parnham and Morris, 2007). The salvo-the synthesis approach applies to organic solvents and amines with diverse structural and chemical features. Mild hydrothermal synthesis reactions have a reaction temperature between 100°C and 240°C, whereas high hydrothermal synthesis reactions have a reaction temperature of up to 1000°C and autogenous pressure. Most zeolite synthesis occurs at lower temperatures and fixed pressure (Bedard, 2010; Von-kiti, 2016).

Zeolite is produced hydrothermally by the direct or metakaolinized synthesis of kaolin. There are three steps in the hydrothermal process of zeolite.

a. The conversion of kaolinite to metakaolinite.

b. Hydrothermal reactions between different alkali media and metakaolinite.

c. Zeolite activation after washing, purification, and cleaning.

Several studies have been conducted on the production of zeolites, and the ideal molar composition for each has been proposed. Some synthetic kaolin/clay-based zeolites are included in table 2:4.

Table 2.4: lists a few developed kaolin- and clay-based zeolites.

Zeolite	Kaolin Deposit location	Synthesis technique	Synthesis parameter	Comments	Reference
A	Bombowha Ethiopia	Conventional hydrothermal and alkali fusion followed by hydrothermal synthesis	Ageing and temperature	Zeolite A was produced from low-grade Bombowha clay using a traditional hydrothermal followed by an alkali fusion technique. Traditional hydrothermal synthesis produced cubic crystal zeolite A with a rounded edge and 75% crystallinity, while alkali fusion produced cubic crystal zeolite A with an 84 percent crystallinity. This show that alkali fusion followed by hydrothermal crystallization is more effective compared to conventional hydrothermal crystallization.	(Ayele *et al.*, 2016)
A	Jordan	Hydrothermal synthesis	Metakaolinization and NaOH concentration	The synthesis revealed zeolite A as the major phase with hydroxyl sodalite (HS) and quartz as minor impurities from the kaolin. XRD pattern presented an excellent relative crystallinity and SEM showing cubic images, which confirmed the morphology of zeolite A. Both XRD and SEM suggested that Jordanian kaolin can be used to synthesize zeolite A.	(Gougazeh and Buhl, 2014)
ZSM-5	G&W mineral resources South Africa	Hydrothermal synthesis	Temperature and time	The technique involved beneficiation using sieving and filtration to upgrade the kaolin. Temperature and time of crystallization varied. The optimization confirmed that both XRD and SEM show excellent SEM images and crystallinity. Finally, established that temperature and time of crystallization are critical in converting kaolin to ZSM-5 zeolite.	(Mohiuddin *et al.*, 2016)

2.13.3 Production of zeolites out of Kaolin

There are several variable factors involved in the production of zeolite from kaolin. The primary stage material composition, such as the quantity of water, crystallization temperature, crystallized duration, and ageing period, are the most important constraints for creating zeolite. Kaolin must be refined to eliminate contaminants like iron, calcium, magnesium, and other substances before zeolite can be made from it. Natural kaolin used in producing zeolite contains some of the contaminants that are also found in kaolin. According to Petrov and Michalev (2012), the presence of these impurities can confer several benefits on zeolite, particularly concerning its catalytic performance, toughness, luminance, and electrical characteristics.

2.13.4 Composition of chemicals and batch reactions for the synthesis of ZSM-5 zeolite.

ZSM-5 zeolite has been created using various techniques using materials mostly composed of silica and alumina, such as kaolin, bentonite, and so on. The primary chemical sources of aluminium are sodium aluminate ($NaAlO_2$), aluminium hydroxide ($Al(OH)_3$), and aluminium nitrate ($Al(NO_3)_3.9H_2O$). In contrast, the primary chemical sources of silica are sodium silicate ($Na_2SiO_3.9H_2O$) and nanoparticles soil (SiO_2 40% by weight). (Zhu et al., 2013; Tang et al., 2016). The rate of zeolite crystallization, product type, shape, and particle volume fraction rely on crystallization (temperature, reaction duration, and ageing period). In general, the elements that influence ZSM-5 formation include the reaction constituent, the type of the starting materials, the crystallization temperature process, crystallization time, and the pH of the mixtures, among many others (Lijalem, 2016).

2.13.5 Different states of catalytic activity

The solid catalysts may either be immediately added to the feedstock in the reactor (known as "in-situ" mixing), or they may be in another reactor down the reaction through which only degradation vapour may flow (ex-situ).

Regarding energy efficiency, the in-situ approach has received widespread adoption. Since the fused polymers and catalysts come into direct contact, the influence of the porous structure is particularly noticeable in this mode (Peng et al., 2022): the potential mass transfer restriction inside the reaction system may delay the evaporation of the polymers degradation products, promoting the reforming processes inside the pores of catalysts. At the same time, the ex-situ method is favored for cracking into olefins (Li et al., 2020). But with fixed-bed reactors, it is considerably more challenging to recycle used catalysts (Kremer et al., 2022).

2.13.6 Recovery of catalytic substances (ZSM-5 Zeolite)

When comparing the economics of catalytic pyrolysis with thermal pyrolysis methods, the cost of the catalyst (both its kind and its amount) becomes an essential element. As a result, research on the deactivation, regeneration, and reuse of catalysts is of the highest importance from the standpoint of industrial amplification (Peng et al., 2022). The majority of the time, catalyst deactivation is reversible, and the accumulated coke may be burned off to eliminate it (Heracleous et al., 2019). The removal of coke from the external surface of the catalyst is simple in this process. Still, the oxidation of the coke within the catalyst depends on the oxygen's capacity to permeate into the catalyst pores (Zhou et al., 2020). The interaction between oxygen and the deactivated catalyst during regeneration may change depending on the catalyst chemistry. There are four key variables that may be easily changed while industrial-scale catalyst regeneration is taking place: temperature, time on stream (TOS), oxygen content, and flow rate. Carbon deposit oxidation is typically conducted at temperatures between 400 and 600 °C and oxygen concentrations between 0.05 and 10 vol %, with TOS variable according to the desired degree of carbon deposit removal.

2.14 Factors affecting optimization in plastic pyrolysis

Within the field of chemical engineering, process optimization is an essential area that aims to maximize the performance of the process while simultaneously reducing the costs associated with carrying out that process. The essential process variables that affect the catalytic pyrolysis process yield are temperature, pressure, catalyst concentration, and reaction time among others. The aforementioned factors can be controlled and adjusted at various settings to produce the desired result. Below are detailed explanations of various process optimization variables.

2.14.1 Temperature

Temperature is one of the most important factors in the decomposition of plastic waste and is crucial for the regulated cracking of polymer molecules. The three primary stages of plastics decomposition are initiation, propagation, and termination (Ali et al., 2021). Once the energy input exceeds the binding enthalpies of C-C, C-H, or C-X bonds, thermal cracking of polymers often occurs (Mhaske et al., 2022). A higher temperature encourages more cracking, which produces lighter monomers and aromatic compounds (Peng et al., 2022). In the case of polyolefins, an increase in contact time causes the development of coke and volatiles like greenhouse gases.

The thermal degrading behaviour of plastic feed is measured using a thermogravimetry analyzer, which generates TG and DTG curves. The chemical makeup and reactivity of the plastic feed have a significant impact on the operating temperature. Similar to this, pyrolysis at lower temperatures (350–500 °C) produces liquid products, but at higher temperatures (>500 °C), the yields of gases and/or solid residue rise.

2.14.2 Reactor Type

The kind of reactor greatly impacts how effectively catalysts and polymers combine, how long they remain inside the reactor for maximal heat transfer, and how quickly they react to create the desired end product.

Plastic pyrolysis is often performed in fluidized beds, fixed-bed reactors, or conical spouted beds, all of which are batch, semi-batch, or continuous-flow reactors found in laboratories (Gebre et al., 2021).

2.14.3 Pressure

High pressure can be used for pyrolysis in a closed reactor, which can substantially influence product dispersion, especially at lower temperatures (Papari et al., 2021). As a result, under high pressure, a lot of gaseous products and lighter hydrocarbons were clearly formed (Shen et al., 2019). However, the influence was less noticeable at higher temperatures (over 450 °C). Contrarily, the reaction in a continuous batch reactor under vacuum and sub-atmospheric pressure efficiently removed product vapours (Dabros et al., 2018). Vacuum pyrolysis, which occurs at high temperatures for a brief period of time, increases the yields of liquid products while reducing the production of gases and char (Al-Rumaihi et al., 2022). Notably, the production of lower molecular weight hydrocarbons was accelerated by a high reaction pressure, whereas the synthesis of double bonds was significantly reduced (Goh et al., 2022).

2.14.4 Catalysts

The goal of utilizing a catalyst in a process is to offer a different route with a low activation energy need. This phenomenon is caused by the chemical interactions that result in the development of intermediate species or transition states. The catalyst may be used frequently because it is renewed throughout a reaction. The catalyst can, however, become inactive in some subsequent reactions in a reactor. Heterogeneous catalysts often have lesser activity than homogeneous catalysts but are easier to separate from one another and have little to no contamination in the product stream. When plastic waste is pyrolyzed, an endothermic process, the reaction temperature is dramatically lowered.

The adoption of a cost-effective catalyst can reduce energy and operational costs. Additionally, various processes used by catalytic reactions often alter how the products are distributed differently.

The generation of low-molecular-weight hydrocarbons and gaseous products with characteristics comparable to conventional fuel during pyrolysis is caused by the increased breaking of intermediate oligomers (Karnjanakom et al., 2020). Conventional acid-base salts and oxides (ZnO, MgO, $CaCO_3$, $CuCO_3$, SiO_2, Al_2O_3), nanoporous and mixed synthetic zeolites, amorphous silica-alumina, MCM-41, kaolin, CaC_2, metal supported on carbon, and simple oxides are among the heterogeneous catalysts employed in the pyrolysis of plastic waste.

In conclusion, the reaction variables during plastic pyrolysis greatly affect the feed reactivity and product distribution; nevertheless, the temperature's impacts on the level of cracking and secondary reaction modifications are of utmost importance. In addition, the inclusion of a catalyst modifies the mechanistic pathways and, consequently, the activation energies of degradation to enable the simultaneous or consecutive upcycling of high-molecular-weight molecules even at low temperatures.

2.15 Applications of pyrolysis products

The idea of converting plastic trash to liquid fuels and other chemicals with additional value is intriguing and has the potential to address health and environmental concerns. The method allows for the quick and efficient processing of nearly all types of plastic waste. The presence of little or no sulfur concentration in pyrolysis oil often provides significant advantages over traditional fuel. This method is designed to replace current plastic waste treatment methods in a sustainable way; however, it is important to note that conventional pyrolysis cannot be used to treat polymeric waste that has been contaminated or made of materials like Polyethlylene terephthalate and other waste electronic and electrical equipment. The product stream is complicated, especially in the case of mixed plastic waste, necessitating further processing in the case of pyrolytic oil. The thermal efficiency of individual feeds enriched with hydrocarbons like Low - density polyethylene, High - density polyethylene, Polypropylene, and Polystyrene is higher, and treatment is not challenging. However, thermal pyrolysis of plastic wastes is an energy-intensive procedure requires high energy to break down the polymers.

However, greater prospects are provided by using effective heterogeneous catalysts with synergistic pyrolysis of plastic waste, which this study seeks to address.

2.15.1 Pyrolysis Oil

Following the process of pyrolysis, the resulting liquid oils predominantly consist of polyaromatic, monoaromatic, aliphatic, and hydrocarbons. However, several contaminants, such as moisture, acids, and char, degrade the quality of the liquid fuels produced and, as a result, limit the potential industrial applicability of the product (Zhao et al., 2012). The quality of the liquid oils can be enhanced by post-treatments such as distillation, homogenization, and neutralizing the acidic content of the chemicals. In fuel applications, the fate of various distillates can be selected based on their physical and unique characteristics. Additionally, high-molecular-weight fractions produced by pyrolysis at low temperatures are useful for heating applications in boilers and power generation for irrigation pumps in the agricultural sector. There has been a growing interest in implementing integrated methods for catalytic or thermal upgradation of pyrolysis oil to derive high-end hydrocarbons, such as petrol, diesel, and Liquidfied Petroleum gas (LPG-grade) hydrocarbons as value-added chemicals, and this is anticipated to boost the economics of waste plastics treatment.

2.15.2 Pyrolysis Gases and Char

Typically, during the pyrolysis process, other products produced apart from the oil are gaseous hydrocarbons and char. These byproducts can be utilized to heat the reactor or for other energy-related purposes. According to Lopez et al. (2011) and Sophonrat et al. (2019), the primary problem of PVC mixed plastic waste is Hydrochloric acid, which can be eliminated or preferentially confined utilizing adsorbent. Alternately, plastic waste can be gasified at high temperatures to generate syngas and/or Liquidfied Petroleum gas (C_3-C_4) hydrocarbons. This process is known as high-temperature gasification. The recent attempts to use char to produce other carbon-related compounds are also worthwhile.

CHAPTER 3: MATERIALS AND METHODS

3.1 Introduction

This chapter presents the materials and methods used for the catalytic pyrolysis of municipal plastic waste and the methodology followed during the preparation and characterization of the kaolin-based ZSM-5 catalyst. The first section enumerated the selected feedstock used for the catalytic process and the characterization techniques carried out on these selected polymer materials, such as FTIR and TGA analysis. Thereafter, the materials and the experimental set-up used to carry out the catalytic pyrolysis experiments are described. In addition, the procedure for the process, as well as the sample analysis methods, are presented.

3.2 Feedstock Materials

Polyethylene (PE), Polypropylene (PP), Polystyrene (PS) and Polyethylene Terephthalate (PET) were used as the raw materials in this investigation. These materials were sourced from the Durban University of Technology's cafeteria garbage bins in Durban, South Africa. The materials were sorted, rinsed, and then shredded into tiny pieces before the commencement of the experiment. As received-kaolin from G&W minerals resources located in the Eastern Cape region of South Africa, served as the alumina source (66.10% SiO_2 and 20.51 % Al_2O_3, respectively). Sodium silicate (26.5% SiO_2 and 10.6% Al_2O_3 composition) solution and Tetrapropylammonium Bromide (TPABr) procured from Sigma Aldrich, Johannesburg, South Africa were used as additional silica source and structural directing agent, respectively. Nitric acid 55%, which was obtained from Ace enterprises chemical association, Johannesburg, South Africa, was used to adjust the pH. Commercial ZSM-5 zeolite powder (SiO_2/Al_2O_3 mole ratio: 50:1, CBV5524G) was obtained from Zeolyst International, Pennsylvania, USA as referencing material. All the chemicals were applied as received with no additional treatment, processing or purification.

3.3 Simulated Mixture of Plastic Waste (SMPW)

A simulated mixture of plastic wastes (SMPW) was prepared to consist of a blended mixture of municipal plastics, which consisted of 50.0 wt. % Polyethylene, 18.0wt. % Polypropylene, 21.0 wt. % Polystyrene, and 11.0 wt. % PET. The proportions were based on data obtained from a short literature review.

3.4 Characterization of feedstock

The thermogravimetric analysis/differential scanning calorimetry (TGA/DSC) and Fourier-transform infrared spectroscopy (FTIR) analysis of the municipal plastic waste (MPW) samples were carried out. An elemental analyzer (Vario EL-II Elementar Analysensysteme GmbH, Hanau, Germany) was used to analyse the samples. Based on the elemental composition of the raw materials, the multiple regression model (Equation 3.1) was used to estimate the higher heating value (HHV) (Boumanchar et al., 2019).

$$HHV\ (MJ\ Kg^{-1}) = 0.4167 * C - 0.57 * H + 0.2590 * O + 0.5989 * N - 5.8291 \quad (3\text{-}1)$$

C, H, N, and O depict the weight percentage of carbon, hydrogen, nitrogen, and oxygen in the MPW, respectively.

The functional groups of samples (PS, PP, PE, PET) were obtained using FTIR (model Bruker Vertex 70 spectrometer, Bruker Optics, Billerica, MA, USA) equipped with a Platinum ATR sampling module.

3.5 Fourier transform infrared (FTIR) spectroscopy

Light may be absorbed by different materials in different ways depending on where in the spectrum it falls. Because of this, a majority of materials absorb infrared light. As a result of these absorptions, the dipole moments of the molecules in these materials shift, affecting their vibrational and rotational patterns. To put it another way, a material's absorption frequencies are governed by its molecular energy bands, and these frequency components impact the efficiency of infrared photon energy transmission (Toninelli et al., 2021). The absorption intensity may be determined by calculating the degree of the infrared photon energy conversion.

Figure 3.1: Bruker Vertex 70 FTIR analyzer

While various infrared spectroscopies may be used to quantify some mid-infrared-absorbing components, FTIR spectroscopy is superior. Due to FTIR's superior signal-to-noise ratio, compared to procedures like HPLC and UV-vis, FTIR analysis is preferred.

Instead of a monochromator and slits, an interferometer is used in FTIR, which is a technological breakthrough. Beams of light are separated into two separate directions to operate. A detector measures the output beam's intensity as a function of path difference after the beams' interference has been allowed to recombine (Birch et al., 2020).

In this study, the FTIR spectroscopy method (Bruker Vertex 70 spectrometer), as shown in Figure 3.1, was employed as both a qualitative (assisting polymers identification based on their individual absorption bands) and semi-quantitative (assessing the polymers degradation degree by quantifying specific absorption bands assigned to carbonyl groups and by calculating the carbonyl index) technique. These investigations produced spectra that functioned as unique chemical identifiers that could be easily separated from other compounds' absorption spectra. FTIR spectra analyses were performed utilizing at least 32 scan images with an average resolution of 4 cm^{-1} IR emission in the frequency range of 400–4000 cm^{-1}.

3.6 Thermogravimetric Analysis (TGA)

Thermogravimetric analysis (TGA), also known as thermogravimetry (TG), is a method that involves measuring the weight of a polymer as a function of temperature or time while the material is being subjected to a controlled temperature program in a regulated environment. Modern TGAs generally have temperature ranges of ambient to 1000 °C or more, which is suitable for polymer applications. Oxygen and hydrogen are examples of purge gases that may be used to generate an inert atmosphere, such as nitrogen, or oxidizing, such as air. Purge gas can have a moisture level of dry to saturated. Polymers usually experience weight loss but regain weight before decomposition in an oxidizing environment at slow heating rates.

Figure 3.2: The 50A Thermogravimetric Analyzer Instrument

In this work, a standardized TGA experiment was conducted on the feedstock PE, PP, PS, and PET to determine the most appropriate process parameters, such as temperature and reaction time, using TA instrument (SDT Q600) to analyze their decomposition behaviour. The samples were heated under N_2 atmosphere at the rate of 40 ^oC/min from ambient to 600 ^oC using a sample size ranging from 15 – 20 mg. The TG Analysis was done twice to analyze the reproducibility and was found to be very low (±0.05%).

3.7 Catalyst Preparation and characterization

In the search for cheaper and more environmentally friendly alternatives to chemical sources, much research has been conducted on the feasibility of kaolin. In this current study, South African kaolin was metakaolinized via thermal activation at 700 ^oC for 2 hours 30 minutes and subjecting it to hydrothermal treatment in a NaOH medium, and then zeolite was produced. The ZSM-5 zeolite catalyst was prepared using a modified method reported by Youssef *et al*. (2018) from the literature.

At the beginning of the synthesis, mineralogical analysis using x-ray diffraction (Philips X-ray diffractometer) was conducted on the three different samples of the kaolin collected from three different sites (G1, G3 and G10) to determine the initial Si/Al ratio. Table 3.1 shows the mineralogical composition of the kaolin samples.

From Table 3.1, it shows that samples G10, G3 and G1 have Si/Al compositional ratios of 3.2, 2.5 and 2.3, respectively. According to Jonscher *et al* (2022), the Si/Al ratio, among other factors, significantly affects the crystallization process and the morphology of the ZSM-5 zeolite formation. The higher the Si/Al ratio, the better the crystals.

Table 3.1: XRF Analysis of raw Kaolin

Sample (Kaolin)	**SiO_2 (%)**	**Al_2O_3 (%)**	**Fe_2O_3 (%)**	**K_2O (%)**	**Na_2O (%)**	**CaO (%)**	**MgO (%)**	**P_2O_5 (%)**	**MnO (%)**	**TiO_2 (%)**
G10__24381	66.1	20.5	0.9	1.8	0.0	0.6	0.0	0.0	0.0	0.7
G3__24379	48.0	19.2	0.6	1.5	0.2	0.6	0.0	0.0	0.0	0.5
G1__24380	46.1	19.5	0.7	1.6	0.0	0.6	0.0	0.0	0.0	0.5

The stages in the synthesis of the catalyst are shown in Figure 3.3. Different amounts (1.0, 0.5, and 0.25 g) of metakaolin (66.1% SiO_2 and 20.51% Al_2O_3) and sodium hydroxide (0.33 g) were dissolved in deionized (DI) water (2.5 ml), and 1.6 ml of TPABr was combined independently with the 20 ml of DI water in the synthesis of kaolin-based ZSM-5. These solutions were mixed together for an hour, and the sodium silicate solution and the NaOH/Kaolin solution were added to the TPABr solution at the same time while stirring for another hour. The pH was controlled using nitric acid until the solution combination was homogeneous.

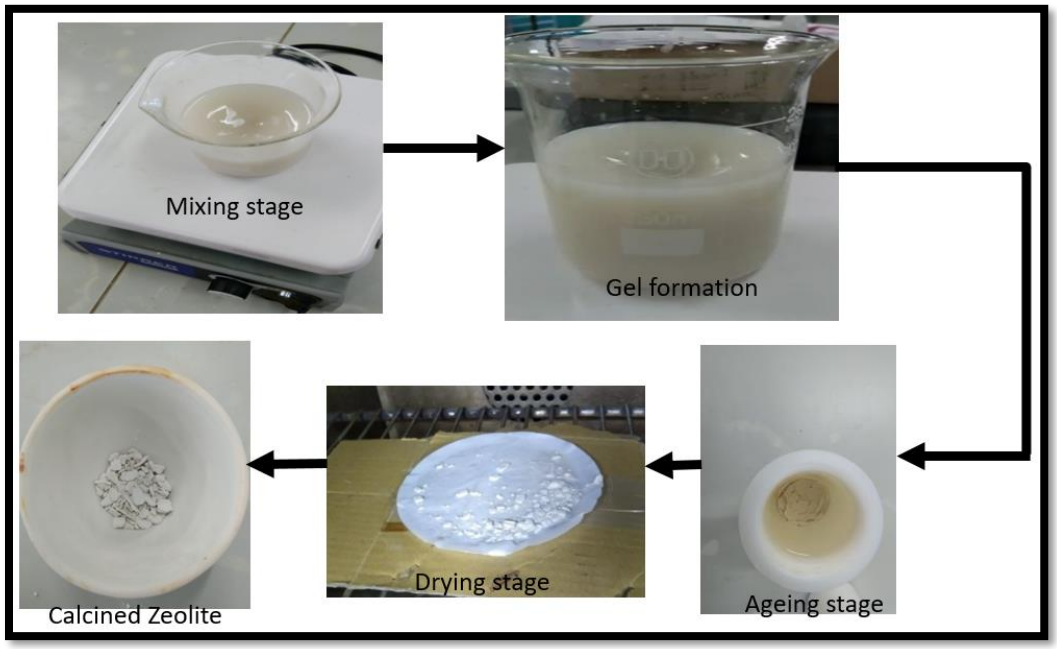

Figure 3.3: Stages of Synthesizing ZSM-5 Zeolite

The formed gel was transferred into a stainless steel Teflon-lined autoclave cup and hydrothermally treated for two days at 180 degrees Celsius. The final product was washed in DI until it had a pH of less than 8. The sample was dried overnight at 80 degrees Celsius and then calcined for five (5) hours at 550 degrees Celsius. The produced dried powder was therefore characterized and analyzed.

3.8 Characterization

Bruker AXS, D8 Advance fitted with Tube (Cu-Ka radiation (lKa1=1.5406 Å) and Detectors Lynx Eye (Position sensitive detector) at V_20 variable slit, 40 kilovolts, and 40mA recorded X-ray diffraction (XRD) patterns and average crystallite size. A 0.5° to 130° 2incremental width was used, with a constant increment of 0.034° and a scan rate of 0.5 sec per step. OriginPro 2020 software was used to analyze the diffraction data and estimate the amount of each phase in the sample.

Scanning electron microscopy FEI Nova NanoSEM 230 with an energy-dispersive laser fitted with a strong absorption lenses were used to analyze the structure. The Oxford X-Max EDS detector was used using INCA software. The BET machine was used to measure and analyze surface area, pore size, and pore volume.

3.8.1 X-ray diffraction (XRD) studies

The primary function of XRD is to measure the degree of phase crystallinity of the materials in samples. About 95 per cent of all solid materials (organic and non-organic) may be classified as crystallographic, meaning they can be diffraction-sensitive and can be studied using this method (Mawson et al., 2020). Even in mixtures of different crystalline substances, a distinct pattern may be seen in every crystalline material (Umarov et al., 2021). To get an idea of how much a certain phase of that element is in the sample, the area beneath the peak of that phase may be measured. Pure substances have X-ray diffraction patterns that are similar to fingerprints, and because of this, polycrystalline phases may be identified and described using XRD. In order to generate the solid material's crystalline structure, atoms are placed in a specific order, which results in the diffraction of X-rays, which results in the XRD patterns. Materials that are amorphous solids are characterized by their random arrangement of atoms. Solid crystals are defined by their three-dimensional arrangement of atoms in a repeating pattern of atoms. A crystal's smallest unit cell has the least possible volume.

Analysis of materials in this study was carried out using a Bruker D2 Phaser XRD (Fig. 3.4) that employed a Cu K radiation source using an output of 40 kV x-ray tubes and 40 mA, respectively, over an angle range of 10 degrees to 130 degrees 2theta. The diffractometer used Bragg – Brentano geometrical design, with an incidence angle specified between the X-ray emitter and the sample and a diffraction angle of 2thetha defined between the incident rays and the sensor (Miller et al., 2020). In contrast to this, the diffraction vector was always parallel to the sample's surface. The samples had to be meticulously prepared before they could be tested.

An almost-flat plane surface was required for pressing the sample with a glass plate for a smoothed, uniform-height surface to be used in this experiment (Fig. 3.4). To follow

phase transitions during calcination and serve as a control, samples from both calcined and non-calcined samples were synthesized in this manner.

Figure 3.4: The Bruker D2 Phaser XRD fitted with a LynxEye detector.

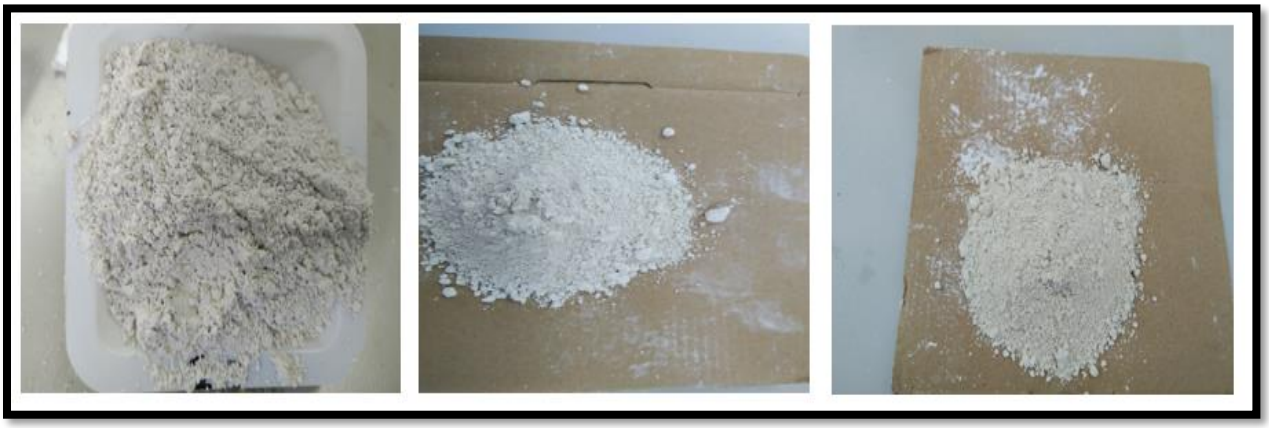

Figure 3.5: Preparation of samples for XRD analysis.

During scanning, samples were rotated every half an hour. A collection of data from the scans was generated, including peak sequences, degree of crystallinity, and Miller indexes. EVA software was used to identify the peak structures by scanning through a library of crystal structures with mirrored phases that appeared at their corresponding 2 theta.

3.8.2 Scanning electron microscopy (SEM)

High-resolution surface imaging is made possible by the use of scanning electron microscopy (SEM). The signals released by test samples are detected by scanning a tiny electron beam across samples. Scanning electron microscopy allows the sample to be excited by an electron beam, which then creates observable signals on the sorts of detectors that use cathode ray tubes to visualize and record the captured images. Secondary electrons, back-scattered electrons, relayed electrons, or specimen currents can all produce visual representations of the sample (Khan et al., 2018). In order for the secondary electron images to be created, the detector must be able to detect both secondary electrons and backscattered electrons. To explain this, it is because secondary electrons are created at a distance of a few nanometers (nm) from the sample.

Advanced SEM equipment has a resolution of about 2 nm. Thus, they are extremely sensitive to the structure of the surface and offer topographical data. The back-scattered electrons are created from deep inside the material and interact considerably more intensely with the material. Consequently, serving as a source of multivariate data (de Silveira et al., 2020).

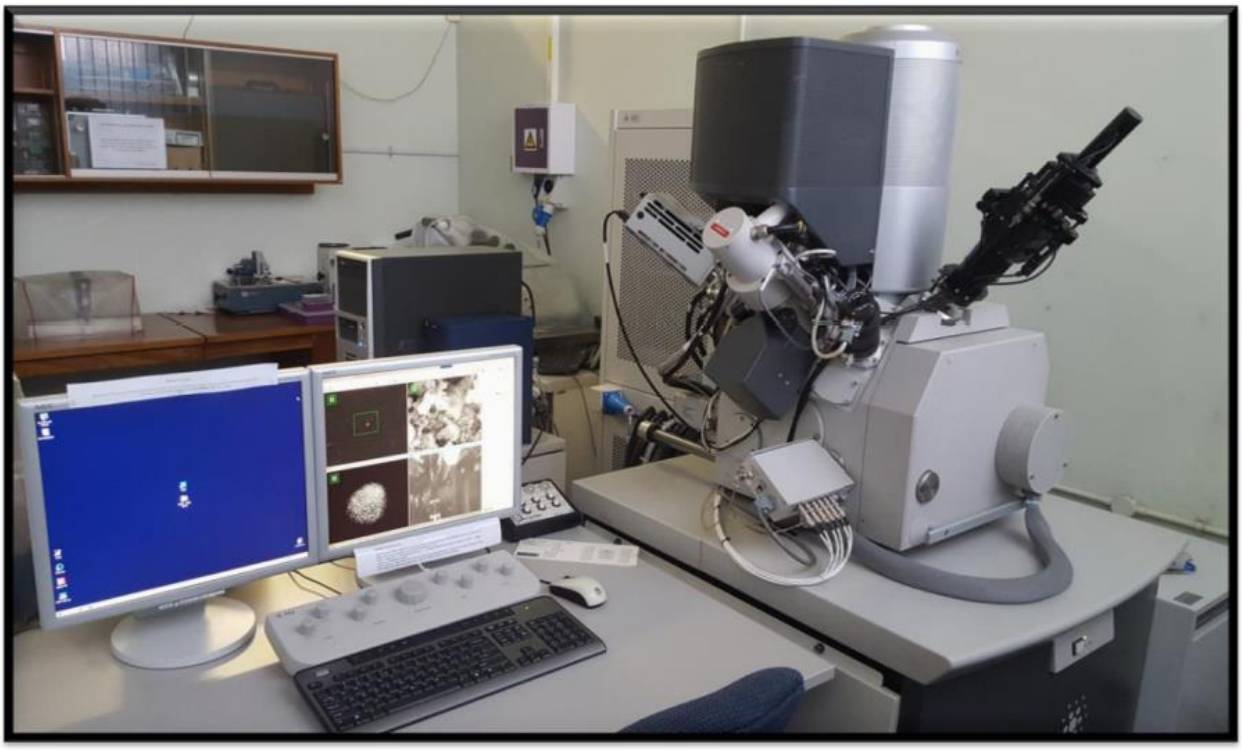

Figure 3.6: The FEI Quanta 200 FESEM with ETD/SSBSED detector.

FEI Quanta 200 FESEM (Oregon, USA) scanning electron microscope was used for this experimental work with the highest voltage reaching a peak of 20 kV. SE and BSE were detected using ETD and Low kV SSBSED (Oregon, USA) detectors. Analysis of morphological structure before and after use was carried out on the G1, G3, and G10 nanoparticles. SEM and EDS were used to characterize the elemental composition of the produced catalysts.

3.9 Pyrolysis Experimentation

The pyrolysis experiment used municipal plastic waste (PE, PS, PP, and PET) as feedstock. The pyrolysis of individual plastic was also carried out for comparison. A stainless steel reactor with the following specifications (length = 450 mm, inner diameter = 100 mm and outer diameter = 150 mm) heated in an electric furnace with the temperature measured by K type thermocouple placed in the reactor was used to carry

out the pyrolysis experiment. Figure 3.7 is the schematic diagram of the pyrolysis experiment, and the procedure by Ajibola *et al.* (2018) was adopted for the pyrolysis experiments. The reactor was in a vertical configuration, and quartz wool was used as a support. Before the pyrolysis experiment, the feedstock was shredded into smaller pieces to increase the combustion rate. 100g each of each sample was used, and the whole reactor system was first purged with N_2 for 30 min at a 30 mL/min flow rate to get rid of residual air in the system and ensure an inert atmosphere. The pyrolysis experiments were performed as follows: At the beginning, the reactor was heated at 10 ^{o}C/min until the temperature reached the set temperature between 350 and 550 °C and held for 60 min. Thereafter, the sweeping gas was allowed to continue to flow until the vapour in the reactor was liquified using a condenser connected to a temperature regulated water bath and kept at 0 ^{o}C. The char was left in the reactor while the condensed liquid product was collected into the storage tank. After allowing the reactor to cool to room temperature, the solid residue was recovered. The gas chromatography-mass spectrometry (GC–MS) was used in analyzing the produced liquid oil. The formula used in calculating the produced liquid oil, gas, and char is shown below (Olagunju and Kiambi 2021). All the pyrolysis experiments were repeated twice, and the mean values were reported.

Char (weight%) = (Amount of Char produced / Amount of feedstock) * 100 (**3-2**)

Liquid oil (weight%) = (liquid yield / Amount of feedstock) * 100 (**3-3**)

Gas (weight%) = 100 - (Char (weight%) + Liquid oil (weight%)) (**3-4)**

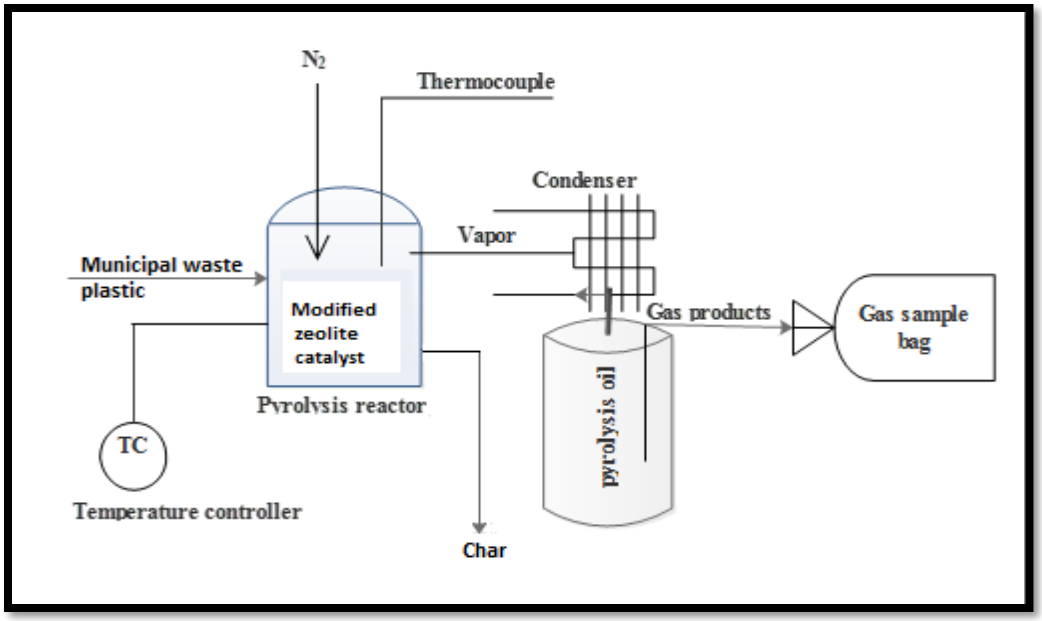

Figure 3.7: Schematic of pyrolysis experimental set-up

3.10 Liquid oil Analysis

Analysis was carried out on the liquid oil produced to determine the properties and attributes of the product oil. The gas chromatography–mass spectrometer was employed to analyze the hydrocarbon mixtures in the catalytic pyrolyzed oil. Furthermore, the physio-chemical analysis was carried out on the oil sample to determine its physical and chemical properties and to ensure it meets both ASTM and SANS standards.

3.11 Gas chromatography-mass spectrometer (GCMS)

The instrument known as gas chromatography/mass spectrometry (Figure 3.8) is capable of separating chemical mixtures (using the GC element) and identifying the constituents in the sample tested (the MS component). For environmental samples, it is one of the most accurate instruments. When heated, a mixture will split into its constituent components. Helium (inert gas) is used to carry the gas through the column. The MS

receives the separated compounds as they exit the column aperture. The analyte molecule's mass is used in mass spectrometry to identify the compounds.

An electronic library of known mass spectra spanning thousands of compounds is accessible via a computer network.

The gas chromatography-mass spectrometer (Agilent 7890-5975C) was used to determine the chemical constituents of the produced pyrolytic oils under the following measurement conditions: DB-1701 column; Helium as carrier gas at flow rate of 1.76 mL/min; 1 µL injection size; and 1: 60 split ratio. Starting GC oven temperature was kept at 42 °C for 1 min; then the temperature was increased to 300 ^{o}C at a rate of 5.5 ^{o}C/min and held for 10 min; Scan mode (35.00 to 550.00 m/z); injector and detector temperature of 220 ^{o}C and 250 ^{o}C respectively.

Figure 3.8: The gas chromatography-mass spectrometer (Agilent 7890-5975C)

The compounds were identified using the National Institute of Standards and Technology (NIST) mass spectral data library. Furthermore, the elemental composition of the liquid oils produced was determined using an elemental analyzer (Vario EL-II Elementar Analysensysteme GmbH, Hanau, Germany), and liquid-oils higher heating value (HHV) were estimated using the earlier mentioned Boumanchar et al., (2019) correlation (Equation 3.1).

3.12 Experimental Design in the optimization process

The process of designing an experiment to get the right data, which is then examined using statistical techniques to provide reliable, factual, and useful results, is known as the design of experiments.

Factorial Design and Response Surface Methodology (RSM) can be used to optimize reaction time, temperature, and catalyst concentration to maximize product yield and composition of liquid oil from plastic mixtures and predict the effect of experimental conditions on product yields formed from pyrolysis of waste mixtures (Ünsal et al., 2020). RSM may be used to predict pyrolysis outcomes with a significant decrease in the number of trials. The information provided by this technique can also help determine how to set up experiments to produce the most of certain gas and liquid compounds (Pezzatti et al., 2020).

A strong analytical method for modelling and assessing the impact of process factors on specific variables that are not known is called factorial design (Leatherdale, 2019). Using a factorial design can integrate experimental design and data analysis in a manner that optimizes findings and reduces the number of experiments by selecting the optimal experimental runs (Beg et al., 2019). Full Fractional Factorial Design enables the exploration of the interactions between numerous input variables and assessing the impact of each input element on the test result (Fang et al., 2018).

CHAPTER 4: INFLUENCE OF SYNTHESIS CONDITIONS ON THE CHARACTERISTICS OF ZEOLITE

4.1 Introduction

Zeolites are hydrated aluminosilicate materials that are microporous in three dimensions. They have an open vacuum with a three-dimensional crystal structure in which aluminum, silicon, and oxygen coordinate with noble metal (Orjioke et al., 2016). As shown in Figure 4.1, the primary components of zeolites are center atoms (Al, Si) and terminal oxygen atoms in a tetrahedral configuration. Zeolites may also generate additional building component by bonding via oxygen-oxygen atoms to form rings, pyramids, and others as shown in Figure 4.2.

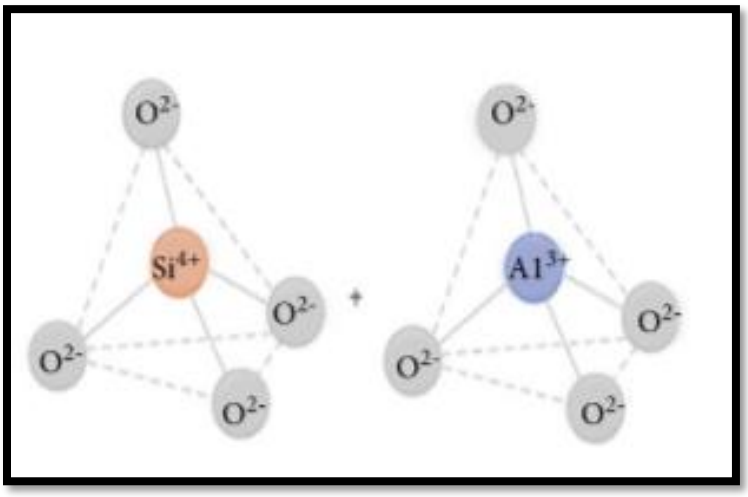

Figure 4.1: Fundamental building component of zeolite (Moshoeshoe et al., 2017)

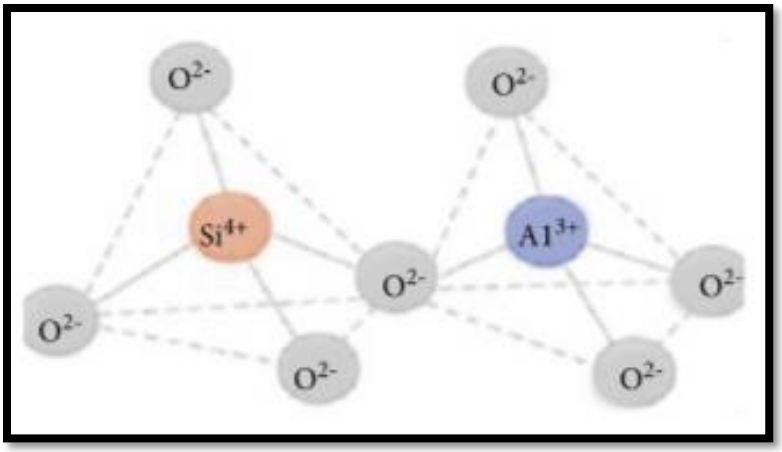

Figure 4.2: Secondary building component of zeolite (Mgbemere et al., 2017)

Zeolites have significant industrial and scientific applications, especially as a solid base catalyst (Verdoliva et al., 2019). Physicochemical qualities and a constant pore structure are characteristics of the frameworks made up of $(SiO_4)_4$ and $(AlO_4)_5$ tetragonal elements (Sadeghpour, and Haghighi, 2022).

There are two main categories of zeolites and these are natural and synthetic zeolites (Chunfeng et al., 2009; Nyankson et al., 2018; Bacakova et al., 2018). Natural zeolites are made from the sedimentary and volcanic rocks such as chabazite, clinoptilolite, and mordenite (Chunfeng et al., 2009). On the other hand, manmade zeolites are produced by heating materials including China clay, kaolin, soda ash, and others (Pan et al., 2019). Additionally, there are several kinds of synthetic zeolites that may be created from various materials, including zeolite A, ZSM-5, Y, and P (Melaningtyas et al., 2019). ZSM-5 zeolites have a reputation for being remarkably stable, and having a substantial amount of empty space (Mgbemere et al., 2017; Melaningtyas et al., 2019). This particular class of zeolites is very significant to the generation of liquid oils when used as a catalyst for the polymer cracking (Ruíz-Baltazar et al., 2015).

4.2 Kaolinite

Kaolin is a natural occurring rich mineral. Also known as Kauling earth or china clay (Prasetyoko et al., 2020). It is whitish in color and has a brown surface. $Al_2Si_2O_5(OH)_4$ is the chemical formula for kaolin, and its theoretical component is SiO_2, 46.54 percent; Al_2O_3, 39.50 percent; and H_2O, 13.96 percent. Kaolin-originating source and location significantly impact both its chemical properties and its crystallographic features (Yaya et al., 2017). Figure 4.3 depicts the pseudohexagonal phase as the ideal state for kaolinite crystals. At the same time, these minerals can also occur in other phases, including the triclinic and pseudo-monoclinic, as well as polymorphs (dickite and nacrite) (Hradil and Hostomský, 2002).

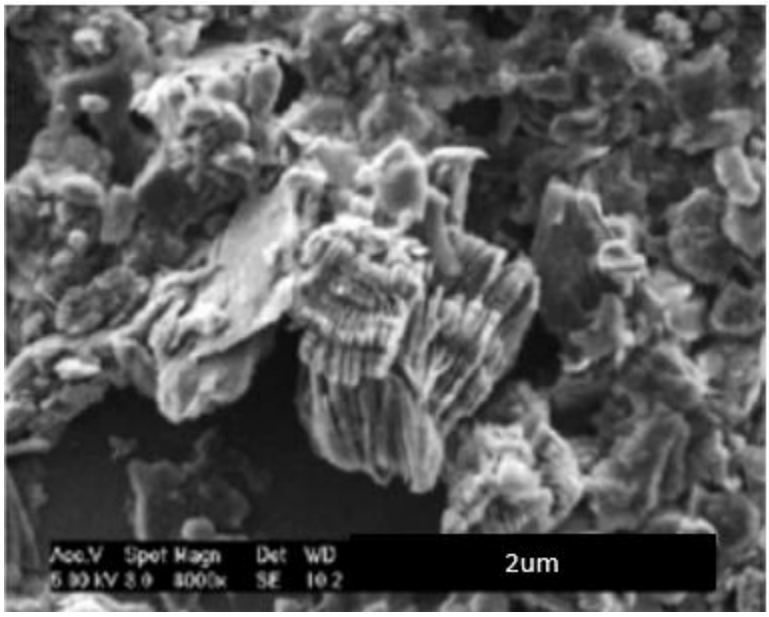

Figure 4.3: The pseudohexagonal forms of kaolinite crystals.

As seen in Figure 4.4, the two layers of Al^+ and Si^- combined to create a compound layer with O_2 atoms serving as the connection between them. (Murray et al., 2011). Kaolinite materials are often used in industrial operations, including in the paint and pharmaceutical sectors, as well as in paper additives and paper surface adhesives.

There are two types of kaolin deposits: primary and secondary. Primary kaolin is produced mainly by hydrothermal process, whereas secondary kaolin is sedimentary in origin.

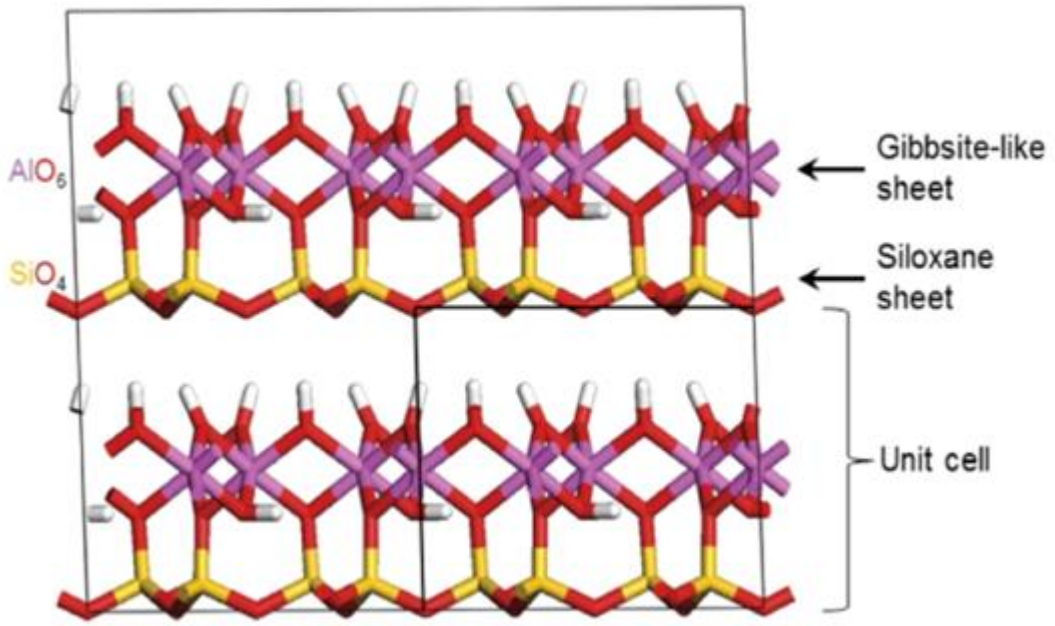

Figure 4.4: The elemental structure of kaolin (Kazemimoghadam and Mohammadi, 2011)

Kaolin deposits are found in several nations, with varying degrees of quality. Improving kaolin's economic worth is one of the objectives of its use in zeolite synthesis. Indonesia, Malaysia, Pakistan, Vietnam, Brazil, Bulgaria, China, the Czech Republic, Spain, South Africa, and the United States are among the nations where kaolin is frequently found as a mineral. The main kaolin reserves in South Africa are located at Grahamstown, Eastern Cape. Kaolin has a wide range of applications, including those for raw materials for ceramics and porcelain, paper manufacturing's loading material, fillers for rubber, fire-resistant material, cement, additives for oil refining, and cosmetics.

4.3 Catalyst Preparation and characterization

In the search for cheaper and more environmentally friendly alternatives to chemical sources, much research has been conducted on the feasibility of kaolin. In this current study, South African kaolin collected from three different sites (G1, G3 and G10) was used as the source material for catalyst synthesis. The ZSM-5 zeolite catalyst was prepared using a modified method reported by Youssef et al. (2018) from the literature. At the beginning of the synthesis, mineralogical analysis using x-ray diffraction (Philips X-ray diffractometer) was conducted on the three different kaolin samples collected from Grahamstown, South Africa, to determine the initial Si/Al ratio.

Table 4.1 depicts the mineralogical composition of the kaolin samples G10, G3 and G1 to have Si/Al of 3.2, 2.5 and 2.3, respectively, and according to Khatmian and Irani (2007), the Si/Al ratio among other factors have a significant effect on the crystallization process and the morphology of the ZSM-5 zeolite formation. The higher the Si/Al ratio, the better the crystals.

Table 4.1: XRF Analysis of raw kaolin

Sample (Kaolin)	SiO_2 (%)	Al_2O_3 (%)	Fe_2O_3 (%)	K_2O (%)	Na_2O (%)	CaO (%)	MgO (%)	P_2O_5 (%)	MnO (%)	TiO_2 (%)
G10__24381	66.1	20.5	0.9	1.8	0.0	0.6	0.0	0.0	0.0	0.7
G3__24379	48.0	19.2	0.6	2.4	0.2	0.6	0.0	0.0	0.0	0.5
G1__24380	46.1	19.5	0.7	3.6	0.0	0.6	0.0	0.0	0.0	0.5

Traditionally, kaolin is calcined to create metakaolin at temperatures between 550 and 900°C. In this project, the muffle furnace, as shown in Figure 4.5, was used for calcining the kaolin samples. The crucible with the quantity of kaolin to be calcined was initially placed into the furnace preheated to 700°C at a heating rate of 15°C/min for 2 hours 30 minutes, following which the furnace was turned off.

The crucible was left in the oven to cool off without opening the furnace. The calcined kaolin was then characterized using XRD, SEM, and TGA analysis.

Figure 4.5: A Bench-top muffle furnace

The stages in the synthesis of the catalyst are shown in Figure 4.6. Different amounts (1.0, 0.5, and 0.25 g) of metakaolin (66.1% SiO_2 and 20.51% Al_2O_3) and sodium hydroxide (0.33 g) were dissolved in deionized (DI) water (2.5 ml), and 1.6 ml of Tetrapropylammonium bromide (TPABr) was combined independently with the 20 ml of DI water in the synthesis of kaolin-based ZSM-5. These solutions were mixed together for an hour, the sodium silicate solution and the NaOH/Kaolin solution were added to the TPABr solution at the same time while stirring for another hour. The pH was controlled using nitric acid until the solution combination was homogeneous.

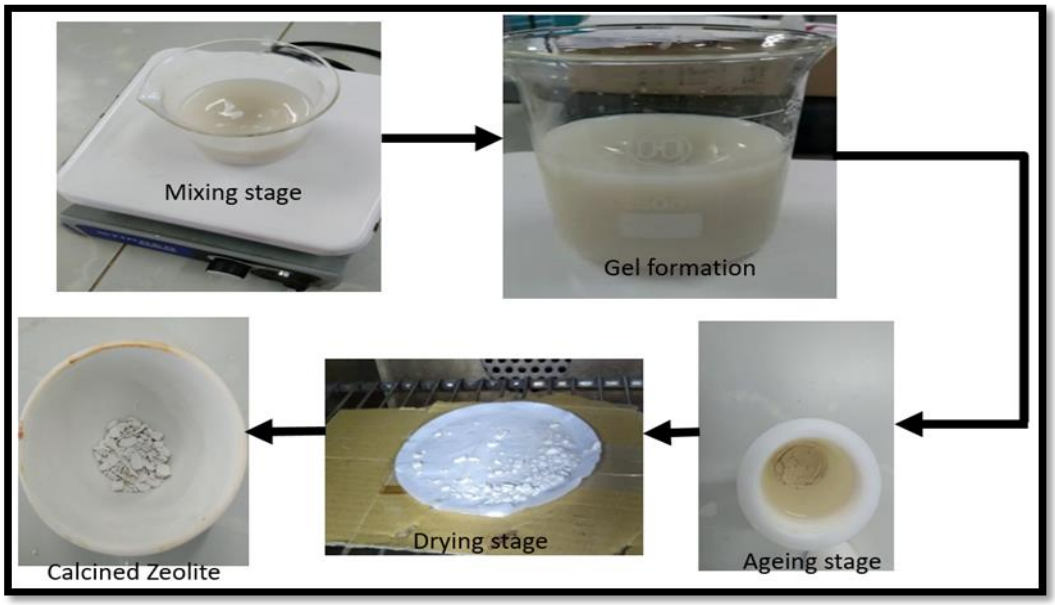

Figure 4.6: Stages of Synthesizing ZSM-5 Zeolite

The formed gel was transferred into a stainless steel Teflon-lined autoclave cup (figure 4.7) and hydrothermally treated for two days at 180 degrees Celsius. The final product was washed in DI H_2O until it had a pH of less than 8. The sample was dried overnight at 80 degrees Celsius and then calcined for five (5) hours at 550 degrees Celsius. The produced dried powder was therefore characterized and analyzed. The schematic diagram of the synthesis steps followed is presented in Figure 4.8.

Figure 4.7: Stainless steel Teflon-lined hydrothermal reactor

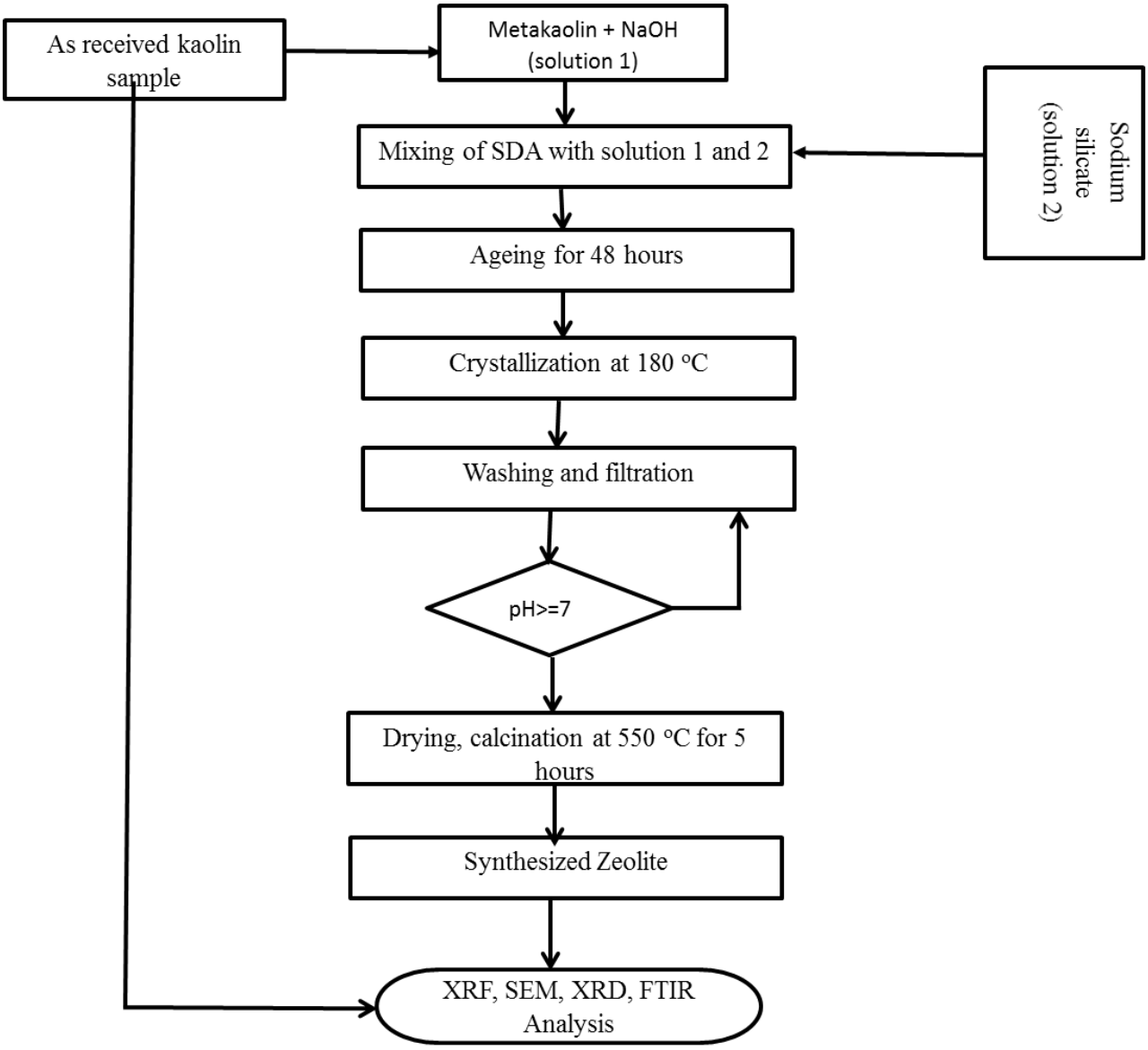

Figure 4.8: Flow diagram of the ZSM-5 zeolite synthesis

4.4 Results and Discussion

4.4.1 Metakaolinization

Using various metakaolinization temperatures, several investigations on the synthesis of zeolites from kaolin have been published in scientific literature. Table 4.1 demonstrates the high potassium oxide content of G&W kaolin, which suggests that samples G1 contain significantly more quartz than G3 and G10.

The XRF data demonstrate that SiO_2 and Al_2O_3 are present in the source material (kaolin). The ratio of silica to alumina in the kaolinite clay from G&W Mineral Resources is 3.2 for sample G10, 2.5 for sample G3, and 2.3 for sample G1. The ratio of silica/alumina of the source material is very critical as this determines the structure of the zeolite to be produced. The Si/Al of the feedstock in this present work are comparable to the predicted values of silica to alumina in the research on clay minerals from the identical area (Mohiuddin *et al*., 2016). Consequently, these ratios make them appropriate starting materials for synthesising high-quality zeolites.

The X-ray peak intensities of the un-calcined kaolin are shown in Figure 4.9. The un-calcined kaolin is composed of poorly crystalline kaolinite, whereas the metakaolin contains highly crystalline kaolinite. Uncalcined kaolin exhibits the presence of mica and quartz as the principal impurities, with mica having typical peaks at 2-theta = 8.9° and quartz having peaks at 2-theta = 20.9 and 26.4°. The kaolinite-specific peaks, however, were located at 2-theta = 12.4 and 24.8°.

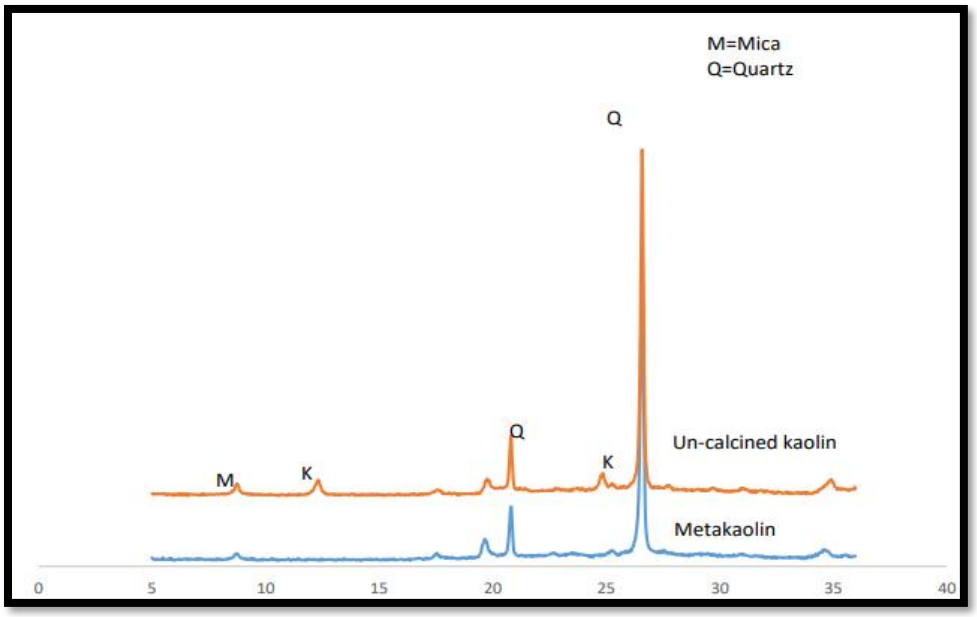

Figure 4.9: XRD peak intensities of un-calcined kaolin and metakaolin

The SEM scan of uncalcined kaolin is shown in Figure 4.10, illustrating the kaolinite's characteristic pseudo-hexagonal structure despite being hidden by quartz impurity. The XRD analysis result demonstrates that the frequency of the diffractogram peaks of the quartz in the metakaolin sample is lower than that of the uncalcined kaolin sample. This is a sign that metakaolin has evolved from kaolin. The kaolinite lattice crystal structure collapsed due to the metakaolinization of kaolin at 650°C, transforming it into an amorphous and disordered structure (Belviso et al., 2013). This proved that kaolin had really been transformed into metakaolin.

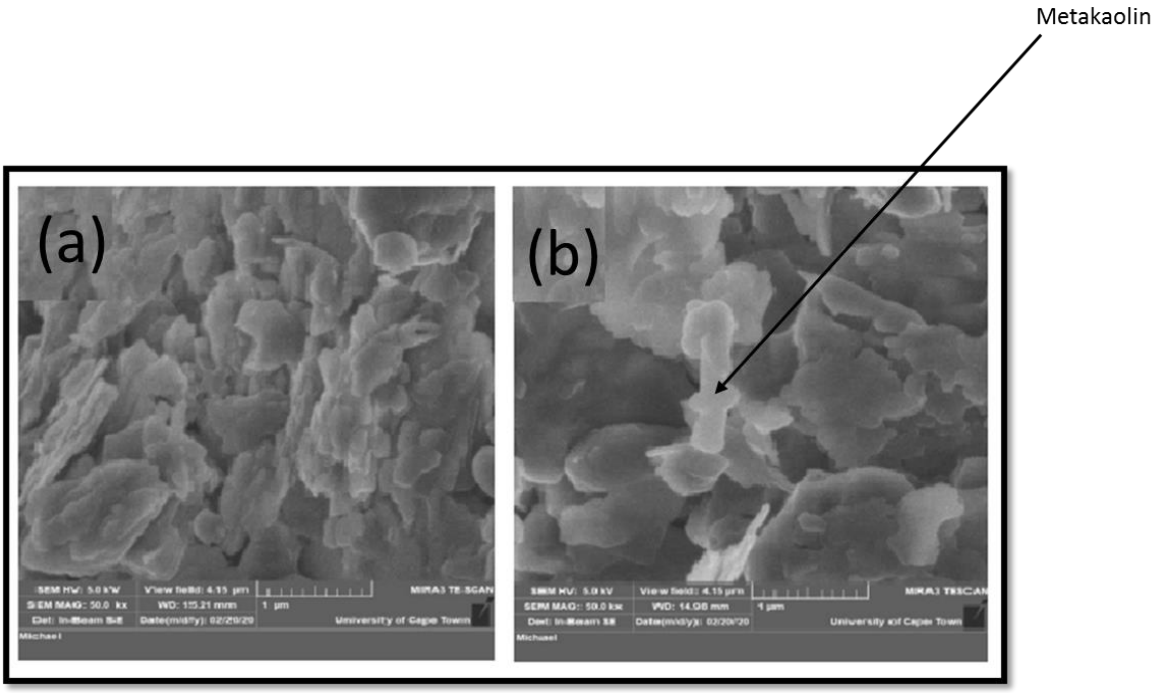

Figure 4.10: The display of SEM scans of un-calcined and calcined kaolin sample

4.4.2 Hydrothermal Synthesis and Characterization of kaolin based ZSM-5 zeolite

The as-received kaolin sourced from three different locations in Grahamstown, South Africa (G1, G3, and G10) was used to synthesise ZSM-5 zeolite using the conventional hydrothermal method, and the results from the process were discussed below.

4.4.3 Effect of crystallization temperature

Figure 4.11 shows the XRD patterns of the synthesized ZSM-5 utilizing metakaolin that was calcined at 650 °C for 2 hours. In Figure 4.11b, the amorphous ZSM-5 occurred on the crystallization of G1/ZSM-5 by the presence of quartz at 2θ 18-35^0. However, the little reflection of ZSM-5 characteristic crystals was noticed at 2θ 7.6, 8.5 and 23.1, although with low intensity. This result showed that zeolite formation is still in the early stage of crystal nucleation. The kaolin requires further purification to remove the quartz before using it for zeolite synthesis.

Figure 4.11c-d shows the XRD pattern of ZSM-5 zeolite on G3/ZSM-5 and G10/ZSM-5 synthesized zeolite. These reflections were noticed at 2θ 7.8, 8.8, 23.1, 23.3, 23.7 and 24.3^0 respectively. These characteristic reflection patterns were seen in both synthesized zeolites suggesting that they are both of the same phase (Mohiuddin et al., 2016). Also, the XRD pattern of G3/ZSM-5 and G10/ZSM-5 exhibits sharp reflections with high intensity, suggesting that the synthesized zeolite are solid crystals (Salou et al., 2021). Investigating the sample reflection based on the XRD powder pattern for zeolite at reflection patterns of 2θ 7.9, 8.8, 23.1and 24.3^0 shows that these samples are in line with the MFI (Inverted Mordenite Framework) zeolite structure type and therefore, G3/ZSM-5 and G10/ZSM-5 synthesized zeolite is of MFI structure (Treacy and Higgins, 2021).

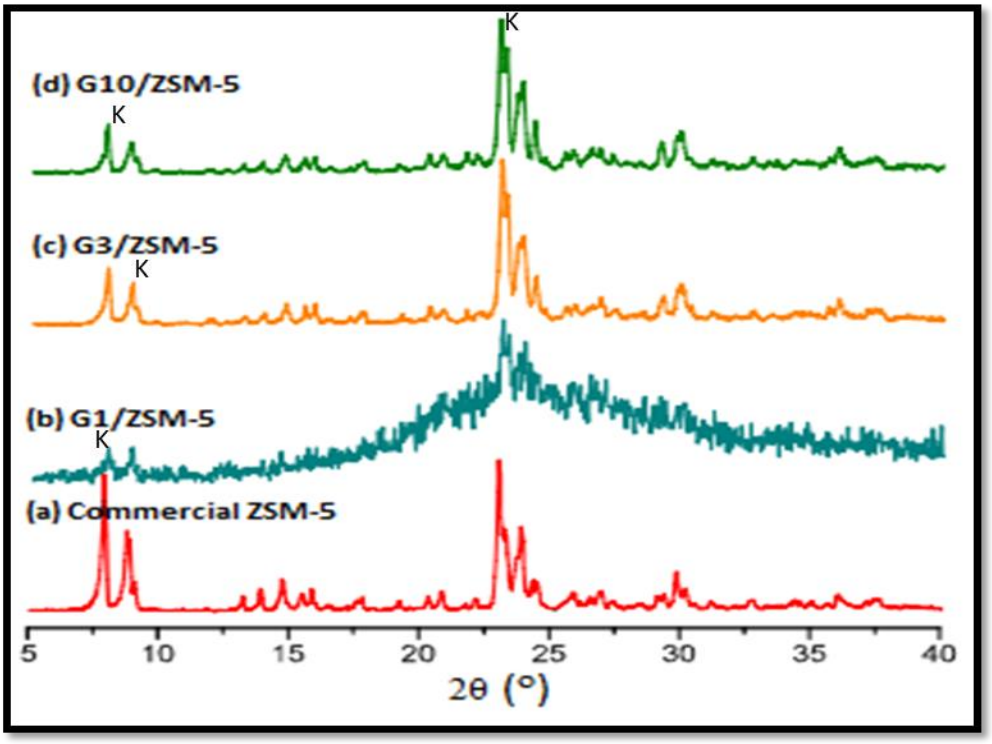

Figure 4.11: XRD patterns of the synthesized ZSM-5 catalysts

4.4.4 Scanning electron microscopy (SEM) studies

SEM is a method for interpreting the form and size distribution of zeolite crystals. ZSM-5 crystals' configuration, formation, and structure are often tightly controlled and dependent on synthesis parameters, including crystallization temperature, duration, and ageing. The surface morphology of the synthesized ZSM-5 zeolite is displayed in Figure 4.12. As shown, Figure 4.12a has the G1/ZSM-5 sample with an irregular shape as fragments with many forms/shapes. The catalyst has sizes ranging from 0.59 – 2.64 microns. This result is in line with the XRD data for synthesising the G1/ZSM-5 sample, which is amorphous. However, the morphology of kaolin-based G3/ZSM-5 and G10/ZSM-5 zeolite nanocrystals produced at 180 ^{0}C, 48hr, and 48hr crystallization temperature, time, and ageing, respectively, form orthogonal aggregate crystal shapes and are well crystalline indicating the presence of an inter-grown crystal, as shown in Figure 4.12(b-c). The aggregation of their high surface Gibbs free energy results in orthogonal nanocrystals (Wu et al., 2013).

These results concur with the crystallization characteristics by XRD and Mohiuddin (2016) work, who investigated the synthesis of ZSM-5 utilizing impure kaolin under various conditions, resulting in various morphologies.

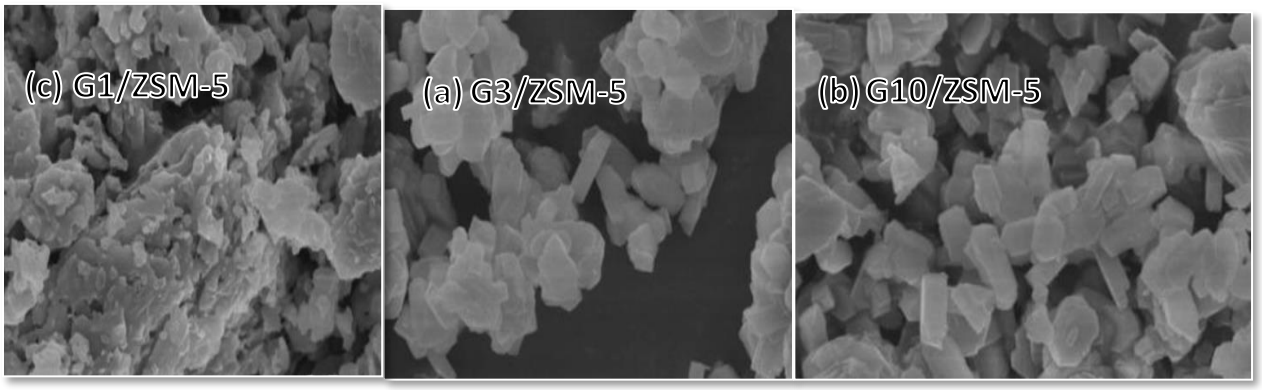

Figure 4.12: SEM images of the synthesized ZSM-5 catalysts

Figure 4.13 displays the XRD patterns of the three distinct ZSM-5 produced from kaolin sources. The three samples were synthesized at 180 ^{0}C, and their typical diffraction peaks at 2 theta equal to 7.91, 8.84, 23.07, 23.91, and 24.41^0 correspond to the five most significant peaks in the XRD study. The peaks at 2 theta match the usual peaks of the MFI structure of ZSM-5 (Aliyu, 2021). In Table 4.2, the equivalent crystallinity was indicated. No peak was found in the synthesis of G1/ZSM-5 at 180^{0}C, which may be caused by excessive quartz. Strong peaks for G3/ZSM-5 and G10/ZSM-5 were observed at 180 ^{0}C, indicating the production of ZSM-5 with relative crystallinities of 77.5 and 65.6 percent, respectively. This result showed that the temperature at which ZSM-5 crystallized impacted its relative crystallinity.

Table 4.2: Temperature-dependent effects on the crystallinity of synthetic ZSM-5 zeolite

Samples at 180 ºC crystallization temperature	Critical peaks at 2 theta	Percentage crystallinity
G1/ZSM-5	8,218	Not available
G3/ZSM-5	13,984	65.6
G10/ZSM-5	14,522	77.5
Commercial ZSM-5	30,147	100

4.4.5 Effect of Crystallization time

Crystallization time plays a major role during the nucleation and crystallization process because it influences crystal growth. The XRD pattern findings in Fig. 4-13 demonstrate that the crystallinity of ZSM-5 was attained for the three independent samples at the 48-hour crystallisation time. This figure displays the MFI zeolite peaks, suggesting that ZSM-5 nucleation remained steady over the 48-hour crystallization time for all three samples. Zeolite nucleation occurred during the initial phase of hydrothermal treatment, followed by crystal growth (Iwakai et al., 2021). However, the peak three samples' intensities fluctuate during the crystallisation time, which may be related to the varying impurities of the samples. At the end of the 48-hour crystallization period, the percentages of proportionate crystallinity for G1/ZSM-5, G3/ZSM-5, and G10/ZSM-5 were 35.37 %, 74.36 %, and 88.24 %, respectively.

Table 4.3: Relative crystallinity of three distinct kaolin-based ZSM-5 samples crystallized after 48 hours.

Samples at 180ºC crystallization temperature	Critical peaks at 2 theta	Percentage crystallinity
G1/ZSM-5	8,218	35.37
G3/ZSM-5	13,984	74.36
G10/ZSM-5	14,522	88.24
Commercial ZSM-5	30,147	100

Furthermore, the SEM images showed that the nucleation rate has an impact on the structure of the ZSM-5 formation (Fig. 4.13). The growth of crystals was aided by the crystallization time as compared to the hydrothermal time. During the zeolite formation, the gel transforms into amorphous crystals with irregularly shaped structured as well as undissolved aluminosilicate due to the extra hydrothermal period. According to Kovo (2011) and Mohiuddin et al., (2017), the agglomeration of zeolite driven by crystallization time encourages the formation of nuclei and octahedral shape. The SEM photos of the samples that were synthesized at a comparable temperature of crystallization of 180°C demonstrate the development of crystals at a time of crystallization of 48 hours for the three distinct kaolin based zeolite.

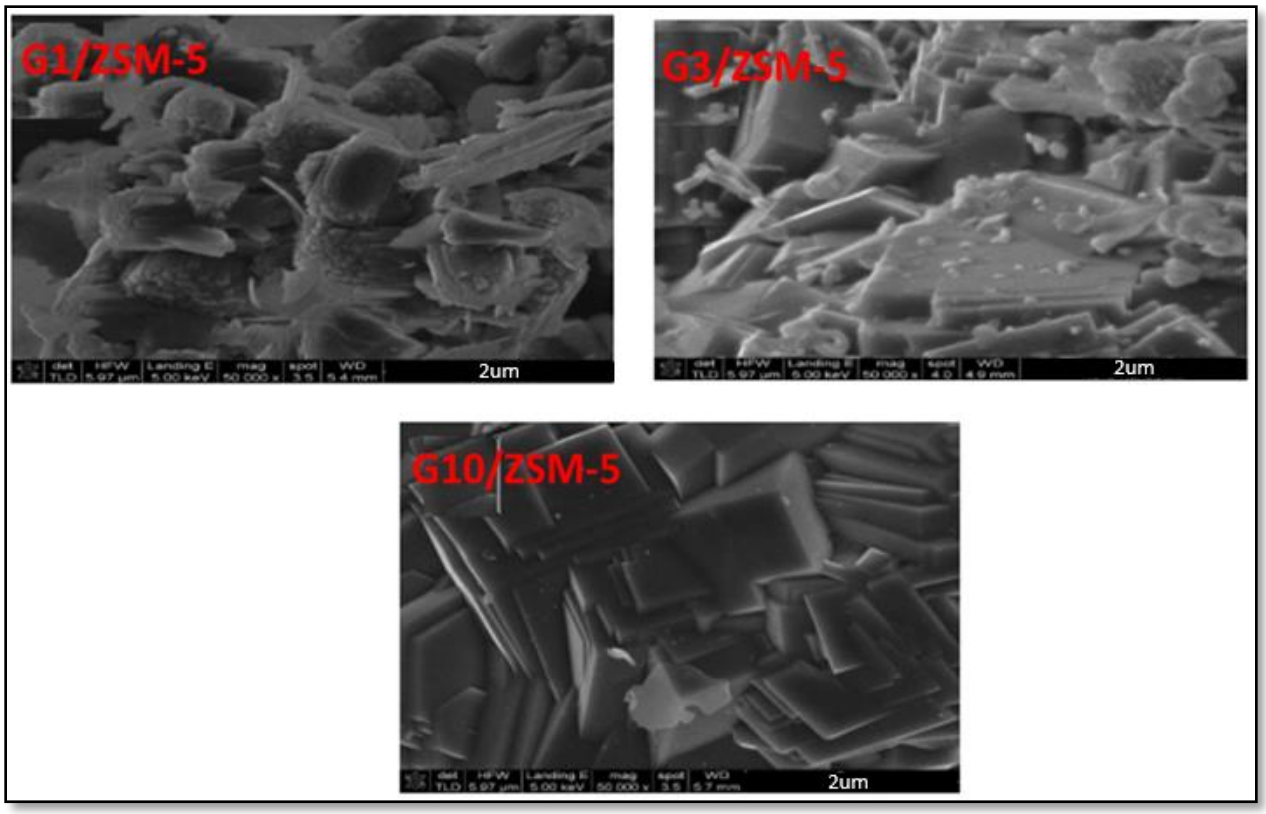

Figure 4.13: SEM photos of ZSM-5 zeolite crystallized after 48 hours of synthesis

4.4.6 FT-IR Analysis

The FT-IR spectra on the influence of crystallization temperature on the crystallinity of ZSM-5 zeolite were studied at a certain crystallization time and aging period. The result is shown in Figure 4.14 and Figure 4.15. The 436 and 457 cm^{-1} bands were allocated internal TiO_4 tetrahedral bending strains. The 545 and 550 cm^{-1} bands were allocated double ring frequency stretches. The bands at 798 and 800 cm^{-1} are linked to exterior symmetric stretching. In bands at 1058 and 1080 cm^{-1}, the external asymmetric stretching vibration is applied (Si-O-T linkage). The band at 1224 cm^{-1} has an accompanying asymmetrical stretched vibration. Figure 4.14 indicates the existence of bands at 550 and 1224 cm^{-1}, with distinctive five-membered rings' visibility at wavenumber of 550 cm^{-1} as the temperature was increased to 180°C (Mohiuddin et al., 2017).

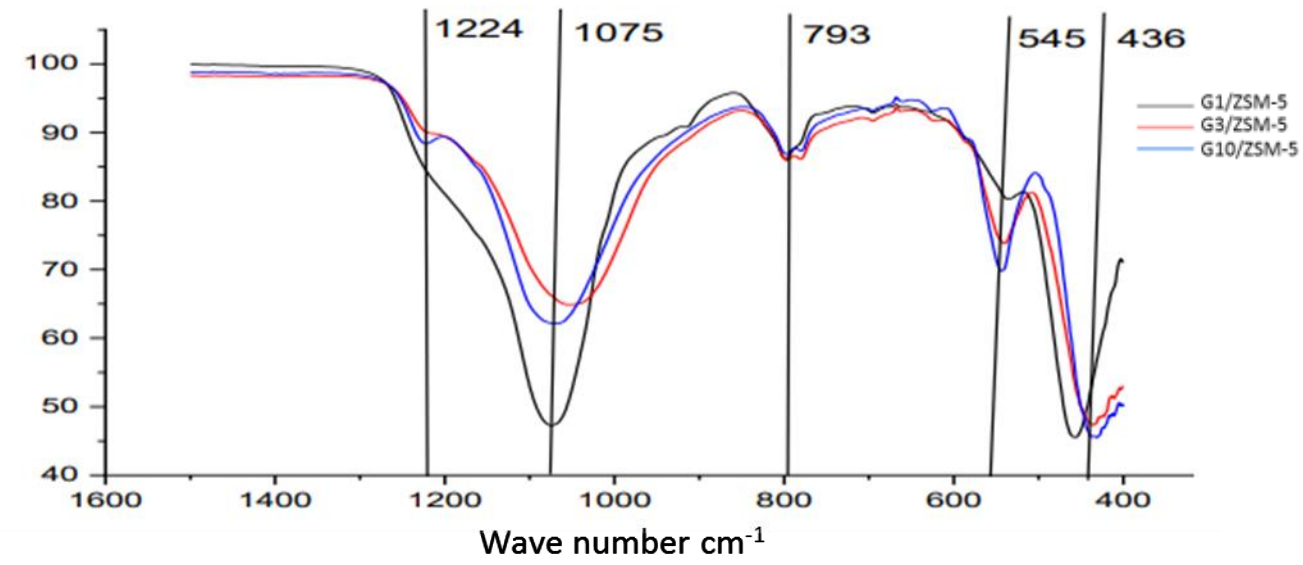

Figure 4.14: FT-IR spectra for ZSM-5 zeolite

Figure 4.15 showed the existence of crystal peaks at the 1224 band which is a distinctive feature of ZSM-5 zeolite formation. Physiological study of the FT-IR bands revealed that the amorphous band of the G1/ZSM-5 zeolite lacks peaks at 1224 cm^{-1}. Contrarily, the G3/ZSM-5 and G10/ZSM-5 zeolites crystalline more rapidly as the temperature increased and by the existence of the 1224 cm^{-1} stretches vibration band, introduced by extrinsic TiO_4 tetragonal interaction. This is a distinctly characteristic of the IR electronic band structure of ZSM-5 zeolite and the result concurs with similar investigation carried out previous researcher (Dey et al., 2021).

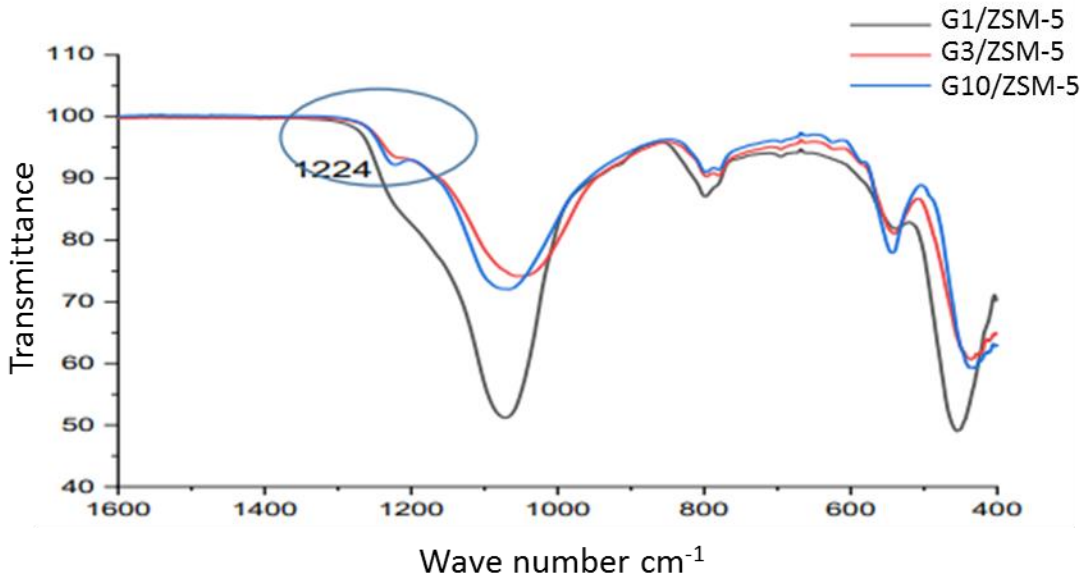

Figure 4.15: FT-IR Spectra for the three kaolin-based ZSM-5 Crystallinity

Table 4.4 lists the micropore volume, BET surface area, and micropore size of the three samples produced from South African kaolin at temperatures and times of 180°C and 48 h, respectively. The specific surface area (SSA) increases as the crystallization duration increases for all the samples that crystallized at 180 °C. At these crystallization conditions, G10/ZSM-5 exhibited a high SSA of 379.5 m^2/g and a pore volume of 0.05 m^3, indicating a well-developed zeolite structure. This pattern was also observed in other samples that crystallized at 180 °C, including G3/ZSM-5 and G1/ZSM-5. G1/ZSM-5 has a total pore volume of 0.04 m^3/g and an SSA of 349.2 m^2/g. G3/ZSM-5 has a pore size of 150.3 m^2/g, which is larger than that of G1/ZSM-5 (120.5 m^2/g), but had a lower SSA of 366.5 m^2/g than G10/ZSM-5. The smaller pore size of G1/ZSM-5 is the result of its lower% relative XRD crystallinity. G10/ZSM-5 had a pore size of 169.4 m2/g, which accounted for the high SSA and pore volume, according to the pore size distribution estimated using the BJH method for the adsorption isotherm (Table 4.4). Additionally, Table 4.4 showed the silica/alumina ratios for G10/ZSM-5, G3/ZSM-5, and G1/ZSM-5 to be 3.2, 2.5, and 1.8, respectively.

Table 4.4: BET Surface Area analysis of the synthesized zeolite

	G1/ZSM-5	G3/ZSM-5	G10/ZSM-5
BET surface (m^2/g)	349.2	366.5	379.5
Pore size (m^2/g)	120.5	150.3	169.4
Pore volume (m^3)	0.04	0.04	0.05
Si/Al	1.8	2.5	3.2

4.5 Conclusion

The kaolin samples (G1, G3, and G10) were gathered from three various locations in the Eastern Cape region of South Africa. These materials were used directly, without beneficiation, to produce zeolites as a substitute source of alumina and silica. They were calcined at 700°C for two hours and 30 minutes to activate the source material. The resulting metakaolin was then employed in the synthesis. South African kaolin has been successfully used to produce ZSM-5 Zeolite. The crystallinity of ZSM-5, produced from South African provenance kaolin, was impacted by the crystallization temperature and crystallization time. For ZSM-5, 180°C was the ideal hydrothermal temperature, and 48 hours were needed for crystallization. Three distinct kaolin-based zeolites G1/ZSM-5, G3/ZSM-5, and G10/ZSM-5 with BET surface areas of 349.2 m^2/g, 366.5 m^2/g, and 379.5 m^2/g respectively were successfully synthesized. To determine the peaks and shape of the generated zeolites, XRD and SEM analyses were also carried out.

CHAPTER 5: INFLUENCE OF PYROLYSIS CONDITIONS ON OIL YIELD USING COMMERCIAL AND LOCALLY SYNTHESIZED ZEOLITE CATALYST (ZSM-5) MADE FROM DIFFERENT KAOLIN MATERIALS

5.1 Introduction

Pyrolysis is the thermal breakdown of organic material into smaller molecules at high temperatures between 500 °C and 900 °C (Miandad et al., 2019). This reaction is carried out in the absence of oxygen, and consequently, the products are hydrocarbons in the form of gas (mainly syngas), oil, and char (Xiang et al., 2018; Sekar et al., 2022). The oil produced from the process is the most valued of all three products. Hence many research studies have focused on the pyrolysis conditions that result in the maximum yield of this product (Miskolczi, Bartha & Deák, 2006; Zhang et al., 2015; Miandad et al., 2019; Mariappan, Panithasan & Venkatesan, 2021; Sekar et al., 2022).

Pyrolysis of plastic is accomplished through free-radical attacks on long-chain polymers (Serrano et al., 2005). Because the free-radical reactions do not occur in specific locations on the polymeric chain, a heterogenous product is formed with a wide spectrum of molecular weight (Serrano et al., 2005; Bhattacharya et al., 2009; Sarker et al., 2020). Despite the lack of a specific product range from the pyrolysis reaction, the majority of the products formed are volatile hydrocarbons which are easily recovered through condensation (Marcilla, Beltrán & Navarro, 2008; Elordi et al., 2012). This broad spectrum of molecules requires further downstream processing to separate the large molecular-weight oils from the small molecular-weight molecules for pyrolysis products to be usable.

Apart from the lack of specificity of the pyrolysis reaction, another of its shortcomings is the unusually high energy required to break down the strong carbon-carbon bonds in the hydrocarbons. Research has shown that the presence of a catalyst in the pyrolysis reaction significantly lowers the activation energy required to initiate the free-radical reactions, thus resulting in significantly lower temperatures required to operate the process (Demirbaş, 2002; Pütün, 2010; Hu et al., 2019; Mohamed et al., 2019; Thahir et al., 2021). Since catalyst are generally selective, they also have the added advantage of narrowing down the product spectrum (López et al., 2011).

The other effect that catalyst have on the pyrolysis process is the reduction in the time required to produce the same amount of product range(Serrano et al., 2005; Serrano, Aguado & Escola, 2012; Miandad et al., 2019). In catalytic pyrolysis processes, longer contact times between catalyst and feedstock has been shown to cause catalyst deactivation due to contamination by products (particularly char) (Zhang et al., 2015; Yang et al., 2017; Sarker et al., 2020).

Zeolites have been shown to be the most excellent and selective catalysts for the production of oil from plastic pyrolysis (Demirbas, 2004; Miskolczi, Bartha & Deák, 2006; Marcilla, Beltrán & Navarro, 2008). There are different types of zeolites, from natural zeolites to synthesized zeolites (Miskolczi, Bartha & Deák, 2006; Pütün, 2010; Serrano, Aguado & Escola, 2012; Janssen et al., 2013). Of all the different types of zeolite catalysts tested on plastic pyrolysis, ZSM-5 proved to be the most suitable catalyst in terms of performance (Sharuddin et al., 2016; Ratnasari, Nahil & Williams, 2017; Mangesh et al., 2020). It is a microporous aluminosilicate crystal with different ratios or proportions of alumina to silica (Miandad, Barakat, et al., 2016; Qian et al., 2021).

Zeolite derived from kaolin is regarded as a low-cost, abundant and a cheap catalytic material (Lijalem Ayele Regassa, 2016). The majority of the research has been done on commercial kaolin, which are primarily employed in the production of zeolite A. The current investigation focused on the application of synthesized ZSM-5 zeolite from kaolin sourced from Grahamstown, South Africa, due to the huge deposit of kaolin available in the location and the tremendous enriching Si/Al concentration in this source material. Also, due to the limited number of reports on the synthesis of ZSM-5 from kaolin in this geological location and its use as a catalyst in the processes of pyrolyzing waste plastics, this research was necessary to fill this gap in the literature. Polyethylene, polypropylene, polyethylene terephthalate, and polystyrene were chosen as feedstock because they are the most prevalent polymers found in municipal solid waste streams.

This study aimed to evaluate the performance of ZSM-5 catalyst produced from South African kaolin in the pyrolysis of plastic wastes (PE, PP, PS, and PET) as a single and mixed feed, while evaluating the effect of catalyst ratio, reaction time and reaction temperature on the maximum pyrolysis product yields in comparison to the commercial ZSM-5 zeolite. One-factor-at-a-time experiments were conducted where two variables were held constant as one was varied over a predetermined range.

5.2 Materials and methods

5.2.1 Sample preparation and characterization

Feed material for pyrolysis was obtained from DUT cafeteria. These materials include plastic types in the categories of PE, PP, PS and PET (see Figure 5.1). These plastics were chosen because they constitute the leading source of plastic garbage in South Africa. In order to achieve uniformity, the materials were sorted, rinsed, and then shredded into tiny pieces prior to the commencement of the experiment. The feedstock used for this experimental work were done individually and then in a mixture of varying proportion as shown in Table 5.1 below. The proportions were based on data obtained from a brief review of the literature.

Figure 5.1: Images of different feedstocks used for the experimental study

ZSM-5 catalyst used in this work was made from kaolin sourced from G&W minerals resources, located in the Eastern Cape region of South Africa. This served as the alumina source (66.10% SiO_2 and 20.51 % Al_2O_3 respectively). Sodium silicate (26.5% SiO_2 and 10.6% Al_2O_3 composition) solution and Tetra propylammonium Bromide (TPABr) procured from Sigma Aldrich, Johannesburg, South Africa were used as additional silica source and structural directing agent, respectively. Nitric acid 55% which was obtained from Ace enterprises chemical association, Johannesburg, South Africa was used to adjust the pH. Commercial ZSM-5 zeolite powder (SiO_2/Al_2O_3 mole ratio: 50:1, CBV5524G) was obtained from Zeolyst International, Pennsylvania, USA as referencing material.

Table 5.1: Experimental feedstock and the operating parameters

Plastic types	Temperature (ºC)	Reaction time (mins)	Catalyst ratio (wt %)
PE (100%)	350 - 550	60 - 150	1:5 – 1:20
PS (100%)	350 - 550	60 - 150	1:5 – 1:20
PP (100%)	350 - 550	60 - 150	1:5 – 1:20
PET (100%)	350 - 550	60 - 150	1:5 – 1:20
PE/PS (50/50)	450	90	1:10
PP/PS (50/50)	450	90	1:10
PP/PE (50/50)	450	90	1:10
PE/PS/PP (40/30/30)	450	90	1:10
PE/PS/PP/PET (40/20/20/20)	450	90	1:10

5.3 Pyrolysis Experimentation

The municipal plastic waste (PE, PS, PP, and PET) were used as feedstock for the catalytic pyrolysis experiment. The synthesized ZSM-5 zeolite from G10/sample kaolin was used as the catalyst having shown a better morphology, and good surface area with little or no impurity among the three synthesized zeolites reported in the previous chapter. A stainless-steel reactor with the following specifications (length = 450 mm, inner diameter = 100 mm and outer diameter = 150 mm) heated in an electric furnace with the temperature measured by K type thermocouple placed in the reactor was used to carry out the pyrolysis experiment. Figure 5.2 is the schematic diagram of the pyrolysis experiment and procedure by Ajibola *et al.* (2018) was adopted for the catalytic pyrolysis experiments. The reactor was in vertical configuration and quartz wool was used as a support. Prior to the pyrolysis experiment, the feedstock was shredded into smaller pieces to increase the combustion rate. 500g of each sample was used, with varying catalyst to feedstock ratio ranging from 1:10 to 1:20. The whole reactor system was first purged with N_2 for 30 min at 30 mL/min flow rate to get rid of residual air in the system and ensure inert atmosphere. The experiments were performed as follows: At the beginning, the reactor was heated at 10 ^oC/min until the temperature reaches the set temperature between 350 and 550 °C and at different temperature range 60 - 150 mins. Thereafter, the sweeping gas was allowed to continue to flow until the vapour in the reactor condensed and kept at 0 ^oC. The char was left in the reactor while condensed liquid product was collected into the storage tank. After allowing reactor to cool to room temperature, the solid residue was recovered from the reactor. The generated liquid oil was characterized in order to ascertain how the content of the feedstock affected the standard of the liquid oil created in the presence of the catalysts. The gas chromatography-mass spectrometry (GC–MS) was used in analyzing the produced liquid oil. The formula used in calculating the produced liquid oil, gas, and char is shown below (Patil *et al*., 2017). All the pyrolysis experiments were repeated twice and the mean values reported.

Char (weight%) = (Amount of Char produced / Amount of feedstock) * 100 (**5-1**)

Liquid oil (weight%) = (liquid yield / Amount of feedstock) * 100 (**5-2**)

Gas (weight%) = 100 - (Char (weight%) + Liquid oil (weight%)) (**5-3)**

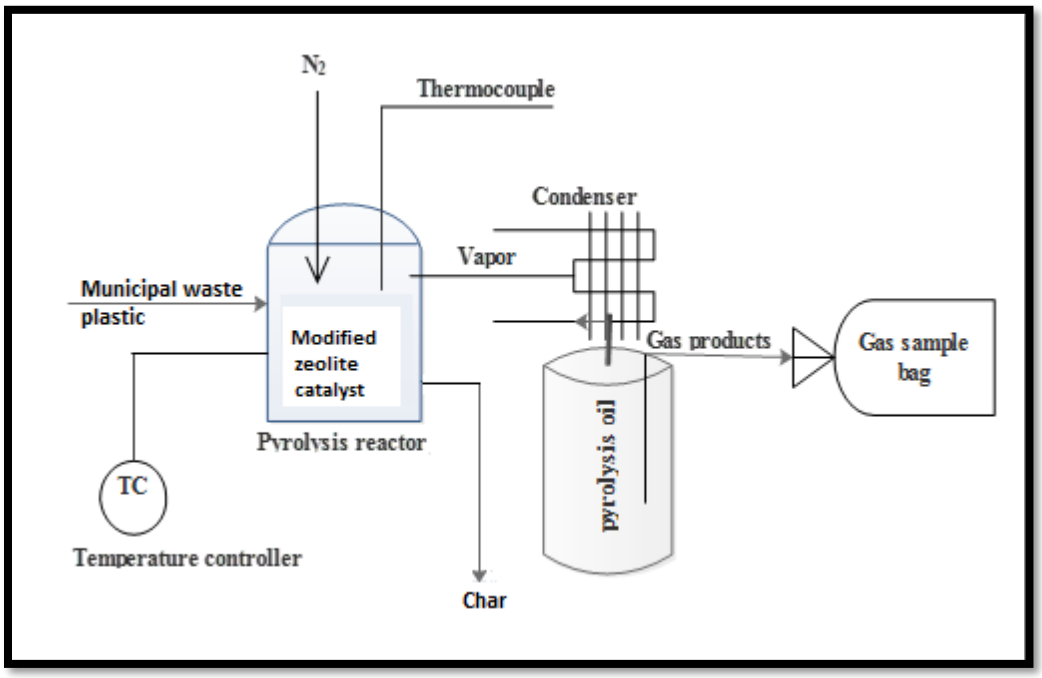

Figure 5.2: Schematic of pyrolysis experimental set up

5.4 Analytical techniques

Thermogravimetric analysis (TGA) was employed to examine the patterns of thermal breakdown in all plastic materials. 10 microng of plastic materials were heated for the TGA analysis at a rate of 10 °C/min from 20 to 800 °C while nitrogen flowed continuously at a rate of 45 ml/min. The pyrolysis liquid oils were then further characterized using a variety of analytical tools, such as Fourier transform infrared spectroscopy (FT-IR), gas chromatography coupled with mass spectrometry (GC-MS), for chemical composition, discovery hybrid rheometer for viscosities, density meter (DMA 35) for densities, AWD-12 pour point tester for pour and freezing points, automatic pensky-martens closed tester

for flash point, and bomb calori meter for HHV by following the standard ASTM methods (APHA, 1998).

Fourier transform infrared spectroscopy (FTIR, Bruker Vertex 70 spectrometer), was used to examined the chemical composition and functional groups in the feedstock and liquid oils from all types of plastic. A minimum of 30 scans were carried out between 500 and 4000 cm^{-1} at an average IR signal with a resolution of 4 cm^{-1}.

The gas chromatography-mass spectrometer (Agilent 7890-5975C) was used to determine the chemical constituents of the produced pyrolytic oils under the following measurement conditions: DB-1701 column; Helium as carrier gas at flow rate of 1.76 mL/min; 1 µL injection size; and 1:60 split ratio. Starting GC oven temperature was kept at 42 °C for 1 min; then the temperature was increased to 300 ^{o}C at a rate of 5.5 ^{o}C/min and held for 10 min; Scan mode (35.00 to 550.00 m/z); injector and detector temperature of 220 ^{o}C and 250 ^{o}C respectively. The compounds were identified using the National Institute of Standards and Technology (NIST) mass spectral data library. Furthermore, the elemental composition of the liquid-oils produced was determined using an elemental analyzer (Vario EL-II Elementar Analysensysteme GmbH, Hanau, Germany) and liquid-oils higher heating value (HHV) were estimated using the earlier mentioned Boumanchar et al., (2019).

The properties of liquid oils derived from pyrolysis were characterized using processes based on established ASTM methodologies. The pour and freeze points were examined using the AWD-12 pour point tester. The temperature range was between -10 °C and -65 °C for one tank (left side tank) (right side tank). The sampling tube was completely filled with samples. The sampling tube was placed in the left-side tank first until the temperature dropped to 0 °C, and then it was moved to the right-side tank. After each 2 °C drop in temperature, the sample tube was periodically removed from the tank to be held horizontally for 4 s to examine the flow. This process was carried out repeatedly until the pour point and freezing point were reached.

The densities of the liquid oils from the pyrolysis process were measured using a portable density meter (DMA 35 from Anton Paar). Prior to performing the subsequent measurements, the density instrument was calibrated with distilled water, cleaned with acetone, and allowed to dry between samples.

By employing a discovery hybrid rheometer (HR1 from TA instruments) with a 40 mm parallel plate geometry, the dynamic viscosities of the liquid oils were quantified. The bottom horizontal plate received a tiny amount of the liquid oil sample. The sample was sandwiched between the two plates after the upper 40 mm plate was lowered gradually. The rheometer's temperature and shear rate ranges were set at 40 °C and 1 to 500 1/s, respectively. Prior to taking actual measurements of liquid viscosity, the rheometer was calibrated using a viscosity standard liquid. Based on the ASTM D 93 technique, the automatic Pensky-Martens closed tester from Koehler in the US determined the liquid oil's flash point. The energy content of the liquid oils used in pyrolysis was calculated using a bomb calorimeter (Parr 6200 Calorimeter, US) using the ASTM D 240 standard. The liquid oil analysis was performed three times, and averaged values and ranges were utilized to make it easier to compare the results to the information in the literature and the characteristics of conventional diesel.

5.5 Thermogravimetric Analysis (TGA)

Thermogravimetric analysis (TGA) of the plastic samples were performed on a Shimazu 50A TGA instrument (see chapter three) to determine the thermal degradation characteristics of the plastics and optimum conditions via plastic weight loss of the sample.

TGA analysis in Figure 5.3 shows that polyethylene (PE) demonstrated a two-stage decomposition process, with the first stage beginning at around 400 °C and reaches over 15% degeneration when the temperature increased to 420°C. The second thermal decomposition of polyethylene began at a temperature of approximately 440°C, reaching 50% degradation at 450°C and reaching maximal degradation (95%) at approximately

465°C. (Fig. 5.3). Wu et al. (2014) claim that even under controlled circumstances, PE raw material requires a higher temperature to breakdown than polystyrene feedstocks. PE is made of a long chain and degrades thermally through a random chain scission mechanism, which calls for a greater temperature (Lee et al., 2012). With a single phase of decomposition, the thermal degradation of the polypropylene (PP) material began at a lower temperature as compared to PE of about 400 °C. It reached its peak depolymerization (95%) at a temperature of about 450 °C. The PP half-carbon chain contains secondary carbons that enhance the carbocation reaction undergoing thermal decomposition, which might cause it to degrade at a lower temperature (Jung et al. 2010). The practical implications are that PP is easier to pyrolyze and require lower temperature to achieve complete conversion to products.

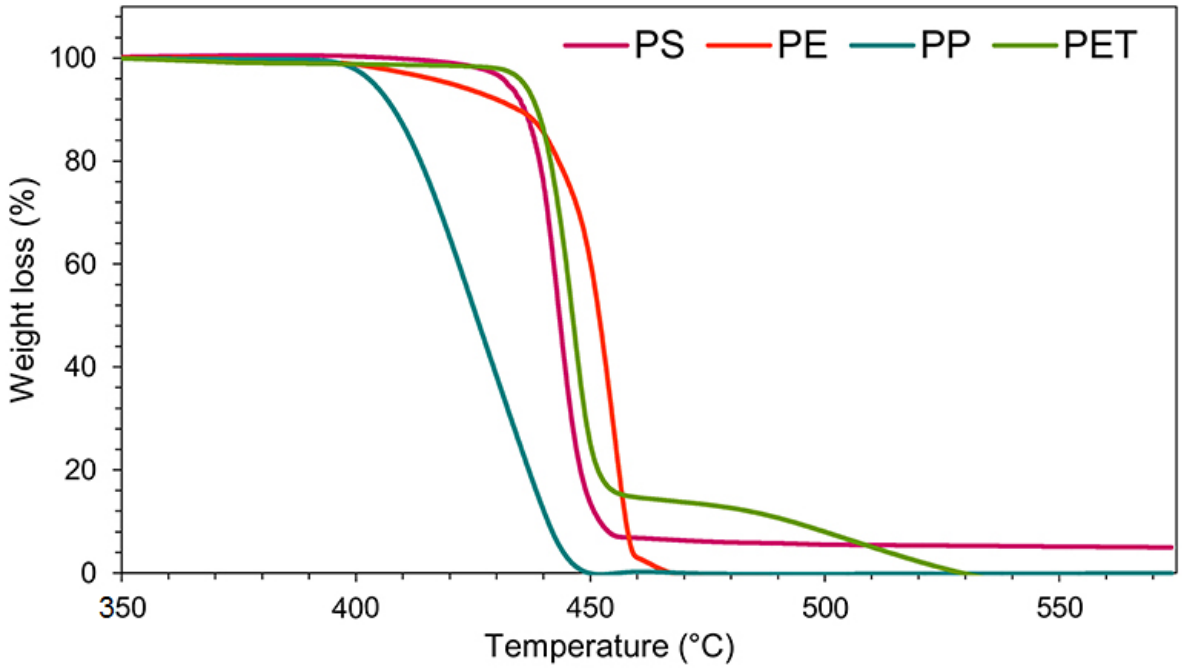

Figure 5.3: TGA of the plastics used in catalytic pyrolysis to obtain liquid oil

The degradation of PET occurred in two stages, with the first stage being a rapid degradation starting at around 430 °C and ending around 460 °C. After this temperature, the weight loss slows down as temperature increases, eventually reaching 0% at 530 °C.

Polystyrene (PS) is the only material that did not achieve 0% weight loss, with about 8% of the initial material remaining. This shows that PS will have a significant amount of char remaining after pyrolysis. PS decomposition is facilitated by both end-chain and random chain scission processes, which improve its degradability (Lee et al., 2012). Overall, the compositions of different plastic feedstocks and the ensuing mechanisms of degradation are what cause distinct TGA trends. The TGA analysis of all the feedstocks revealed that the highest decomposition occurred between 400 °C and 470 °C (Fig. 5.3). According to Lopez et al. (2011), the addition of a catalyst may result in reduction of the operating parameters (reaction time and temperature).

The behavior towards the degradation of individual plastic waste as well as for their blend is shown in Figure 5.4 – Figure 5.7. At a heating rate of 40 °C/min, PS had the fastest reaction rate, followed by PE, PET and lastly, PP. Even though PE had a higher reaction rate compared to PET and PP, the reaction temperature was significantly higher at around 525 °C, in comparison to <500 °C for PET and PP. Mixing different plastics in different proportions reduced the reaction rate while increasing the pyrolysis temperature. The maximum reaction rate for the mixed waste is close to that of PE because it contained a higher percentage of this material.

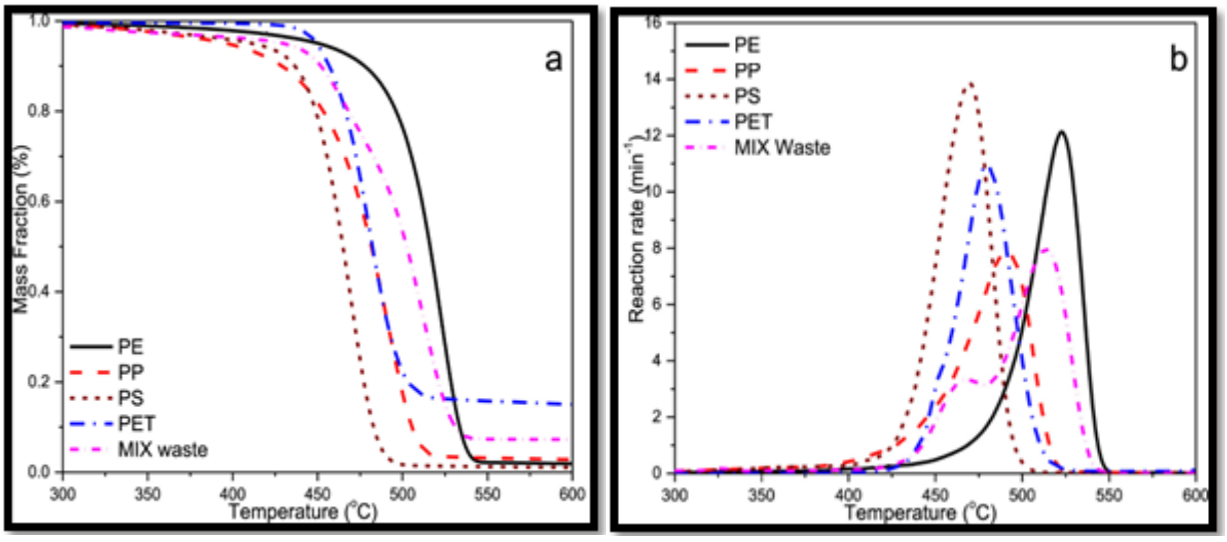

Figure 5.4: Pyrolysis of individual and mixed plastic waste at a heating rate of 40°C/min: a) Mass loss vs. temperature curve; b) Reaction rate vs. temperature curve

Figure 5.5 shows that mixing PE and PP increased the reaction rate while slightly decreasing the temperature at which the maximum rate of reaction is obtained. When compared to the calculated reaction rate, the experimental reaction rate shows that there is interaction between the two plastics that results in a higher reaction rate than expected. The calculated rate is obtained from the summation of the individual weight degradation components (Heikkinen et al., 2004).

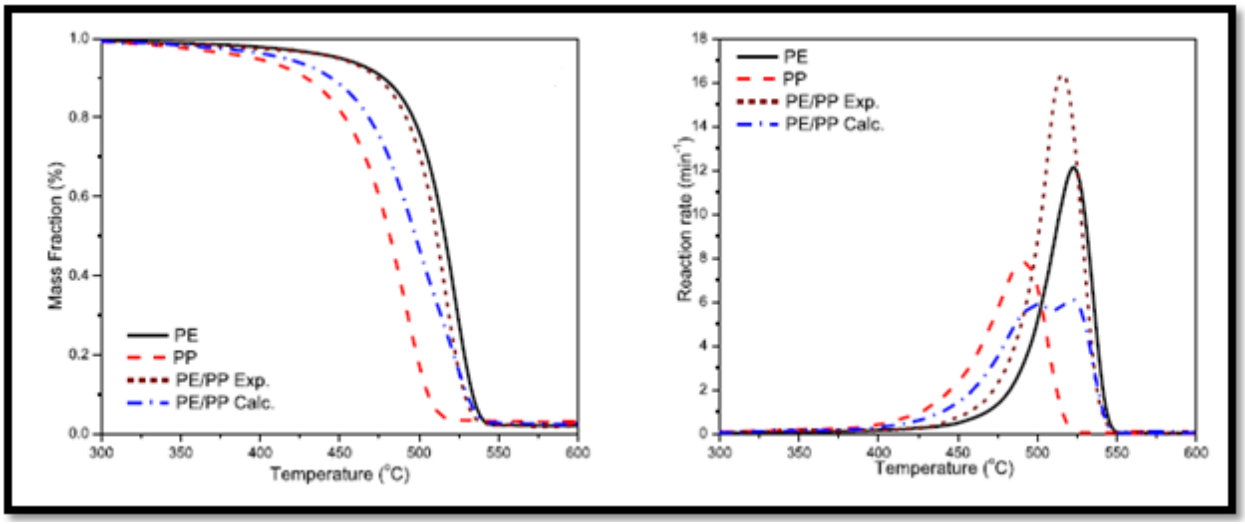

Figure 5.5: Mass loss and reaction rate curve at the heating rate of 40 °C/min. for PE, PP and PE/PP

Mixing PE and PS shows less interaction as opposed to that observed for the pair PE and PP (Figure 5.6). for the PE/PS pair, the experimental reaction rate is significantly lower than that of the individual plastics. This means that PS is interacting negatively with PE, resulting in a low reaction rate. However, the reaction rate profile for the mixed pair closely follows the predicted reaction rate profile.

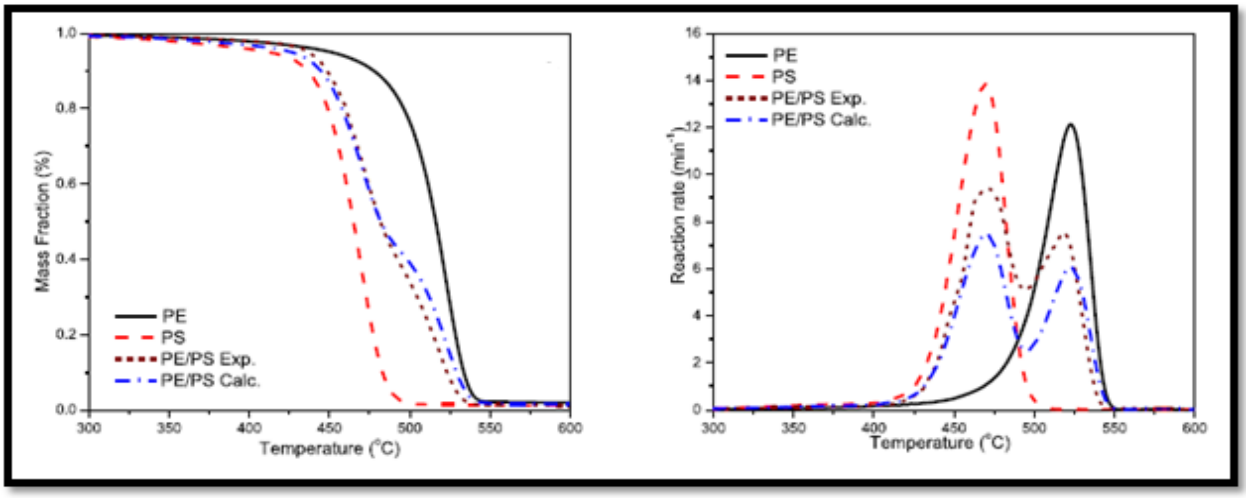

Figure 5.6: Mass loss and reaction rate curve at the heating rate of 40 °C/min for PE, PS and PE/PS.

Figure 5.7 shows PE and PET mix. It was observed that there was an initial delay in PET degradation, whereas PE degradation was accelerated. The delayed degradation of PET was caused by PE due to scission of alkyl oxygen bond via random chain scission. Under thermal degradation, PET does not fully volatilize and it produces a large amount of coke/char as residue (Singh *et al*., 2019). To further investigate the significance of the operating parameter range obtained from the TGA analysis, a catalytic pyrolysis experiments were conducted.

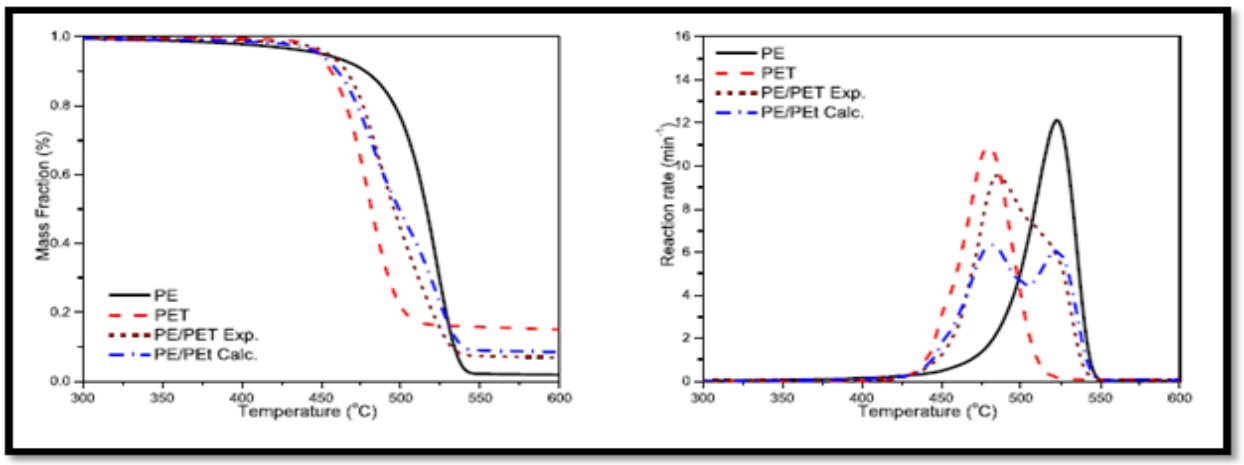

Figure 5.7: Mass loss and reaction rate curve at the heating rate of 40 °C/min for PE, PET and PE/PET.

5.6 Results and discussions

5.6.1 Effect of pyrolysis temperature

Two catalysts, G-10/ZSM-5 and G-3/ZSM-5 were used to determine the oil yield at variable temperatures ranging from 350 – 550 °C. for these tests, pyrolysis time was maintained at 60 minutes and the catalyst ratio was 1:10. The G-1/ZSM-5 catalyst was not used for pyrolysis experiments because of low crystallinity that was caused by the presence of a significant amount of quartz.

For the G-10/ZSM catalyst, Fig 5.8 shows that 450 °C resulted is the highest liquid oil for PE, PP and PS while the highest yield for PET was obtained at 400 °C. Oil yields increased as temperature increased from 350 °C and reached a maximum at 450 °C before decreasing as temperature was further increased to 550 °C. However, the oil yield at 550 °C was still higher than that at 350 °C. Although, this oil yield was accompanied by a significant increase in gas yield and a decrease in char yield.

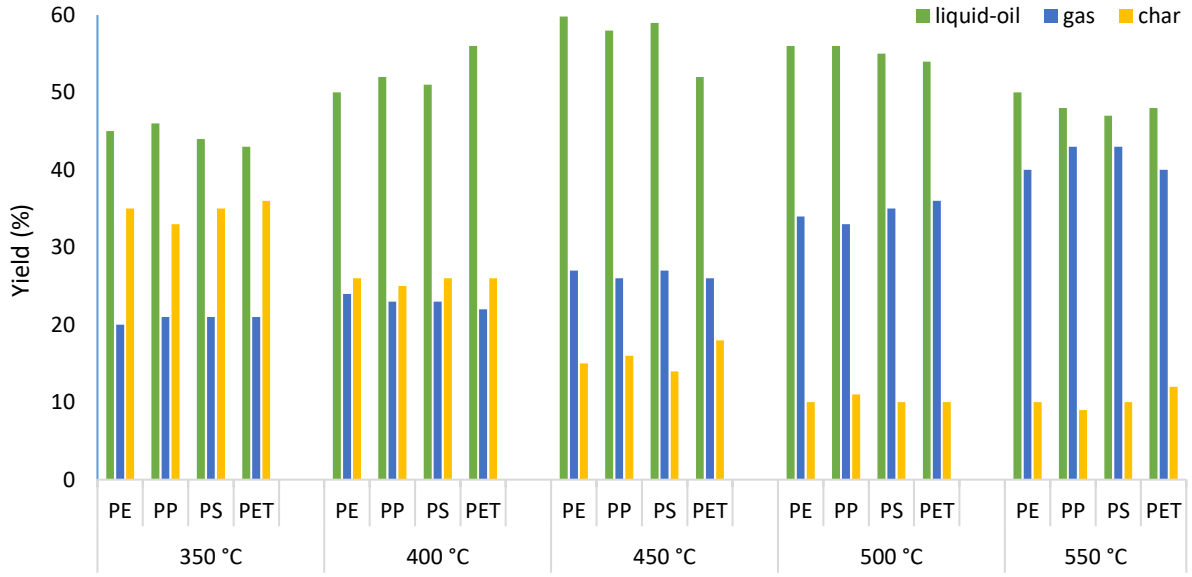

Figure 5.8: Effect of temperature on yield during pyrolysis of different plastics using G-10/ZSM-5 catalyst.

There was an observed decrease in the char yield as pyrolysis temperature increased. Coupled with an increase in gas yield, rising pyrolysis temperatures shows that coke formation becomes less dominant while further breakdown of molecules occurred. This is in contrast with the study by Ahmad *et al.* (2015), where they observed that coke formation started to dominate as temperature increased, resulting in a reduction in product conversion.

The effect of G-3/ZSM-5 (Figure 5.9) showed the same trend as G-10/ZSM-5 catalyst. Operating temperature of 450 °C resulted in the highest oil yield, while increasing temperature from 350 °C to 550 °C increased the gas yield and simultaneously a reduction in char obtained was observed. Paired comparisons between G-3/ZSM-5 and G-10/ZSM-5 show that the catalyst also have the same performance. For example, the oil yield using PE at 450 °C is 57.8% using G-3/ZSM-5 and 59.8% using G-10/ZSM-5. The small difference in performance between G-3/ZSM-5 and G-10/ZSM-5 could be attributed to the differences in relative crystallinity, with G-3/ZSM-5 having a crystallinity of 74.36%, and G-10/ZSM-5 with 88.24% relative to commercial ZSM. These results of G-3/ZSM-5 are in agreement with studies done by Sakata *et al.* (1999) and Fakhrhoseini *et al.* (2013), where high yields of liquid oil using PP were obtained at temperatures in the range 380 – 500 °C. This data shows that the optimum pyrolysis temperature is around 450 °C for PE, PP and PS. However, it is slightly lower for PET, at around 400 °C. The generally low yields for PET could be attributed to the low volatile matter content. Sharuddin *et al.* (2016) and Miandad *et al.* (2016) made a similar observation where PET had low oil yields compared to other types of plastic because of the low volatile matter content.

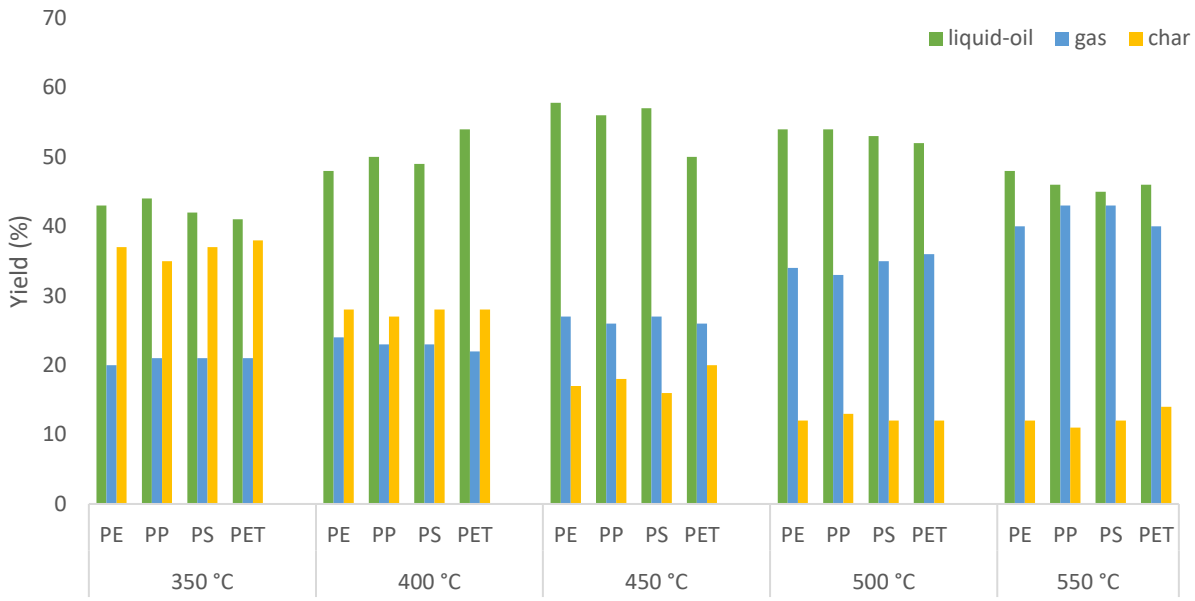

Figure 5.9: Effect of temperature on yield during pyrolysis of different plastics using G-3/ZSM-5 catalyst.

5.6.2 Effect of pyrolysis time

Oil yield ranged from 43% to 60% over a pyrolysis time ranging from 30 minutes to 150 minutes (Figure 5.10). Pyrolysis time showed a similar trend as pyrolysis temperature, with oil yields increasing to a maximum at pyrolysis time of 90 minutes. The yield dropped as pyrolysis time increased from 90 minutes to 150 minutes. This profile seen in Figure 5.10 suggests that 90 minutes of the optimum reaction time for efficient conversion of plastic to liquid oil. This is higher than the optimum pyrolysis time of 75 minutes obtained by Miandad, Nizami, *et al.* (2016) for the pyrolysis of PS at 400 °C. The difference, as Miandad, Nizami, *et al.* (2016) pointed out, could be attributed to reactor dimensions, heat transfer rates and configuration.

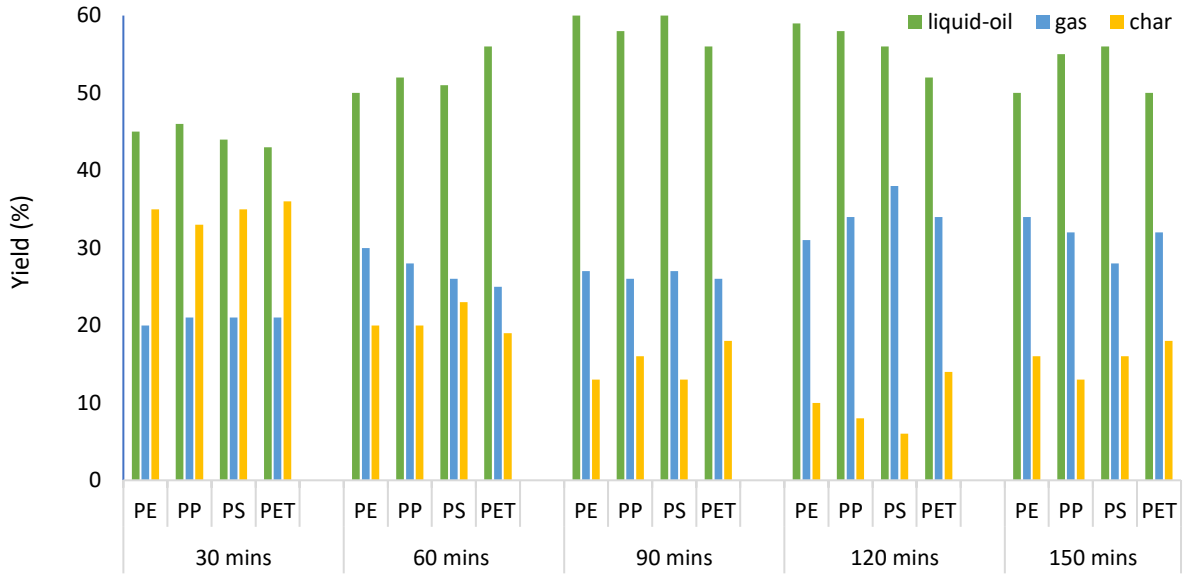

Figure 5.10: Effect of pyrolysis time on yield during pyrolysis of different plastics using G-10/ZSM-5 catalyst.

G-3/ZSM-5 catalyst performed poorly at low reaction time of 30 minutes (Figure 5.11), all plastics producing roughly equal amounts of liquid oil and char. This means that 30 minutes was not sufficient to convert both the feed material and the coke that is formed during the free-radical reactions into liquid oil or gas. Miandad, Nizami, et al. (2016) made a similar observation in their study where they evaluated the effect of pyrolysis time on oil yields.

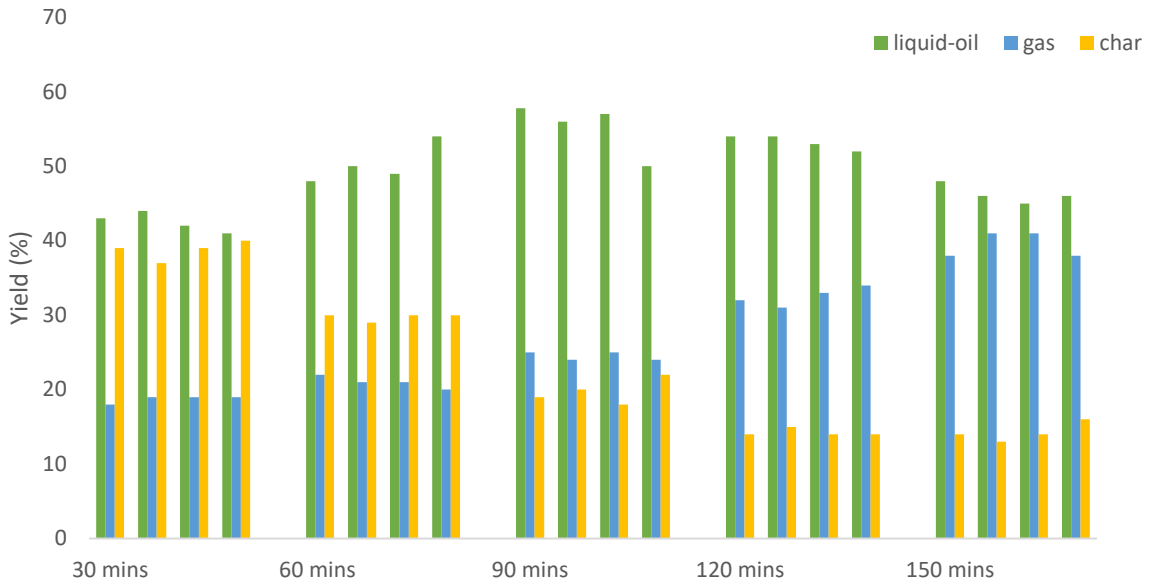

Figure 5.11: Effect of pyrolysis time on yield during pyrolysis of different plastics using G-3/ZSM-5 catalyst.

5.6.3 Effect of catalyst ratio

The ratio of catalyst is an essential variable as it determines the theoretical number of active sites for chemical reactions to take place on. Figure 5.12 shows that reducing catalyst ratio (increasing the amount of plastic to catalyst) resulted in a significant increase in gas yield, at the expense of oil yield. Oil yield increases to a maximum when the catalyst ratio was reduced from 1:1 to 1:5. The yield then significantly decreased when the catalyst ratio was decreased to 1:20. This is because a higher catalyst ratio compensates for catalyst deactivation caused by coke and char formed during pyrolysis (Sebestyén et al., 2017).

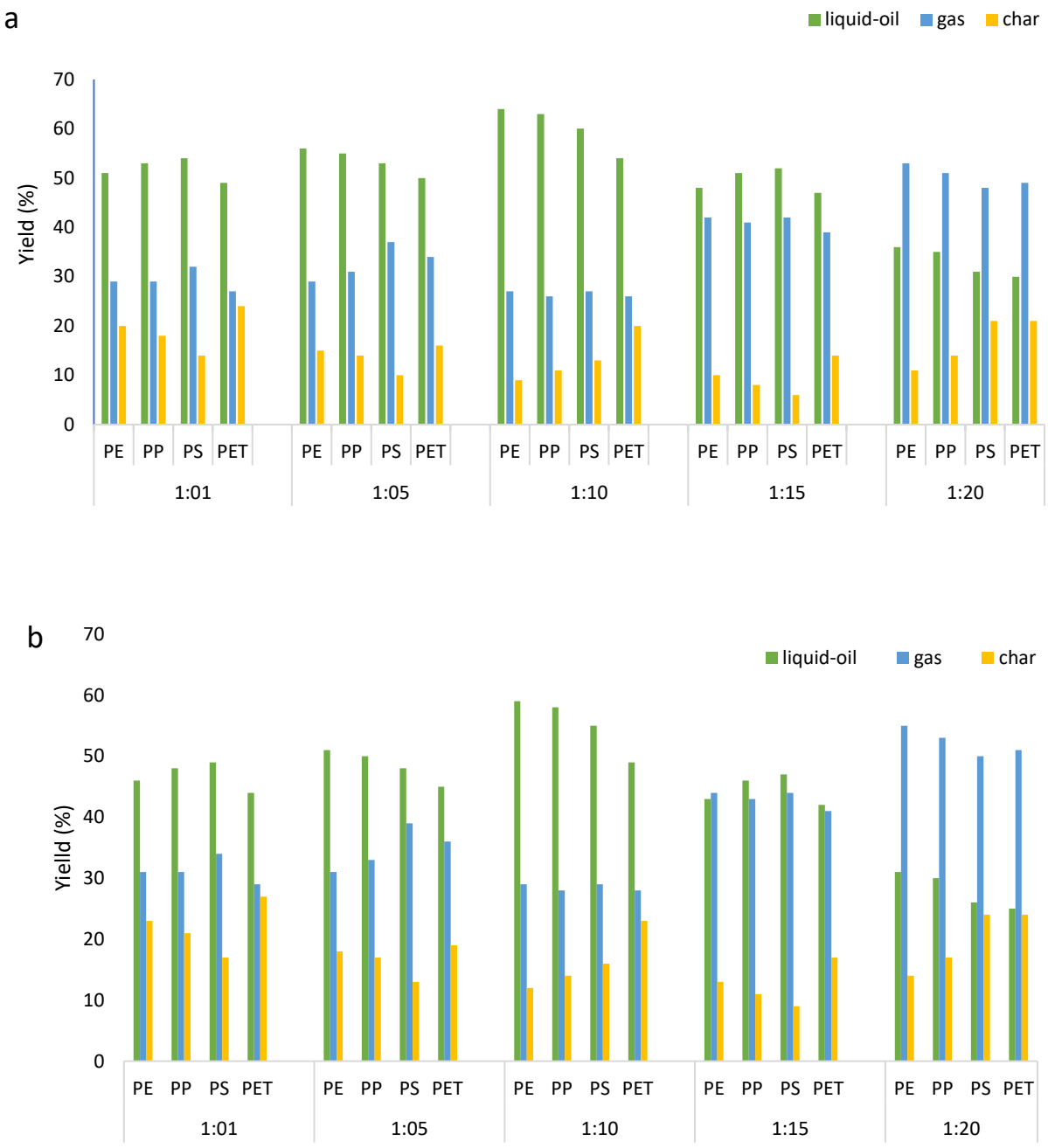

Figure 5.12: Effect of catalyst ratio on yield during pyrolysis of different plastics using a) G-10/ZSM-5 catalyst, and b) G-3/ZSM-5.

The optimum catalyst ratio was 1:10 for all types of plastic used in the pyrolysis reaction. Aisien *et al.* (2021) obtained a similar result where the highest yield of oil was obtained at a catalyst ratio of 1:10. However, this was contrary to what was observed by Panda (2018) and Hakeem *et al.* (2018), where a catalyst ratio of 1:3 was the optimum ratio for the pyrolysis of individual and mixed plastics.

5.6.4 Effect of synthesized ZSM-5 zeolite from South African kaolin and commercial ZSM-5 zeolite on the pyrolytic products yield

Commercial and synthesized zeolite catalysts were used to study the impact of catalysts on the products at 450 ^{o}C and 90 minutes, especially on the liquid oil (Fig. 5.13 – Fig. 5.17 and Table 5.2 – Table 5.5). Relative to all the other feedstocks examined, PS feedstock produced the most liquid oil (Fig. 5.13). When PS was pyrolyzed catalytically, commercial zeolite generated higher efficiency of liquid oil (56%) together with char (11.2%) and gases (32.8%) than synthesized zeolite, which generated 51 % liquid oil, 13.4 % char, and 35.6 % gas (Table 5.2).

Table 5.2: Product yields from PS plastic waste and liquid oil constitutes using commercial and synthesized ZSM-5 zeolite catalysts.

Feedstock	Catalyst used	Pyrolytic yield (%)			Liquid oil constitutes (%)
		Oil	Gas	Char	
Polystyrene (PS)	Commercial ZSM-5	56	32.8	11.2	Ethylbenzene (60.8) Benzene (3.8) Styrene (7.6) alpha-Methylstyrene (10.7) Indene (3.3) Azulene (4.8)
	Synthesized ZSM-5	51	35.6	13.4	Ethylbenzene (10) Styrene (15.8) Benzene (16.3) Propenylbenzene (4.2) Propylbenzene (3.5) Isopropylbenzene (8) alpha-Methylstyrene (38.3)

This can be attributed to the commercial zeolite's low BET surface area, acidity, and microporous structure. This result agrees with the experiment conducted by Lee et al. (2001). Mesoporous synthetic catalysts with high BET surface and acidity generated decreased liquid oil production, according to Seo et al. (2003). Rehan et al. (2017) performed both thermal and catalytic pyrolysis on PS and reported that thermal pyrolysis produced 80% liquid oil yield, followed by catalytic pyrolysis of 54% using commercial zeolite and synthetic zeolite of 50% catalysts.

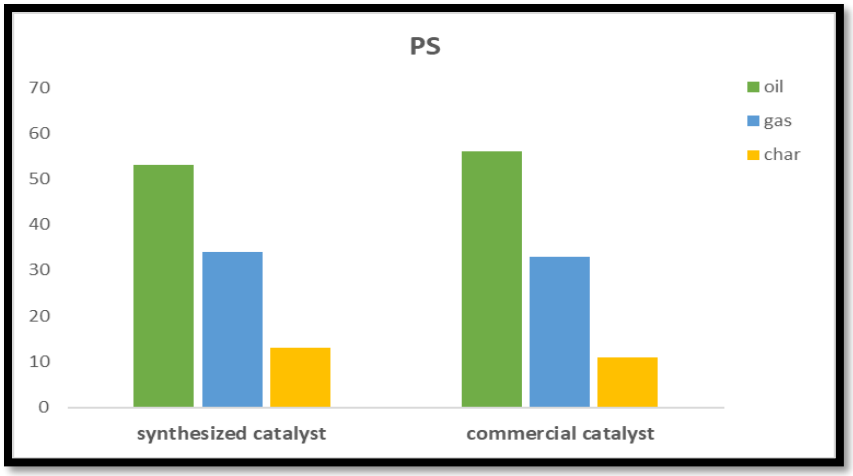

Figure 5.13: Effect of synthesized and commercial ZSM-5 zeolite on PS plastic waste

Using commercial and synthesized zeolite catalysts for PP experiment, the liquid oil generated were 38 % and 44.7 % respectively, while the gas yields were 50.3 % and 47.2 % respectively. (Fig. 5.14). Additionally, Obal et al. (2012) demonstrated that the catalytic pyrolysis of PP using alumina-loaded mesoporous catalysts resulted in the highest gas output. Kim et al. (2002) provided an explanation of how zeolite with low BET surface area, microporous structure, and low acidity facilitate the early breakdown of PP that may boost the generation of gases, as seen in this work (Table 5.3).

Table 5.3: Product yields from PP plastic waste and liquid oil constitutes using commercial and synthesized ZSM-5 zeolite catalysts.

Feedstock	**Catalyst used**	**Pyrolytic yield (%)**			**Liquid oil constitutes (%)**
		Oil	Gas	Char	
Polypropylene (PP)	Commercial ZSM-5	38	50.3	11.7	Ethylbenzene (7.1) o-Xylene (8.8) alpha-Methylstyrene (3.9)

					Benzene, 1-propenyl (7.1) 1H-Indene (6.2) Benzene, 1,3-diethenyl (9) Benzene 1-methyl-2-cyclopropen (4) Naphthalene, 1-methyl (6.2)
	Synthesized ZSM-5	44.7	47.2	8.1	Azulene (7.6) Benzoic acid, 2,6-bis[(trimethylsilyl)oxy] (3.6) Phenanthrene (4.4) Cyclononasiloxane, octadecamethyl-(22.8) Cyclooctasiloxane, hexadecamethyl-(4.1) Phenol, 2,2′-methylenebis[6-(1,1-dimethylethyl)-4-methyl-(3.8) 1,2-Benzenedicarboxylic acid, mono(2-ethylhexyl) ester (19.7) Tetracosamethyl-cyclododecasiloxane (28.9)

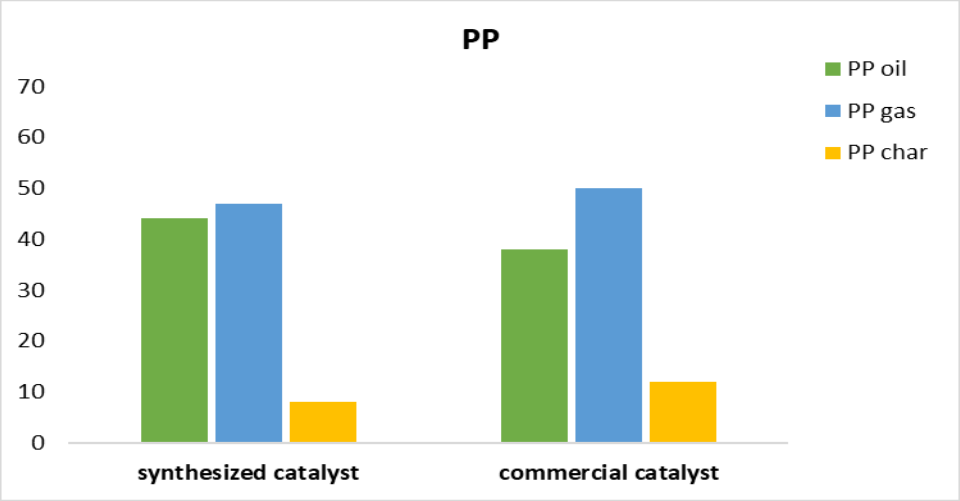

Figure 5.14: Effect of synthesized and commercial ZSM-5 zeolite on PP plastic wastes

The liquid oil production of 56 % and 48 % from the catalytic pyrolysis of polyethylene (PE) using both commercial and synthesized zeolite respectively was recorded. Commercial zeolite produced a high yield of char (19%) during catalytic pyrolysis but a lower yield of gas (25 %), whereas synthetic zeolite produced a higher yield of gases (38 %) and a lower yield of char (14 %). (Fig. 5.15 and Table 5.4).

Table 5.4: Product yields from PE plastic waste and liquid oil constitutes using commercial and synthesized ZSM-5 zeolite catalysts.

Feedstock	**Catalyst used**	**Pyrolytic yield (%)**			**Liquid oil constitutes (%)**
		Oil	Gas	Char	
Polyethylene (PE)	Commercial ZSM-5	56	25	19	Ethylbenezene (4.2) Styrene (10.2) Napthalene (3.4)
	Synthesized ZSM-5	48	38	14	Toluene (15.3) Ethylbenzene (10.4)

					1,3,5,7-Cyclooctatetraene (46.5) Benzene, (1-methylethenyl) -(6.8) Azulene (5.2) Naphthalene, 1-methyl-(3.3)

When compared to commercial zeolite catalyst, G10/ZSM-5 zeolite has a larger BET surface area and acidity, which may contribute to its higher catalytic efficiency and higher gas output (Miandad et al., 2017a). These findings concur with those made by Batool et al. (2016), who likewise found the highest gas output from the catalytic pyrolysis of PE using a synthetic catalyst (ZSM-5). 97% of the gases produced by PE catalytic pyrolysis using a very acidic synthetic zeolite catalyst were reported by Zeaiter (2014). High acidity and BET surface area in mesoporous catalysts support larger gas yields, whereas low acidity and BET surface area in microporous catalysts favor higher liquid oil and char yields (Lopez et al., 2011).

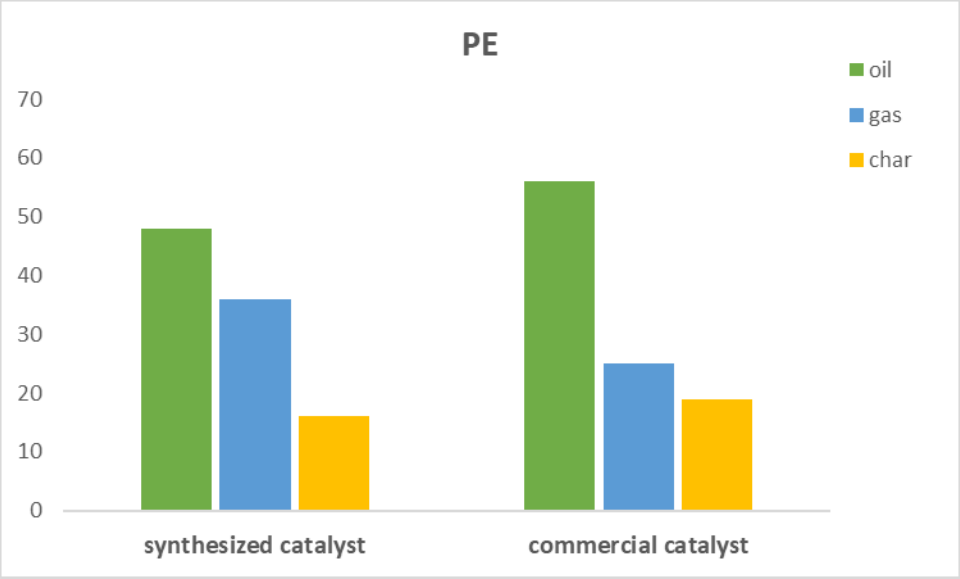

Figure 5.15: Effect of synthesized and commercial ZSM-5 zeolite on PE plastic wastes

In Figure 5.16, it was revealed that mixing PS with other plastic wastes resulted in lower liquid oil yields compared to pure PS feedstock. The yields of liquid oil from all PP and PE mixes were also found to be less than those from individual PE and PP materials (Fig. 5.16). Although pyrolysis of PE with other plastics was expected to have synergistic effects throughout the degradation process, according to Xue et al. (2017), and the synthesis and transfer of hydrogen from PE should accelerated the degradation process.

Table 5.5: Product yields from mixed plastic wastes (PE/PS, PP/PS and PP/PE) and liquid oil constitutes using commercial and synthesized ZSM-5 zeolite catalysts.

Feedstock	Catalyst used	Pyrolytic yield (%)			Liquid oil constitutes (%)
		Oil	Gas	Char	
Polystyrene (PS) + Polypropylene (PP)	Commercial ZSM-5	49	40.6	10.4	Ethylbenezene (4.2) Styrene (10.2) Napthalene (3.4)
	Synthesized ZSM-5	42	43.6	14.4	Toluene (15.3) Ethylbenzene (10.4) 1,3,5,7-Cyclooctatetraene (46.5) Benzene, (1-methylethenyl) -(6.8) Azulene (5.2) Naphthalene, 1-methyl-(3.3)
Polystyrene (PS) + Polyethylene (PE)	Commercial ZSM-5	33	42.7	24.3	Azulene (11) Naphthalene, 2-ethenyl-(5) Benzene, 1,1′-(1,3-propanediyl)bis-(3.5) Phenanthrene (11.7) Anthracene, 9-ethenyl-(4.4)

					Naphthalene, 2-phenyl- (8) Phenol, 2,2′-methylenebis[6-(1,1-dimethylethyl)-4-methyl-(7.1) 1,2-Benzenedicarboxylic acid, mono(2-ethylhexyl) ester (3.3)
	Synthesized ZSM-5	38	45.6	16.4	Azulene (12.1) Naphthalene, 2-methyl- (3.2) Phenanthrene (5.3) 1,2-Benzenedicarboxylic acid, mono(2-ethylhexyl) ester (3.9) Tetracosamethyl-cyclododecasiloxane (50) 13-Docosenamide, (Z)- (5) Hexacontane (10.1)
Polypropylene (PP) + Polyethylene (PE)	Commercial ZSM-5	22	65.3	12.7	Azulene (16.9) Naphthalene, 2-methyl- (5.5) Naphthalene, 1-methyl- (4)

					Biphenyl $$ 1,1′-Biphenyl (5.3) Acenaphthene (4.7) Phenanthrene (9.9) Acetic acid n-octadecyl ester (3.1) Phenol, 2,2′-methylenebis[6-(1,1-dimethylethyl)-4-methyl (12.2) 1,2-Benzenedicarboxylic acid, mono(2-ethylhexyl) ester (35.9)
	Synthesized ZSM-5	30	56.7	13.3	Phenanthrene (3.7) Phenol, 2,2′-methylenebis[6-(1,1-dimethylethyl)-4-methyl-(5.4) 1,2-Benzenedicarboxylic acid, mono(2-ethylhexyl) ester (51.3) Cyclononasiloxane, octadecamethyl-(9.1) Tetracosamethyl-cyclododecasiloxane (20.3)
Polypropylene (PP)	Commercial ZSM-5	42	38.2	19.8	Ethylbenezene (10.6) Styrene (6.6)

+ Polyethylene (PE) + Polystyrene (PS)					alpha-Methylstyrene (8.3) Naphthalene 2-methyl (5) Biphenyl (4.5)
	Synthesized ZSM-5	63	24.4	12.6	Benzene, 1,1′-(1,3-propanediyl)bis-(4) 1,2-Benzenedicarboxylic acid, mono(2-ethylhexyl) ester (25) Cyclononasiloxane, octadecamethyl-(32.8) Cyclodecasiloxane, eicosamethyl-(3.7) Cyclooctasiloxane, hexadecamethyl-(4.6) Tetracosamethyl-cyclododecasiloxane (18.4)
Polypropylene (PP) + Polyethylene (PE) + Polystyrene (PS) +	Commercial ZSM-5	54	28.1	17.9	Azulene (10.7) Naphthalene, 2-methyl-(4.3) Biphenyl (4.4) Phenanthrene (9) Naphthalene, 2-phenyl-(3.3) Phenol, 2,2′-methylenebis[6-(1,1-

Polyethylene Terephthalate (PET)					dimethylethyl)-4-methyl-(5.5) 1,2-Benzenedicarboxylic acid, mono(2-ethylhexyl) ester (52)
	Synthesized ZSM-5	58	24.7	17.3	Azulene (11.2) Naphthalene, 2-methyl-(6.3) Biphenyl (4.9) Phenanthrene (9.3) Naphthalene, 2-phenyl-(3.3) Phenol, 2,2′-methylenebis[6-(1,1-dimethylethyl)-4-methyl-(5.8) 1,2-Benzenedicarboxylic acid, mono(2-ethylhexyl) ester (47)

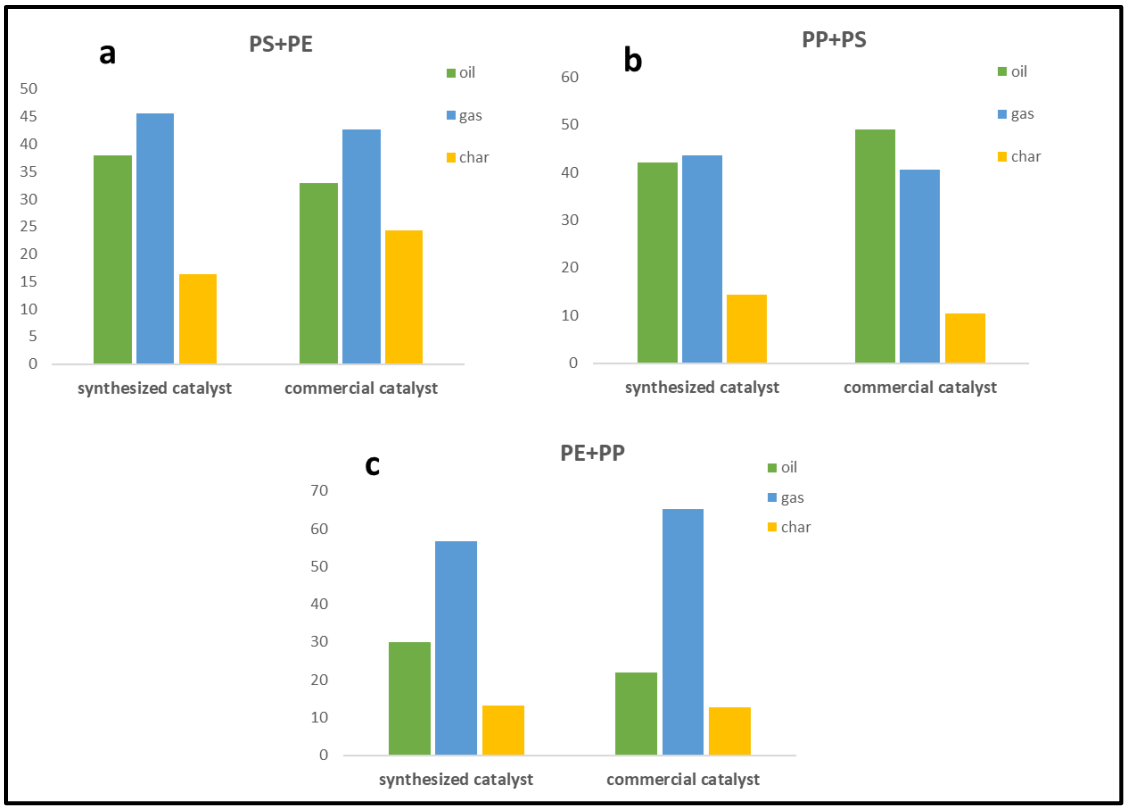

Figure 5.16: Effect of synthesized and commercial ZSM-5 zeolite on mixed feedstock a) PS and PE plastic wastes b) PP and PS plastic wastes c) PE and PP plastic wastes

Both commercial and synthesized zeolite catalysts were also used individually to catalyze the pyrolysis of mixed plastic wastes in various ratios (Table 5). As shown in Figure 5.17, there was a marginally better oil yields achieved in PS/PE/PP and PS/PE/PP/PET samples using the locally synthesized zeolite catalyst. In mixed plastic wastes, the PS/PE/PP sample with the synthesized G10/ZSM-5 zeolite had the maximum liquid oil output of 63%, and the PP/PE sample with commercial zeolite catalysts had the lowest liquid oil yield of 22% and the maximum gas yield of 65.3% and char yield of 24.3% were obtained from PS/PE.

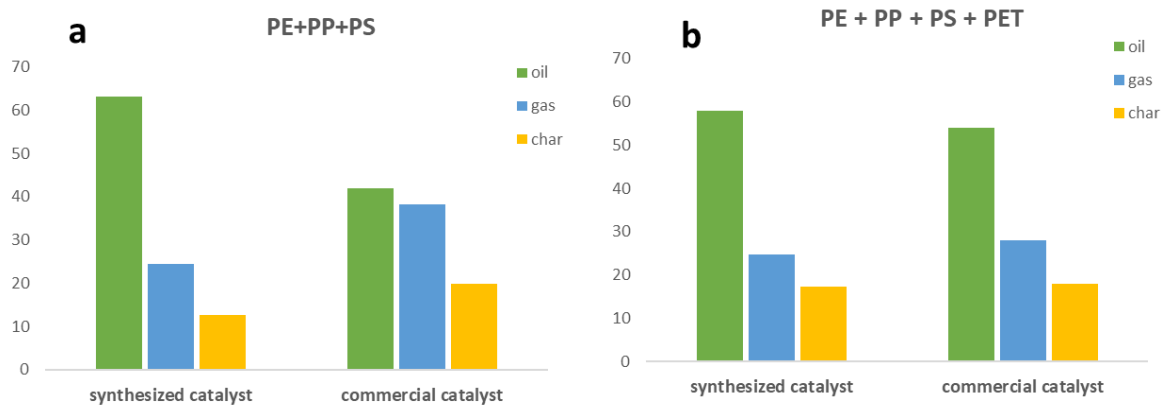

Figure 5.17: Effect of synthesized and commercial ZSM-5 zeolite on mixed feedstock a) PE, PP, and PS. b) PS, PP, PE and PET plastic wastes

5.6.5 Effect of natural and synthetic zeolite catalysts on liquid oil composition

The liquid oils obtained from the catalytic pyrolysis of various plastic wastes (individual and mixed) at 450 degrees Celsius for 90 minutes in the presence of commercial and synthesized ZSM-5 zeolite catalysts contained various hydrocarbons (Figs. 5.18; Table 5). Most of the aromatic hydrocarbons were present in the liquid oil generated from the experiments conducted on polystyrene (PS) using both catalysts. With the commercial zeolite catalyst, ethylbenzene was present in the highest concentration (60.8%), however, with the locally synthesized ZSM-5 catalyst, ethylbeneze was also present but in the lower concentration (10%). Styrene (7.6% and 15.8%) and alpha-methylstyrene (10.7% and 38.3%), were the other prevalent chemicals in significant amounts. Table 5 has the quantitative listing of all other chemicals. Indene, benzene, styrene, and alpha-ethylstyrene are the main chemicals detected in the generated liquid oil, and according to studies conducted by Artetxe et al. (2015), and Bartoli et al. (2015), these were similar hydrocarbons reported. According to Onwudili et al. (2009), the generation of toluene and ethylbenzene may result from additional styrene breakdown. Furthermore, with a decrement in styrene formation, the high temperature and contact time also promote the production of alpha-methylstyrene, toluene, and ethylbenzene (Artetxe et al., 2015). Secondary reactions that reduce styrene and enhance its derivate compounds have been found to occur at high temperatures by Ukei et al. (2000) and Shah and Jan (2014).

The gas chromatography–mass spectrometry (GC-MS) analysis confirmed that polypropylene (PP) plastic waste catalyzed by both catalysts yielded a liquid oil with a more complicated composition than that of other plastic feedstocks (Table 5). Also, it was observed that compound forms and quantities varied between the liquid oils produced using these catalysts. With commercial zeolite as the catalyst, the highest concentration of o-xylene (8.8%) was observed, whereas synthesized zeolite produced the highest concentration of cyclononasiloxane, octadecamethyl (22.8%). The use of catalyst boosted the production of naphthalene and poly-aromatic compounds through aromatization, oligomerization, and deoxygenation on the catalyst's active acidic sites. Abbas-Abadi et al. (2014) reported the synthesis of aliphatic, paraffinic, aromatic, and naphthenic hydrocarbons when PP was catalytically pyrolyzed using an FCC catalyst. Dawood and Miura (2002) also confirmed that using a modified HY-zeolite catalyst improves the conversion of PP plastic into aromatics and olefins. Table 5 listed more hydrocarbons along with their quantities.

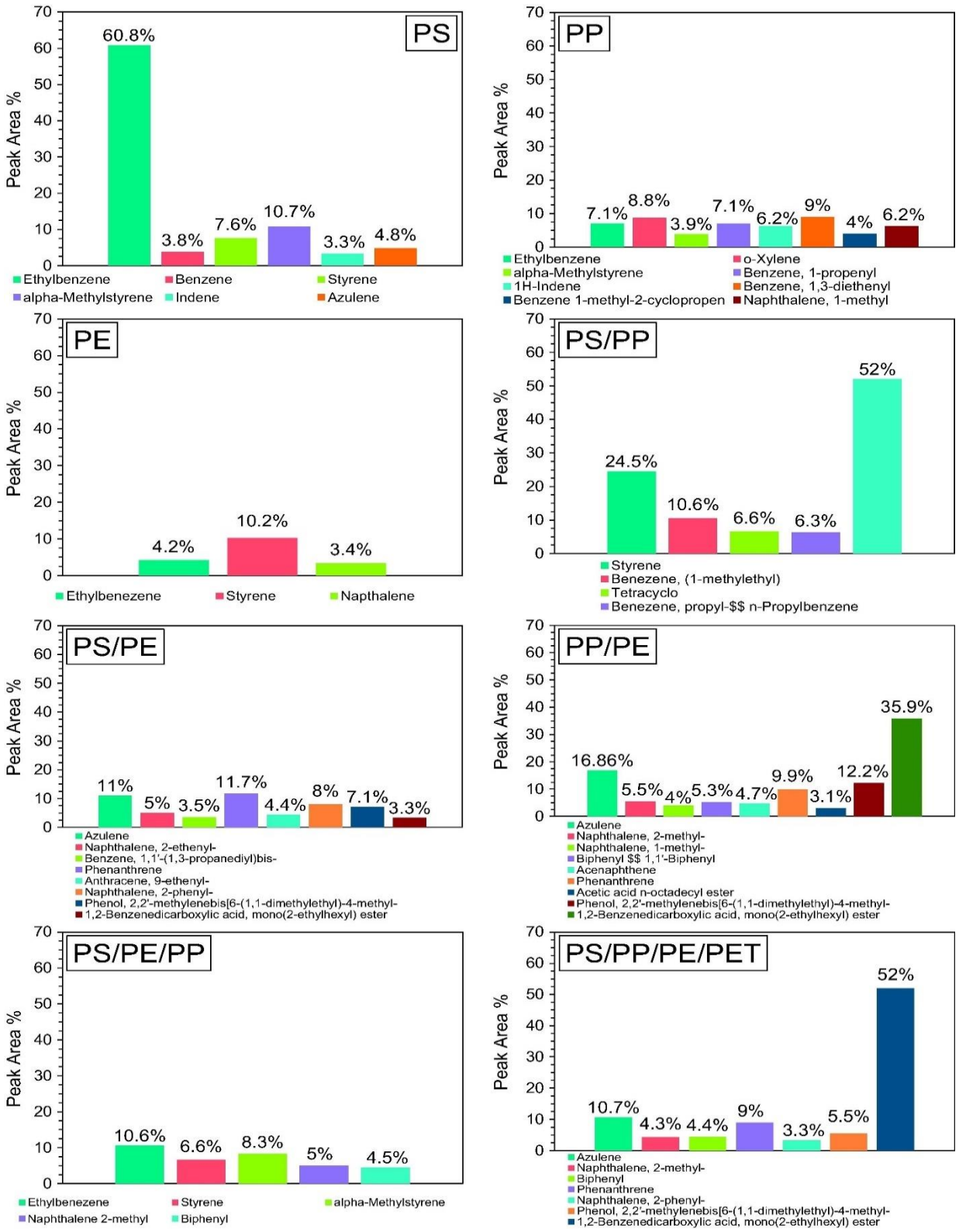

Figure 5.18: GC–MS analysis of liquid oil compositions from catalytic pyrolysis using commercial ZSM-5 zeolite

Fewer types of chemicals, primarily aromatic hydrocarbons, were detected in the liquid oil synthesized by the catalytic pyrolysis of PE using commercial and synthesized ZSM-5 zeolite. Ethylbenzene and naphthalene were the hydrocarbons that were present in both experiments performed. The PE was broken down during catalytic pyrolysis via: carbenium ion reaction caused by proton attack or hybrid ion abstraction involving Lewis acid sites. (Rizzarelli et al., 2016). De Stefanis et al. (2013) also confirmed that the carbenium ion mechanism by proton addition (Bronsted acid sites to C-C bonds) or hybrid ion abstraction by Lewis acid sites to the PE molecules is responsible for the catalytic degradation of PE. Once the breakdown process commenced, light hydrocarbon molecules were produced sequentially. High-carbon chain compounds and significant char deposition were recorded as a result of the higher molecules being degraded on the catalyst's exterior surface while being prevented from entering by the microporous catalyst (Lopez et al., 2011).

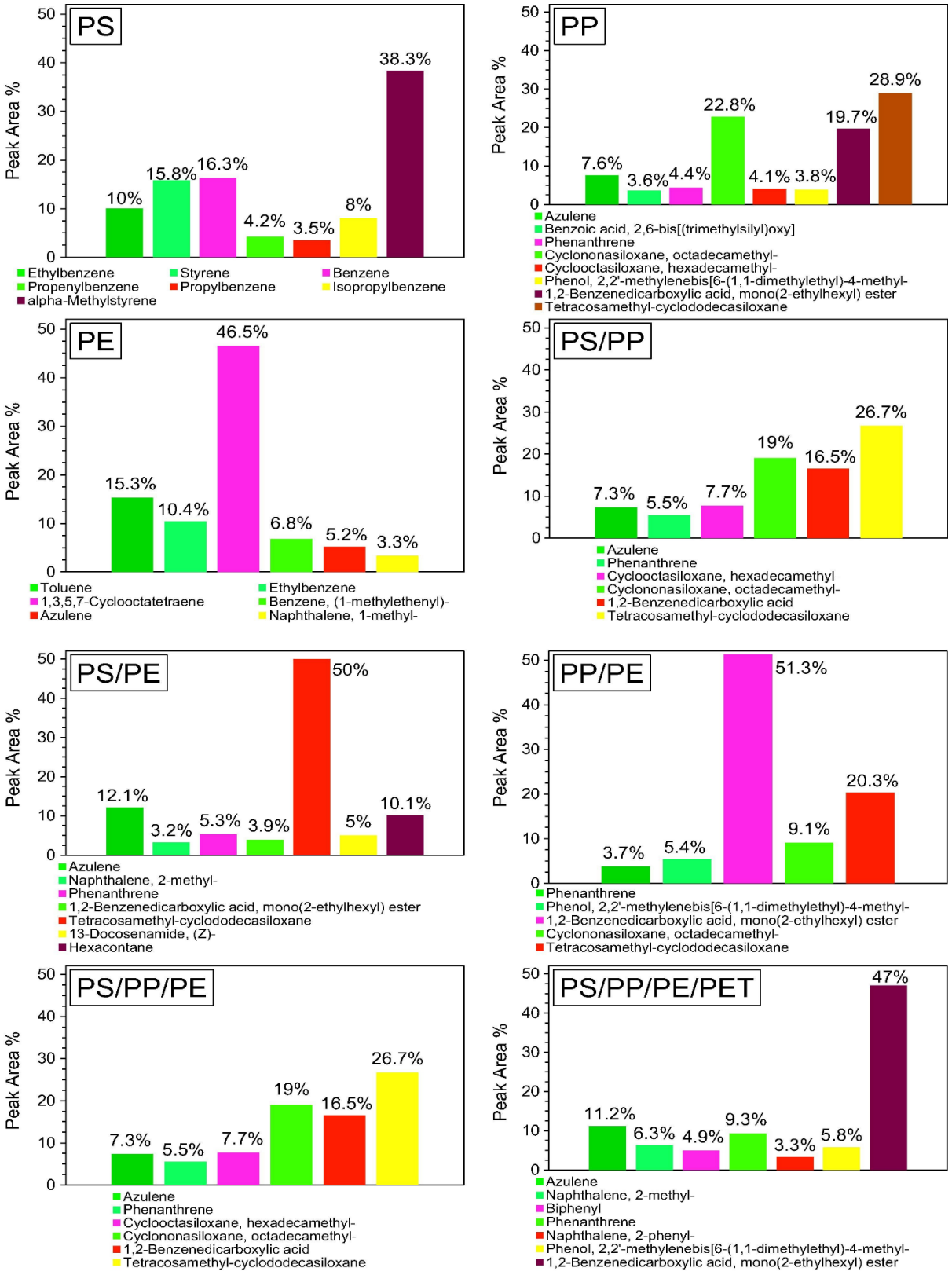

Figure 5.19: GC–MS analysis of liquid oil compositions from catalytic pyrolysis using synthesized ZSM-5 zeolite

Majority of the hydrocarbons were found in the liquid oil generated from the individual and the combined feedstock used in the catalytic pyrolysis processed involving the use of both commercial and the locally synthesized ZSM-5 zeolite as shown in Table 5.5. However, different samples of mixed feedstock had various types and compositions of hydrocarbon chemicals. The majority of the samples included aromatic hydrocarbons. Table 5 displays the names of the specific compounds and their quantities for each feedstock. Due to the risk of errors at such low concentrations and for the sake of specificity, several additional chemicals that were below 3% were excluded from Table 5.5, Figs. 5.18 and 5.19.

High amounts of polycyclic aromatic hydrocarbons (PAH) were found to be present in the liquid oils generated from these experiments. This is not usual as PAHs are present in petroleum products as natural components of fossil fuels in a relatively significant amount (Qi et al., 2017). It was discovered that the liquid oils produced PS contains more of the PAHs. According to Budhwani (2015), PAHs are organic molecules made of carbon and hydrogen arranged in a number of aromatic rings. Several researchers have investigated the conversion of these PAHs molecules into other benefit products (oxygenated molecules), including aldehydes, carboxylic acids, and ketones (Rivas et al., 2000).

Fourier-transform infrared spectroscopy (FTIR) analysis was used to assess the existence of the functional groups in the liquid oils obtained from the catalytic pyrolysis of the plastic wastes. This technique utilizes infrared adsorption spectrum created by chemical bonding in the liquid molecules to detect the functional groups in the liquid oils (Rehan et al., 2017). In the presence of both zeolite catalysts at 450 ^{o}C for 90 minutes, the formed liquid oil from independent and combination of plastic waste feedstocks constituted alkenes, alkanes, and aromatic as well as a minuscule portion of phenol group (Figs. 5.20 and 5.21). All compositions of hydrocarbons found, were consistent with the GC-MS observations (Figs. 5.18 and 5.19). Evidently, a distinct peak that denotes the presence of aromatic hydrocarbons (C-H) was seen at the beginning of each evaluation of liquid oil generated from the commercial ZSM-5 zeolite. Alkanes (C-H stretch), alkenes (=C-H bend), and aromatic compounds (C-C stretch in the ring) predominated in the

middle (Fig 5.20). Across all liquid oil samples, a prominent alkane (C-H stretch) peak was found at a wavelength of 2930 cm^{-1} (Figs. 5.20 and 5.21). Also, a weak peak of phenol and alcohols (O-H stretch, H-bonded) functional groups were found in the generated liquid oil of PP, PE, and the mixture of all plastic categories.

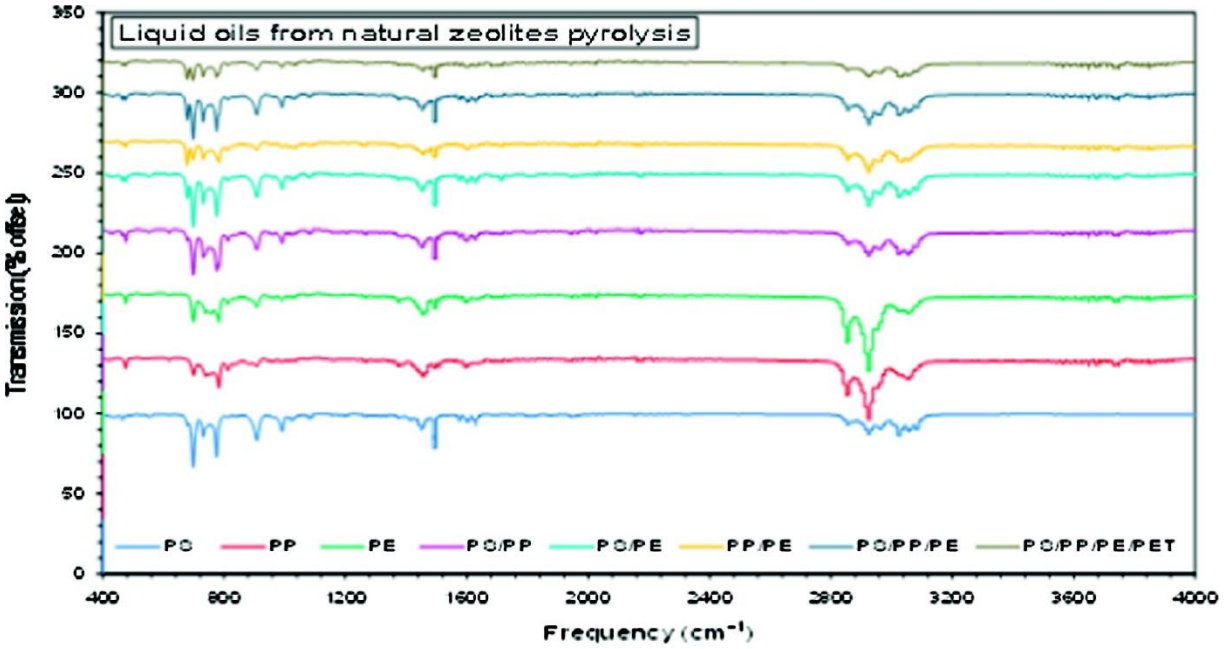

Peaks	PS	PP	PE	PS/ PP	PS/PE	PE/PP	PS/PP/ PE	PS/PP/P E/PET	Bond	Functional Group
697	✓	X	✓	✓	✓	X	✓	✓	C-H "oop"	Aromatics
776	✓	X	✓	✓	✓	X	✓	X	=C-H bend	Alkenes
910	✓	X	✓	✓	✓	X	✓	X	=C-H bend	Alkenes
990	✓	X	X	✓	✓	X	✓	X	=C-H bend	Alkenes
1,450	✓	✓	✓	✓	✓	X	✓	X	C-C stretch (in ring)	Aromatics
1,500	✓	X	X	✓	✓	X	✓	X	C-C stretch (in ring)	Aromatics
2,860	X	✓	✓	X	X	X	X	X	C-H stretch	Alkanes
2,930	X	✓	✓	X	X	X	X	X	C-H stretch	Alkanes
3,030	✓	X	X	✓	✓	✓	✓	✓	C-H stretch	Aromatics
3,060	X	✓	✓	✓	X	X	X	✓	O-H stretch, H-bonded	Alcohols, phenols

Figure 5.20: FT-IR analysis of liquid oil produced from catalytic pyrolysis of plastic waste with natural zeolite.

As displayed in Figure 5.21, aromatics, phenols, alkenes, alkanes, alkynes, alkyl halides, and alcohol functional groups were present in the liquid oils generated by catalytic pyrolysis with the synthesized zeolite. Additionally, aromatic molecules predominated, demonstrating the catalyst's high aromatization capacity. With the exception of individual PS feedstock and the mixed of plastic material, all liquid oil products showed a minor peak of alkynes at the beginning (-C=C-H:C-H bend). Interestingly, practically all liquid products derived showed a significant aromatic peak at a wavelength of 697 $cm^{-}1$. Figure 5.21 showed the liquid oil products of PP, PE, and mixed PE-PP, had a moderate peak of 1, 2 amines at wavelength of 785 $cm^{-}1$ (Fig. 5.21). In the intermediate spectrum of wavelength, alkenes (=C-H bend) and aromatics (=C-C stretch in the ring) hydrocarbons predominated. Also, an intermediate peak of alkanes (C-H stretch) were detected between 2860 and 2930 $cm^{-}1$ in all liquid fuel blends. At a wavelength of 3030 $cm^{-}1$, additional prominent aromatic (C-H stretch) peak was found. However, in PE, PP, and related combination with PET, a low peak of phenol and alcohol (O-H stretch, H-bonded) was found (Fig. 5.21). The existence of aromatic, alkane, and alkene hydrocarbons in the liquid products obtained from polymers was reported by Siddiqui and Redhwi (2009) and Sarker and Rashid (2013). Both Tekin et al. (2012) and Panda and Singh (2013) performed FT-IR analyses on the liquid oil produced from polymeric materials and found that primarily aromatic hydrocarbons along with a few alkanes and alkenes were present.

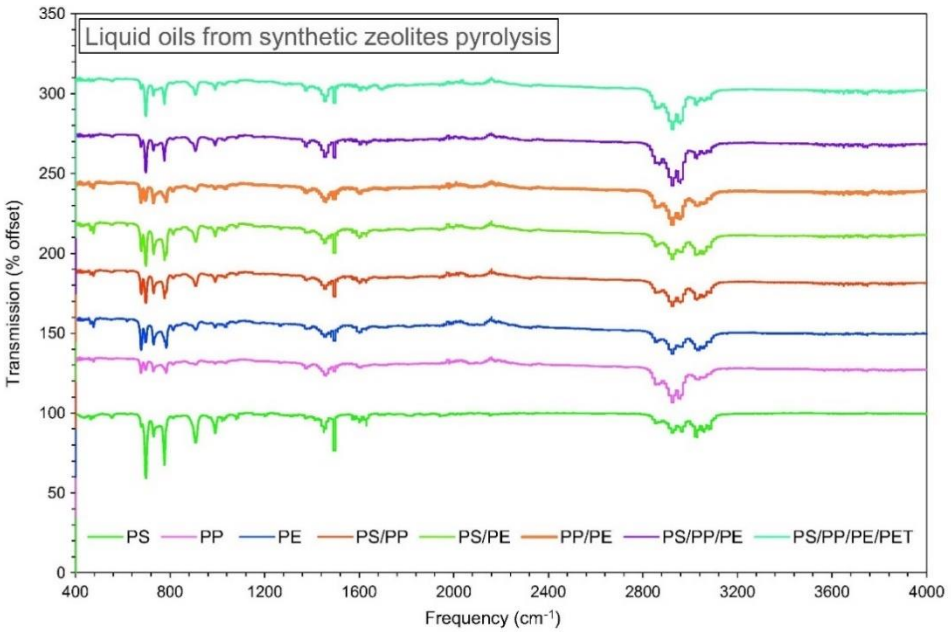

Peaks	PS	PP	PE	PS/ PP	PS/PE	PE/PP	PS/PP/ PE	PS/PP/ PE/PET	Bond	Functional Group
677	X	✓	✓	✓	✓	✓	X	X	-C≡C-H: C-H bend	Alkynes
697	✓	X	X	✓	✓	X	✓	✓	C-H "oop"	Aromatics
729	✓	✓	✓	✓	✓	✓	✓	✓	C-Cl stretch	Alkyl halides
776	✓	✓	X	✓	✓	X	✓	✓	=C-H bend	Alkenes
785	X	✓	✓	X	X	✓	X	X	N-H wag	1°, 2° amines
910	✓	X	X	✓	✓	X	✓	✓	=C-H bend	Alkenes
990	✓	X	X	✓	✓	X	✓	✓	=C-H bend	Alkenes
1,460	✓	✓	✓	✓	✓	✓	✓	✓	C-C stretch (in ring)	Aromatics
1,500	✓	X	X	✓	✓	X	✓	✓	C-C stretch (in ring)	Aromatics
2,860	✓	✓	✓	✓	✓	✓	✓	✓	C-H stretch	Alkanes
2,930	✓	✓	✓	✓	✓	✓	✓	✓	C-H stretch	Alkanes
3,030	✓	✓	✓	✓	✓	✓	✓	✓	C-H stretch	Aromatics
3,060	X	✓	✓	✓	X	X	X	✓	O-H stretch, H-bonded	Alcohols, phenols

Figure 5.21: FT-IR analysis of liquid oil produced from catalytic pyrolysis of plastic waste with synthesized ZSM-5 zeolite.

5.7 Proximate and Ultimate Analysis of the feedstock using the synthesized catalyst

A significant consideration in the design of a liquid oil-based pyrolytic plant is the elemental analysis of the product oil. The final study revealed differences in the elemental makeup of pyrolytic liquid-oil produced from the feedstocks (PE, PP, PS, and PET) under various temperature regimes (Table 5.6).

The proximate, ultimate analysis and HHV of the pyrolytic liquid-oil produced from MPW (PE, PS, PP and PET) at temperatures of 400 °C and 450 °C are presented in Table 5.6. At 400 °C, the carbon content (89 wt%) of the pyrolytic liquid-oil obtained from PS was higher than that of PET (78 wt%) and PE (79 wt%) but almost the same with PP (87 wt%). With increasing the temperature to 450 °C, the carbon content of PET (75 wt%) slightly decreased while little or no change was observed on the carbon content of PS, PE and PP (see Table 5.6). For all the feedstock composition considered, there was no significant change in the hydrogen content of the liquid-oils under the influence of temperature variation.

Table 5.6: The ultimate analysis of the different municipal plastic wastes

Plastic waste	Carbon	Hydrogen	Oxygen	Nitrogen	Sulphur
		Temperature: 400 ºC			
PE	79	14	4	0.07	0.07
PS	89	15	1	0.03	0.05
PP	87	14	1.5	0.08	0.06
PET	78	14	6	0.18	-
		Temperature: 450 ºC			
PE	78	13	4.3	0.06	0.05
PS	88	16	1.4	0.02	0.04
PP	85	13	1.8	0.07	0.05
PET	75	12	9	0.20	-

However, the oxygen content of the liquid-oil from PS (1 wt%) and PP (1.5 wt%) was lower when compared to PE (4 wt%) and PET (6 wt%) at 400 °C. The PET plastics produced higher oxygen content at both 400 °C and 450 °C. In the same vein, the high oxygen composition of the liquid-oil from PET collaborated its lower HHV when compared to other feedstock. There was no significant difference observed between the H/C ratio for all the pyrolytic liquid-oils because of the closeness of their hydrogen values. Another reason is attributed to the fact that their hydrogen contents were significantly lower to the carbon contents. Interestingly, a significant difference was observed when the nitrogen content of liquid-oil from PS (0.03 wt%) was compared to PET (0.18 wt%) at 400 °C.

Table 5.7: The proximate analysis of the municipal plastic wastes

Plastic waste	Moisture content	Carbon content	Volatile content	Ash content	HHV (MJ/Kg)
PE	0.2	0.0	99.8	0.5	46.5
PS	0.3	1.3	97.6	1.6	46.5
PP	0.2	0.3	99.4	0.1	41.8
PET	0.6	8.0	90.7	0.3	30.3

With the PE, the nitrogen content (0.07 wt%) was similar to that obtained with PP (0.08 wt%). The N/C ratio further confirms the PS liquid-oils with the lower nitrogen when compared to PE and PET. Notably, increasing the temperature to 450 °C has little or no effect on the nitrogen content of both PS and PP possibly due to complete decomposition of the volatile content of the feedstock at the temperature of 400 °C. This suggests that the nitrogen content of pyrolytic liquid-oils was more dependent on feedstock composition than temperature.

The sulphur content from all the raw materials and that of liquid-oils produced at all conditions considered were found to be < 1 wt% and fall within the range of 0.1 to 1.5 wt% reported for petroleum crude (Saber et al. 2016). These findings have shown that nitrogen content in the feedstock could enhance the pyrolytic liquid-oil yield as well as reduce the nitrogen content present in the liquid-oil significantly. Thus, it could be seen as a promising approach to produce high-quality pyrolytic liquid-oil from MPW.

5.8 Summary of the findings

The study demonstrated the potential of locally synthesized zeolite from South African kaolin as a substitute promising low-cost catalyst in pyrolysis technology. Four primary types of plastic waste, including PE, PS, PP, and PET, were catalytically pyrolyzed using zeolite catalysts from commercial and synthesized materials in a fixed bed reactor. The optimum temperature, pyrolysis time and catalyst ratio were 450 °C, except for PET which had an optimum temperature of 400 °C, 90 minutes and 1:10 respectively. These results are comparable to what has been reported by other researchers using similar types of plastics under the same operating conditions. According to GC-MS and FT-IR research, the liquid oils formed by all types of plastic waste employing both catalysts primarily contained aromatic hydrocarbons such styrene, ethylbenzene, benzene, azulene, naphthalene, and toluene with a little amount of aliphatic hydrocarbon compounds. With the help of both catalysts, liquid oils made from all types of plastic waste showed high HHV (30.3 – 46.5 MJ/kg), which is comparable to regular diesel. For the conversion of plastic waste into liquid oil and value-added products like char for possible energy and environmental applications, catalytic pyrolysis can be a promising method. For the liquid oil to be acceptable as a fuel for transportation, an energy source, or valuable chemicals, post-treatments like refining or blending with regular diesel are necessary.

CHAPTER 6: OPTIMIZATION OF PROCESS PARAMETERS IN THE CATALYTIC PYROLYSIS OF PLASTIC WASTE USING RESPONSE SURFACE METHODOLOGY

6.1 Introduction

Plastics are a vital component of the global economic system and everyday life. Since plastic is a crucial component in many industries, including packaging, building, transportation, electronics, and healthcare, its use has grown significantly over time. These industries use plastics because of their dependability, adaptability, corrosion resistance, lightweight, superior thermal and electrical insulation, and low manufacturing costs (Hahladakis and Lacovidou, 2018; Millet et al., 2018; Harussani et al., 2022). When evaluating the end of a plastic's useful life, these qualities, which characterize usability, could lead to problems (Napper and Thompson, 2020). Municipal plastic wastes (MPW) and industrial plastic wastes (IPW) are the two primary categories of plastic wastes (Anene et al., 2018). Polyethylene (PE), Polyethylene Terephthalate (PET), Polystyrene (PS), and Polypropylene (PP) are commonly found in these waste categories (Zhu et al., 2019; Peng et al., 2022). Materials for packaging make up between 50 and 70 percent of MPW (Lebreton and Andrady, 2019).

Plastic wastes are non-biodegradable and persist in the environment for a long time, leading to research into various management strategies, such as waste-to-energy (WTE) operations, reuse, regeneration, and dumping in landfill space (Velvizhi et al., 2020; Nanda and Berruti, 2021). Examples of this WTE or plastic-to-fuel (PTF) technology include the combustion of refuse-derived fuel (RDF), including pyrolysis, gasification, and plasma arc gasification (Anene et al., 2018; Alam et al., 2022). Pyrolysis can be catalytic or thermal (Patel et al., 2022). The benefits of catalytic pyrolysis include producing liquid products with a lower boiling point, enhanced selectivity, quicker and better reactions, shorter residence times, reduction of the formation of unsuitable products, decomposition at lower temperatures (high energy efficiency), and decreased residence times (Dwivedi et al., 2019; Zhou et al., 2021). Alumina and silica-alumina (Busca, 2020; Lee et al., 2022), zeolites (Król, 2022), FCC catalysts, and reformed catalysts (Huang et al., 2022) are the most often employed promoters in this methodology. Numerous investigations for the

pyrolysis of waste plastics to produce liquid fuel have been described at different scales and with differing degrees of success (Zhou et al., 2021; Idumah, 2022).

The yield of liquid produced by catalytic pyrolysis is dependent on the interaction between the process parameters. Regarding modelling and optimization of the pyrolysis process, only a few researchers focus on enhancing process optimization. To the best of our knowledge, ZSM-5 zeolite produced from South African kaolin has not yet been utilized to catalyze mixed plastic wastes. Moreover, typical optimization via one-factor-at-a-time is time-consuming and expensive when a large number of tests are conducted (Abdel-Rahman et al., 2020; Xiao et al., 2022). To minimize time and expenses, researchers are utilizing tools such as design experts, MATLAB, and so on, to design experiments, model the data gathered, and enhance the impact of process parameters on yields (Knoll and Golkar, 2018; Singh Sivam et al., 2022).

Istadi et al., (2020) developed a Hybrid Artificial Neural Network-Genetic Algorithm (ANN-GA) method to simulate and optimize the conversion of plastic waste into liquid fuels over modified residual catalytic cracking catalysts. To predict how experimental variables will affect the product yields produced by pyrolysis, Pinto et al. (2020) employed response surface methodology (RSM). To increase the yield and composition of liquid products from the evaluated plastic waste, an experimental factorial design was employed to optimize reaction duration, temperature, and startup pressure (Ma et al., 2020). In order to create liquid fuel, Li et al. (2021) investigated the thermal decomposition of a waste tire and waste plastic mixture. The response surface analysis was used to conduct the regression algorithm on the experimental data.

Response surface methodology (RSM) provides the benefit of reducing the number of costly experiments by identifying the optimal experimental settings. Response surface methodology (RSM) can therefore be a technique utilized to address the optimization problem with the intended purpose of maximizing the liquid yield. This work aimed to optimize the catalytic pyrolysis of mixed plastic wastes and to assess the impact of process variables, including temperature, reaction time, and catalyst concentration, on the product yield while utilizing the locally-made catalyst (G10/ZSM-5). The experimental data were modelled using the RSM based on central composite design (CCD), and the

coefficient of determination was used to compare the predictiveness of the models. In addition, analysis of variance (ANOVA) was utilized to assess the reliability and validity of the RSM model. The PS/PE/PP plastic waste mixture was employed as the feedstock for this experiment. The laboratory-scale batch reactor was used for the pyrolysis experiments, and the catalyst's impact on the amount and quality of the pyrolysis products was investigated. The resulting liquid was analyzed using gas chromatography-mass spectrometry (GC–MS).

6.2 Materials and methods

The waste plastic mixtures (PE, PP, and PS) used in this experiment were collected from the DUT cafeteria bin. These plastic mixtures were selected based on the high oil yield performance compared to other mixtures in the OFAT experiments conducted in the previous chapter (See chapter 5). The feedstock composition of 40 wt% PE, 30 wt% PP and 30 wt% PS was used.

6.3 Design Evaluation

The process parameters for pyrolyzing mixed plastic waste into liquid fuel were optimized using the response surface approach and a design technique known as central composite design (CCD). RSM is a collection of mathematical and statistical models that proved advantageous in establishing an empirical connection for improving and maximizing process parameters. RSM is an effective approach for fitting a quadratic model that may be used to both optimize process parameters and examine how those parameters interact. Three processes were involved in optimization: firstly, the experimental runs were statistically constructed; secondly, the mathematical model's coefficient was computed; and lastly, the responses and suitability of the model were predicted. For the statistical experiment in this study, three independent variables, namely: A-temperature, B-reaction time, and C-catalyst to feedstock ratio, were selected and varied at three levels: a high level, represented as (+1), a low level represented as (-1) a middle point (0).

These three independent variables were represented as X_1, X_2, and X_3 with three output or dependent variables, liquid oil yield (Y_1), gas yield (Y_2), and char yield (Y_3), as illustrated in Table 6.1. The independent variables were selected based on their significance in the preliminary experiments.

Table 6.1: Independent factors, their CCD levels, and the output

Variables	symbol	-1	0	1
Temperature (ºC)	X_1	400	450	500
Reaction time (mins)	X_2	90	120	150
Catalyst to feedstock ratio (wt%/wt%)	X_3	1:5	1:10	1:15
Output				
Liquid oil yield	Y_1			
Gas	Y_2			
Char	Y_3			

The CCD has 8 cube points, 6 cube-centred points, 6 axial points, and 0 axial-centred points. As a result, 20 experiments were conducted using the CCD in this study. Table 6.2 contains the design of the CCD matrix for three different variables in coded form, the experimental response (oil, gas and char) and the RSM response (oil, gas, char). To minimize the impact of inexplicable variance in the observed response produced by unrelated factors, all tests were carried out at random. Following the completion of the experiments, the data were fitted to a quadratic model to simulate the system response specified in Eq (6.1)

$$Y = \beta o + \sum_{i=1}^{n} \beta i \times Xi + \sum_{i=1}^{n} \beta ii \times Xi^2 + \sum_{i=1}^{n} \sum_{j>1}^{n} \beta ij \times XiXj \qquad (6\text{-}1)$$

where Y is the predicted output; n indicates the number of trials; βo, βi, βii, and βij are regression coefficients for the constant, linear, quadratic, and interaction components, respectively; Xi, and Xj, are the independently coded factors. For each response, generated equations were used to calculate predicted values. These variables were utilized to generate contour plots for the optimization procedure.

The study made use of Design Expert software version 16.4.0. For a simple analysis of the impact of experimental factors on the responses, three-dimensional response surfaces and contour plots were used. Both variables were held constant at their centre locations to produce the individual response surface and contour plots. Multiple regression analysis was used to obtain the model coefficients for one response. The coefficients of correlation and determination of the models were used to assess how well they fit the data. Fisher F-test analysis of variance (ANOVA) was used to assess each model's suitability. The objective of this test is to determine the link between the response variable and a subset of the independent factors.

Table 6.2 represent the results of 20 experimental runs using the CCD design matrix for the catalytic pyrolysis of mixed plastic waste (PE, PP, PS). The findings consist of the investigated factors in coded form, the experimental results, and the model-predicted response factor results. The experimental values are the calculated liquid oil yield, gas yield and char yield (using equation 3.1 – 3.3), while the predicted values are computed from the model (Equation 6.1). These results were subjected to four-step processes of the RSM analysis: (i) the statistical significance of the model developed was tested using ANOVA, (ii) the diagnostic and response plots were used to establish the optimum region and interactive conditions, (iii) a numerical optimization technique was used to optimize the desired goals fixed for maximum liquid oil yield (%), gas yield (%) and char yield (%), and (iv) validation was conducted. The coefficient of determination (R^2), adjusted R^2, standard deviation (SD) and coefficient of variance (CV), and adequate precision (AP) demonstrated the model's fit. In addition, Fisher’s F-values and associated p-values with a 95% confidence level were utilized to determine the relevance of the model equations for each output parameter (Table 6.3).

Table 6.2: The central composite design matrix of experimental and yield responses

	Factor			Experimental Response			RSM Predicted Response		
Run	A: Temperature	B: Reaction time	C: Catalyst ratio	Oil yield	Gas yield	Char	Oil yield	Gas yield	Char
	°C	mins		%	%	%	%	%	%
1	-1	-1	-1	70,11	26,09	3,61	70,05	26,08	3,62
2	0	0	0	71,24	24,56	3,84	71,2	24,64	3,77
3	1	-1	-1	69,56	26,47	4,3	69,72	26,46	4,3
4	-1	1	-1	71,04	26,11	4,19	71	26,1	4,2
5	0	0	0	70,98	24,56	3,84	71,2	24,64	3,77
6	0	0	0	71,24	24,56	3,84	71,2	24,64	3,77
7	-1	1	1	72,9	24,41	2,97	72,78	24,39	2,99
8	-1	0	0	71,49	25,34	2,69	71,36	25,39	2,65
9	0	0	0	70,29	24,56	3,84	71,2	24,64	3,77
10	0	-1	0	70,75	26,11	2,96	70,72	26,16	2,92
11	0	0	0	71,24	25,2699	3,23	71,2	24,64	3,77
12	0	1	0	71,66	24,62	3,32	71,69	24,67	3,27
13	-1	-1	-1	70,11	26,09	3,61	70,05	26,08	3,62
14	1	1	-1	68,1	26,96	3,37	68,14	26,93	3,39
15	0	0	0	71,24	24,56	3,84	71,2	24,64	3,77
16	1	-1	1	71,42	26,96	2,91	71,5	26,94	2,93
17	1	0	0	71,92	25,3	3,07	71,05	25,36	3,02
18	0	0	1	71,63	24,24	4,23	71,5	24,28	4,19
19	1	1	1	72,31	23,95	3,03	72,48	23,95	3,04
20	0	0	-1	69,77	24,84	5,53	69,73	24,9	5,48

6.4 Analysis using the central composite design

The acquired findings were then examined using ANOVA to determine the "goodness of fit" (Ghafari *et al.* 2009; Singh *et al.* 2020a). ANOVA assesses the interactions between variables and their corresponding responses (Galan *et al.* 2021; Pandit *et al.* 2021; Usman *et al.* 2021; Rifi *et al.* 2022). Equations 6.2 to 6.4 represent the software-generated models for the liquid oil, gas and oil yields in coded form for the mixed plastic waste catalytic process. The predicted results had been defined as the summation of a constant and three first-order effects (terms in A, B and C), three interaction effects (AB, BC, and AC), and the quadratic effect (C^2) as a result of temperature (A), reaction time (B), and catalyst concentration (C). The quadratic model was found to be the most acceptable in terms of three responses (liquid oil, gas, and char).

$$\text{Oil yield} = 71.2 - 0.1551A + 0.4849\,B + 0.8873\,C - 0.6349\,AB + 0.6409\,AC + 0.6409\,BC - 0.5889\,C^2 \quad (6.2)$$

$$\text{Gas yield} = 24.64 - 0.0153\,A - 0.7423\,B - 0.3088\,C + 0.1116\,AB - 0.319\,AC - 0.8665\,BC + 0.\,7256\,A^2 + 0.7706\,B^2 - 0.0544\,C^2 \quad (6.3)$$

$$\text{Char} = 3.77 + 0.1841\,A + 0.1721\,B - 0.6466\,C - 0.3726\,AB + 0.2132\,AC + 0.2557\,BC - 0.9323\,A^2 - 0.6723\,B^2 + 1.07\,C^2 \quad (6.4)$$

6.5 Model fitting and statistical analysis

Using Design-Expert software, regression analysis and ANOVA were used to investigate the statistical fitness of the created model at the 95% confidence level (Singh et al. 2020a; Pandit et al. 2021; Rifi et al. 2022). F-value describes the variation in responses, which can be verified by the regression equation, whereas the p-value ascertains the statistical fitness of the developed model.

For a model to be significant, the p-value cannot be greater than 0.05, whereas the p-value for the lack of fit (LOF) test must be more than 0.05 (Singh et al. 2020a; Khui et al. 2021; Sada 2021; Wu et al. 2022; Zubair et al. 2022). The R^2 values for liquid oil, gas, and char were 0.9184, 0.9732, and 0.9601, respectively, indicating a solid relationship between dependent and independent variables. This also revealed that the total variance explained by the developed model was 91.84%, 97.32%, and 96.01%, respectively, and that 8.16, 2.68, and 3.99 % of the overall variance was not addressed by the produced model. The adjusted R^2 for liquid oil, gas, and char was determined to be 0.8709, 0.9492, and 0.9241, respectively, which were extremely close to the R^2 values presented in Tables 6.3 to 6.5. As a result, the prediction of experimental data is perfect, with a difference of less than 0.2. The models were well verified since all of the LOF were not significant, indicating the model's capacity to adequately capture the functional agreements between the experimental components and the response variables (Chen et al. 2022; Nocera et al. 2022).

Furthermore, the appropriate precision values were larger than 4, indicating that the model is adequate and may be securely utilized to explore the whole design space (Ghafari et al. 2009; Baytar et al. 2020; Chen et al. 2022). The coefficient of variance (CV), described as the ratio of the standard deviation of estimation to the mean value of the observable response, determines the repeatability and reliability of the model (Jalilibal et al. 2021; Wang et al. 2021b; Arachchige et al. 2022). In this situation, the CV for liquid oil, gas, and char were determined to be 0.5419, 0.8334, and 5.02%, respectively, indicating that the models are replicable since their CV was less than 10% (Singh et al. 2020a; Jalilibal et al. 2021; Khui et al. 2021; Pandit et al. 2021; Arachchige et al. 2022; Chen et al. 2022; Rifi et al. 2022).

Table 6.3: ANOVA for response surface quadratic model for liquid oil yield

	ANOVA model statistics					
Source	**Sum of Squares**	**df**	**Mean Square**	**F-value**	**p-value**	
Model	19.98	7	2.85	19.3	< 0.0001	**significant**
A-Temp	0.1788	1	0.1788	1.21	0.2931	
B-Reaction time	1.75	1	1.75	11.82	0.0049	
C-Catalyst ratio	5.55	1	5.55	37.51	< 0.0001	
AB	2.25	1	2.25	15.23	0.0021	
AC	2.16	1	2.16	14.58	0.0024	
BC	2.16	1	2.16	14.58	0.0024	
C^2	1.48	1	1.48	10	0.0082	
Residual	1.77	12	0.1478			
Lack of Fit	1.05	6	0.1747	1.44	0.3335	**not significant**
Pure Error	0.7261	6	0.121			
Cor Total	21.75	19				
R^2 **(0.9184)**	Adjusted R^2 **(0.8709)**	Predicted R^2 **(0.7511)**	Adeq Precision **(19.0649)**	Std. Dev. **(0.3845)**	Mean **(70.95)**	C.V. % **(0.5419)**

Table 6.4: ANOVA for response surface quadratic model for gas yield

ANOVA model statistic						
Source	**Sum of Squares**	**df**	**Mean Square**	**F-value**	**p-value**	
Model	16.14	9	1.79	40.41	< 0.0001	**significant**
A-Temp	0.0017	1	0.0017	0.0386	0.8481	
B-Reaction time	4.03	1	4..03	90.7	< 0.0001	
C-Catalyst ratio	0.6501	1	0.6501	14.65	0.0033	
AB	0.0683	1	0.0683	1.54	0.2433	
AC	0.5139	1	0.5139	11.58	0.0067	
BC	3.79	1	3.79	85.44	< 0.0001	
A^2	1.42	1	1.42	31.95	0.0002	
B^2	1.6	1	1.6	36.04	0.0001	
C^2	0.008	1	0.008	0.1796	0.6807	
Residual	0.4438	10	0.0444			
Lack of Fit	0.0239	4	0.006	0.0852	0.9839	**not significant**
Pure Error	0.42	6	0.07			
Cor Total	16.58	19				
R^2 (0.9732)	Adjusted R^2 **(0.9492)**	Predicted R^2 **(0.9067)**	Adeq Precision **(20.1001)**	Std. Dev. **(0.2107)**	Mean **(25.28)**	C.V. % **(0.8334)**

Table 6.5: ANOVA for response surface quadratic model for char yield

ANOVA model statistic						
Source	**Sum of Squares**	**df**	**Mean Square**	**F-value**	**p-value**	
Model	7.9	9	0.878	26.71	< 0.0001	**significant**
A-Temp	0.2476	1	0.2476	7.53	0.0207	
B-Reaction time	0.2164	1	0.2164	6.58	0.0281	
C-Catalyst ratio	2.85	1	2.85	86.7	< 0.0001	
AB	0.7602	1	0.7602	23.13	0.0007	
AC	0.2296	1	0.2296	6.99	0.0246	
BC	0.3303	1	0.3303	10.05	0.01	
A^2	2.34	1	2.34	71.23	< 0.0001	
B^2	1.22	1	1.22	37.04	0.0001	
C^2	3.07	1	3.07	93.42	< 0.0001	
Residual	0.3287	10	0.0329			
Lack of Fit	0.0186	4	0.0046	0.0899	0.9822	**not significant**
Pure Error	0.3101	6	0.0517			
Cor Total	8.23	19				
R^2 (0.9601)	Adjusted R^2 **(0.9241)**	Predicted R^2 **(0.8562)**	Adeq Precision **(22.0812)**	Std. Dev. **(0.1813)**	Mean **(3.61)**	C.V. % **(5.02)**

Figure 6.1 depicts the relationship between predicted and experimental liquid oil, gas, and char values. These diagnostic plots aided in determining the model's suitability. They showed a good agreement between the experimental data and the predicted results of the models, implying that the models are well-matched to form a relationship between independent and dependent variables during the mixed plastic waste catalytic process (Baytar *et al.* 2020; Singh *et al.* 2020a; Galan *et al.* 2021; Pandit *et al.* 2021; Wu *et al.* 2022). Furthermore, all AP values were greater than four (Tables 6.3 to 6.5). This show that all anticipated models may be employed to explore the design space (Ghafari *et al.* 2009; Baytar *et al.* 2020; Jalilibal *et al.* 2021; Wu *et al.* 2022).

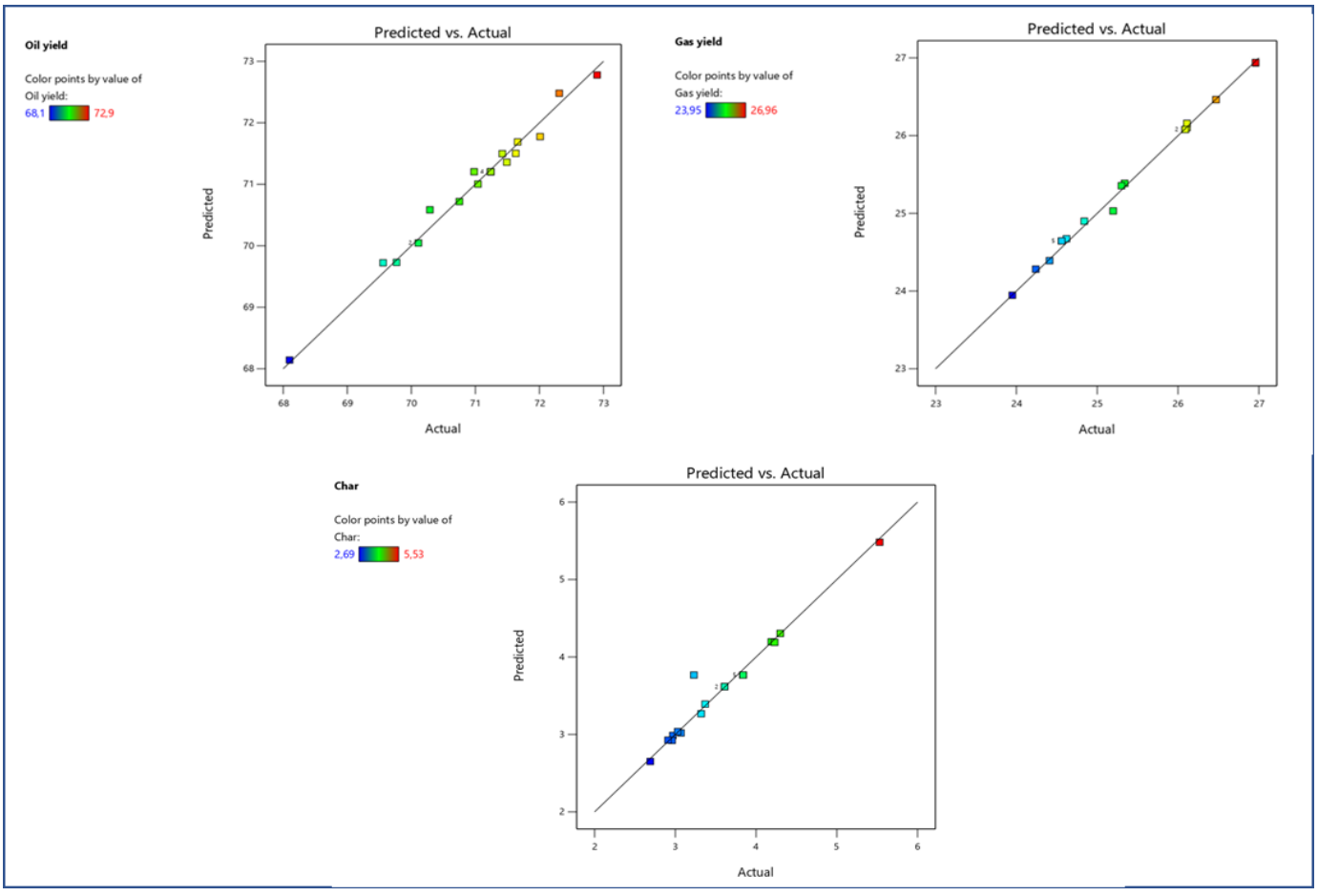

Figure 6.1: Design expert plot, predicted vs. actual plots (a) liquid oil, (b) gas, and (c) char

6.6 Effects of process parameters on optimum oil yield

The graphical depiction of the effects of temperature and reaction time on liquid oil, gas, and char yield is shown in 3D and contour plots in Figures 6.2 to 6.4, with regard to each response regression model. The independent variables were chosen based on the variables' sensitivity to the responses, as shown in previous preliminary experiments (see chapter 5). All the 3D graphs exhibit distinct peaks, showing that the optimal conditions for maximal response values in the design space are attributable to reaction time and temperature and were established to be within the design space's range.

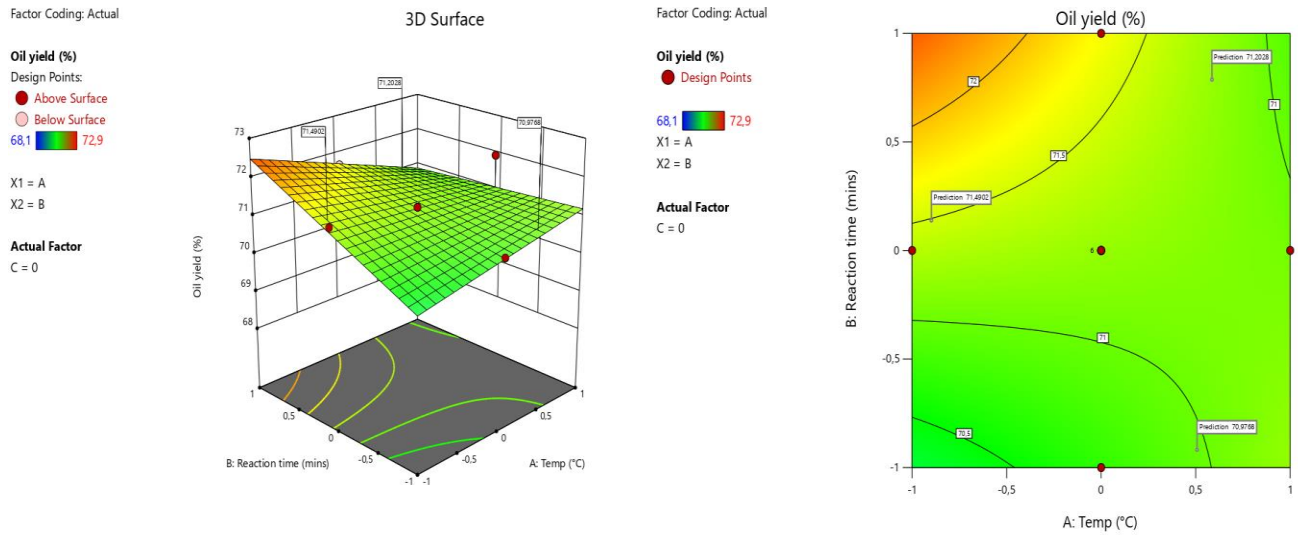

Figure 6.2: Response surface plots showing cross-factor interactions (reaction time and Temperature for liquid oil yield (%); (a) 3D plot (b) contour plot

According to Fig. 6.2, liquid fuel yield increases as temperature rises from 400 ^{o}C to 450 ^{o}C. It then decreases as the temperature increases from 450 ^{o}C to 500 ^{o}C because more non-condensable gaseous/volatile fractions are produced as a result of vigorous cracking at higher temperatures. This result agrees with those reported in the literature, where higher reaction temperature and reaction time cause a higher production of liquid oil (Budsaereechai et al., 2019).

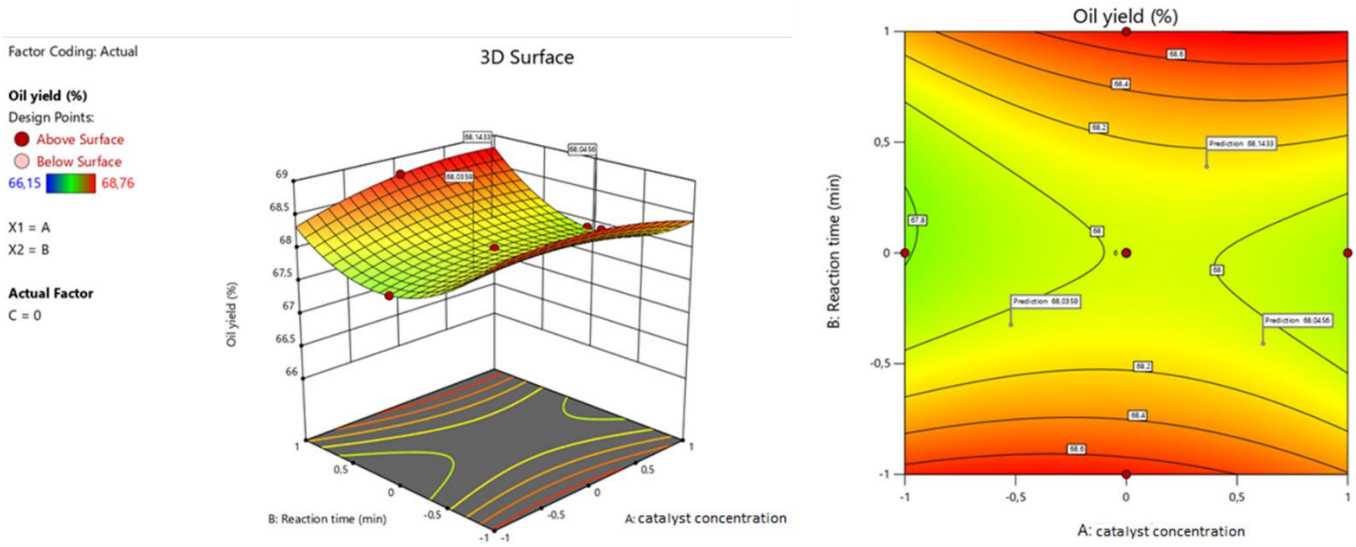

Figure 6.3: Response surface plots showing cross-factor interactions (reaction time and catalyst concentration) for liquid oil yield (%); (a) 3D plot (b) contour plot

The optimum reaction time for the catalytic pyrolysis process was determined by varying the reaction periods at 90, 120, and 150 min. The relationship between the reaction time and catalyst concentration was established using the three-dimensional reaction surface curves of the reaction time factor pair and the catalyst concentration. More liquid oil was produced when the catalyst concentration was increased from 1:5 to 1:10 by weight ratio during the reaction's 90-minute duration. After that, the reaction time was extended to 120 minutes, but the volume of liquid oil tended to decline (see Fig. 6.3.). This resulted from the applied reaction time being excessively long and reaching equilibrium (Adams et al., 2015). Thus, it was unnecessary to increase the reaction time further. The liquid oil that was produced was comparable. However, at higher catalyst concentrations (1:10 to 1:15), a reduction was seen in the yield. The decrease in yield at higher amounts of the catalyst can be attributed to the possible leaching of the catalyst into the reaction medium.

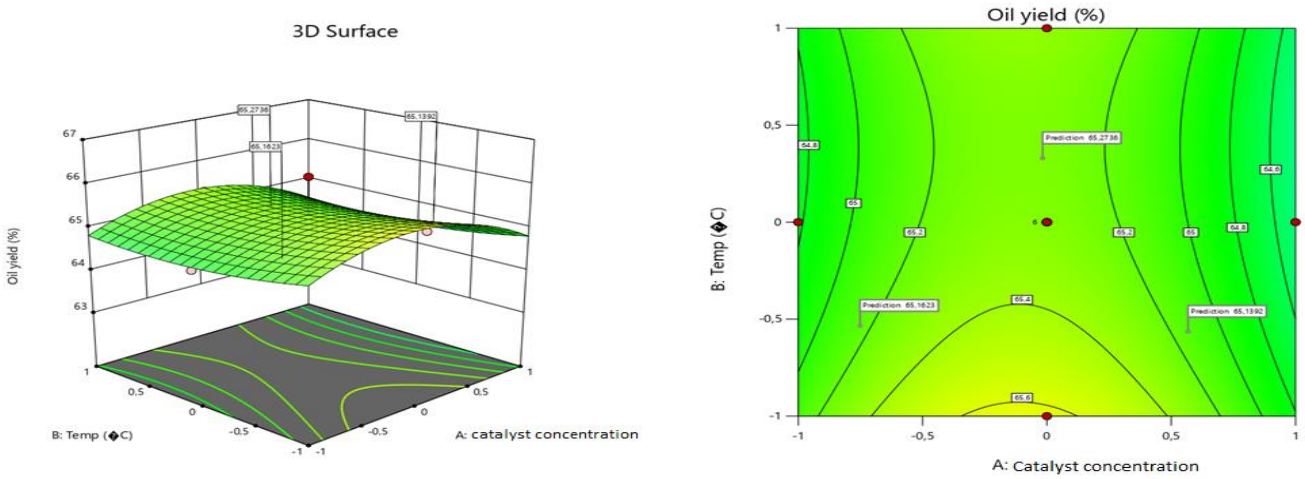

Figure6.4: Response surface plots showing cross-factor interactions (Temperature and catalyst concentration) for liquid oil yield (%); (a) 3D plot (b) contour plot

Considering the three-dimensional reaction surface curves of the temperature factor pair and the catalyst concentration, it was found that more liquid oil product was produced when the temperature was increased. The relationship between these factors can be seen in Figure 6.4, demonstrating that the yield of liquid oil increases as the ratio of catalyst to feed increases from 1:5 to 1:10 in relation to an increase in temperature from 400 ^{o}C to 450 ^{o}C but drops as the ratio further increases from 1:10 to 1:15 due to the increase in reaction rate and production of a wax-like product.

6.7 Numerical optimization using the desirability functions

Utilizing design expert software, the numerical optimization method was applied to the catalytic pyrolysis reaction of mixed plastic wastes. The scale of the desirability function runs from d = 0, which denotes that the response is utterly unacceptable, to d = 1, which denotes that the response is more desirable. Depending on the complexity of the problem, the response's objective may be maximum, minimum, in the range, target, or equal to. When the value obtained is one, the desirability function varies linearly. The constraints shown in Table 6.6 were defined to generate the optimum region using Design expert software:

(1) The temperature was set in the range of 400 ^{o}C to 500 ^{o}C. This is because extending the temperature range above the maximum for this experiment will cause the formation of more gaseous products, and below the temperature range will form more char.

(2) The catalyst ratio was set in the range of 1:5 to 1:15. However, excess of the catalyst could cause leeching in the reaction medium.

(3) In industry, time is an important factor. The aim was to achieve maximum liquid oil production in a short period. Therefore, the range of 90 minutes to 150 minutes was the selected reaction time for the optimization.

Based on the defined boundaries, optimization of the process was carried out to develop the most effective solutions.

Table 6.6: Numerical optimization results and constraints for the factors/response

Parameter	Goal	Experimental region	
		Lower	Upper
Temperature (^{o}C)	In range	400	500
Reaction time (min)	In range	90	120
Catalyst concentration	In range	1:5	1:15
Yield (%)	Maximize		

The optimal experimental conditions were obtained at a temperature of 450 ^{o}C, a reaction time of 90 min, and a catalyst ratio of 1:10 under these operating conditions. The optimal yield of liquid oil was 72.8%, gas yield of 24.6%, and char of 2.6% with a desirability value of 0.982, as shown in Fig. 6.5. The validity of this prediction was checked by triplicate confirmatory experiments under the optimized parameters. Overall, the results obtained from experimental data were in good agreement with data obtained from numerical optimization using desirability functions.

The experimental results of the CCD are in close agreement with the predicted results of the desirability functions, which further confirms the validity and accuracy of the CCD model.

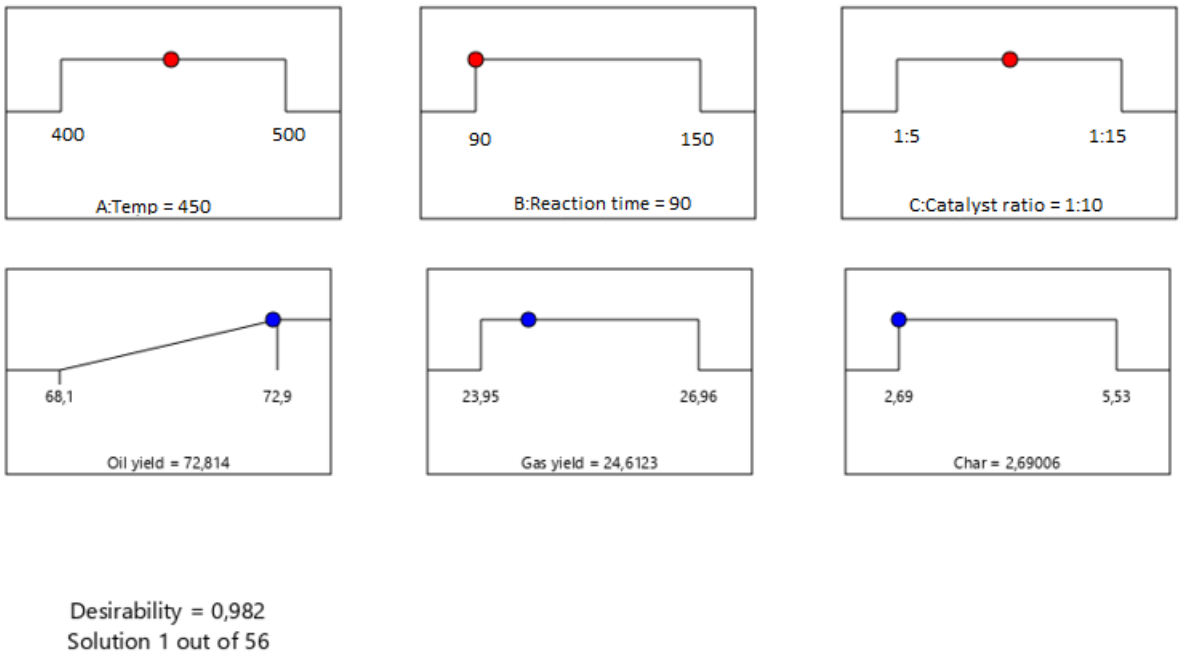

Figure 6.5: Desirability ramps on process optimization of three independent variables for catalytic pyrolysis of mixed plastic wastes yield (%).

6.8 Characterization of the liquid oil produced

The physical and chemical properties of the produced liquid oil were measured according to the test methods recommended by the American Society for Testing and Materials (ASTM) and South African National Standard (SANS) as follows; viscosity at 40 ^{0}C, water content, density at 20 ^{0}C, ash content, cetane number, total contamination, gross calorific value, sulphur and flash point. The results of these characterizations are listed in Table 6.7.

Table 6.7: Physical properties of liquid fuel obtained by catalytic pyrolysis of mixed plastic wastes at optimized conditions.

Characteristic	Test	Units	Result	SANS 342 specification
Density @ 20 ºC	IP 365	g/ml	0.821	0.800 min
Flash point	IP 34	ºC	56	55 min
Viscosity @ 40 ºC	IP71	cSt	2.84	2.2 – 5.3
Ash content	IP4	% m/m	<0.01	0.01 max
Sulphur content (XRF)	-	% m/m	0.01	0.05 max
Cetane number	ASTM D613	-	48	45 min
Water content	ASTM D4377	% m/m	-	0.05 max
Total contamination	-	Mg/kg	1	24 max
Gross calorific value	-	MJ/kg	41.82	40 – 45

The results show that the liquid produced from catalytic pyrolysis of mixed plastic wastes at optimized conditions is within SANS 342 standard specifications and the American Society for Testing and Materials (ASTM) diesel fuel specification. The properties are numerous, but the most important ones are those that have a direct impact on the performance of the engine, such as viscosity because of its effect on the atomization of the fuel being injected into the engine combustion compartment, the flash point, which is much higher than diesel, density which is lesser than water and so on. All these properties help to increase the engine's lifespan, give better lubrication and complete combustion so that the engine can produce a higher energy output.

6.9 Summary

The response surface methodology (RSM) was used to optimize the catalytic pyrolysis process of chosen mixed plastic waste (PE, PP, and PS), and three independent experimental variables (temperature, reaction duration, and catalyst concentration) were considered in order to increase the liquid fuel production.

RSM successfully completed an optimization procedure with less expensive experiments (< number of experimental runs). For a maximum liquid fuel yield of 72.7%, gas yield of 24.6%, and char of 2.6% with optimization desirability of 98.2%, the experimental variables' optimal values were 450 ^{o}C, 90 min, and 1:10 for the reaction temperature, reaction duration, and catalyst-to-waste plastic ratio, respectively. The derived quadratic model has a high R^2 determination coefficient and matches the response well (0.9184). The liquid fuel's properties achieved under these optimal conditions met ASTM requirements with a high heating value of (41.82 MJ/kg).

The final product demonstrated that plastic wastes could serve as an inexpensive source of raw materials for the production of liquid fuel. It is thought to be another strategy for mitigating environmental issues brought on by plastic waste management and is a promising option to valorize plastic garbage.

CHAPTER 7: CONCLUSION AND RECOMMENDATIONS

Plastics appear to be an integral part of our daily life, but only about 25% of the plastic that ends up in landfills is recycled. Due to the rapid growth in population and urbanization, the amount of waste produced annually is predicted to increase by 70% to over 3.4 billion tonnes in 2050. The issue of what happens to plastic beyond its useful life is a concern because it is currently very difficult to find a substitute. The plastics life cycle involves energy significantly. The world is challenged with finding the proper fuel that won't exhaust finite supplies while simultaneously lowering environmental issues due to the rising demand for energy. From a sustainability perspective, energy spent in production should be recovered by the time a product has reached the end of its useful life.

To address the continually expanding volume of plastic waste and satisfy the rising energy demand, catalytic pyrolysis of waste plastic is the most practical way. In this study, locally produced ZSM-5 zeolite derived from South African kaolin, catalytic pyrolysis was used to convert independent and mixed plastic garbage into liquid oil and other value-added products. Three kaolin samples (G1, G3, and G10) from different locations in Grahamstown, South Africa, were chosen for the synthesis of ZSM-5 due to their availability, abundance, and high alumina/silica content. There is a need to find a local substitute because commercial ZSM-5 zeolite is costly and hard to come by. From the local kaolin raw materials, ZSM-5 zeolite was effectively produced. In this study, crystallization temperature, ageing time, and crystallization duration all influenced the formation of crystalline ZSM-5 zeolite. When compared to other synthesized catalysts (G1/ZSM-5, G3/ZSM-5), the analysis revealed that G10/ZSM-5 had higher specifications, including good crystallinity structure, pore size, and Si/Al ratio.

In order to investigate the operational conditions and determine the ideal ranges for the optimization studies, preliminary tests were conducted on chosen individual and combined plastic wastes (PP, PE, PS, PET, PP/PS/PE, and so on).

The pyrolysis reaction of feedstock into liquid oil, gas, and char was successfully accomplished through the use of the locally synthesized ZSM-5 catalyst. The findings of the experiments demonstrated the outstanding activity and stability of the produced zeolite during the catalytic pyrolysis process. As a result, using ZSM-5 zeolite made from South African kaolin as a solid catalyst is effective and can be used as a substitute for ZSM-5 zeolite that is sold in stores.

Using commercial and synthetic zeolite catalysts, respectively, the catalytic pyrolysis of PS yielded the highest percentages of liquid oil (56 and 51%) compared to PP (38% and 44.7%) and PE (56% and 48%). According to the results of the preliminary experiments, the impacts of parameters such as temperature, reaction duration, and catalyst concentration were significant. Using GC-MS to evaluate the pyrolysis oil's chemical components, it was discovered that most of the liquid oil produced had a high aromatic content and some aliphatic and other hydrocarbon components. The FTIR analysis, which revealed distinct peaks for aromatic and other hydrocarbon functional groups, further supported these findings. Additionally, liquid oil produced from various sources of plastic waste had greater heating values (HHV) that were comparable to regular diesel and ranged from 30.6-46.5 MJ/kg. As a result, with further processing and refinement, the produced liquid oil may be used for various varieties of energy and transportation purposes.

Data analysis and model equation generation for the response variables were done using the Response Surface methodology based on Central Composite Design (CCD). The optimization desirability plot displayed the optimal response region based on the model equation's generated results. Surface and contour plots were utilized efficiently to determine the optimal factor combinations for producing the highest yield.

Overall, it can be concluded that the feedstocks employed (single and mixed plastic waste) are good sources for producing a variety of valuable chemicals and hydrocarbons.

At the optimum temperature of 450 ^{o}C, reaction period of 90 min, and catalyst concentration of 1:10, various hydrocarbons were generated with a maximum conversion rate of 72.10 %. The liquid fuel produced contained components similar to those found in fossil fuels and can therefore be used as an alternative to fossil fuels.

7.1 Recommendations for future

From the above results, it can be concluded that ZSM-5 synthesized from South African kaolin work very well in the pyrolysis of individual and mixed municipal plastic wastes. However, further studies are required to materialize the process. The followings are the recommendations for future work.

- Development of a continuous process for plastic pyrolysis using a suitable catalyst.
- Development of business case for pilot plant and commercial scale production.
- Further research is needed to understand the detailed composition of produced gases, their health and environmental concerns, and their potential to be used as an alternative fuel.
- Explore further applications of produced liquid oil, gases and char to make this technology more economically sustainable.
- Comprehensive life cycle assessment (LCA) of catalytic pyrolysis, including feedstock, to fully understand the economic, environmental and overall sustainability of this technology

REFERENCES

Adams, D.J., Dyson, P.J. and Tavener, S.J., 2015. *Chemistry in alternative reaction media*. John Wiley & Sons.

Ahmad, I., Ismail Khan, M., Khan, H., Ishaq, M., Tariq, R., Gul, K. and Ahmad, W. 2015. Pyrolysis study of polypropylene and polyethylene into premium oil products. International Journal of Green Energy. 12(7):663–671. DOI: 10.1080/15435075.2014.880146.

Aisien, E.T., Otuya, I.C. and Aisien, F.A. 2021. Thermal and catalytic pyrolysis of waste polypropylene plastic using spent FCC catalyst. Environmental Technology and Innovation. 22:101455. DOI: 10.1016/j.eti.2021.101455.

Ajibola, A.A., Omoleye, J.A. and Efeovbokhan, V.E., 2018. Catalytic cracking of polyethylene plastic waste using synthesised zeolite Y from Nigerian kaolin deposit. Applied Petrochemical Research, 8(4), pp.211-217.

Alam. S.S., Husain Khan. A., and Khan. N.A., 2022. Plastic waste management via thermochemical conversion of plastics into fuel: a review. *Energy Sources. Part A: Recovery. Utilization. and Environmental Effects*. *44*(3). pp.1-20.

Ali, S.S., Elsamahy, T., Abdelkarim, E.A., Al-Tohamy, R., Kornaros, M., Ruiz, H.A., Zhao, T., Li, F. and Sun, J., 2022. Biowastes for biodegradable bioplastics production and end-of-life scenarios in circular bioeconomy and biorefinery concept. Bioresource Technology, p.127869.

Ali, S.S., Elsamahy, T., Koutra, E., Kornaros, M., El-Sheekh, M., Abdelkarim, E.A., Zhu, D. and Sun, J., 2021. Degradation of conventional plastic wastes in the environment: A review on current status of knowledge and future perspectives of disposal. Science of The Total Environment, 771, p.144719.

Al-Rumaihi, A., Shahbaz, M., Mckay, G., Mackey, H. and Al-Ansari, T., 2022. A review of pyrolysis technologies and feedstock: A blending approach for plastic and biomass towards optimum biochar yield. Renewable and Sustainable Energy Reviews, 167, p.112715.

Al-Salem, S.M., Antelava, A., Constantinou, A., Manos, G. and Dutta, A., 2017. A review on thermal and catalytic pyrolysis of plastic solid waste (PSW). Journal of environmental management, 197, pp.177-198.

Alwai Alcheikhhamdon, Y., 2021. Propylene-propane separation using mixed matrix films made of functionalized polymers and zeolitic-imidazolate frameworks (Doctoral dissertation, University of British Columbia).

Andler-Osorio, R., 2020. Bacterial and enzymatic degradation of poly (cis-1, 4-isoprene) rubber: Novel biotechnological applications.

Anene. A.F., Fredriksen. S.B., Sætre. K.A. and Tokheim. L.A., 2018. Experimental study of thermal and catalytic pyrolysis of plastic waste components. Sustainability. 10(11). p.3979.

Arabella Ruiz, 25 Plastic Waste Statistics That Will Shock You https://theroundup.org/plastic-waste-statistics/

Bacakova, L., Vandrovcova, M., Kopova, I. and Jirka, I., 2018. Applications of zeolites in biotechnology and medicine–a review. Biomaterials science, 6(5), pp.974-989.

Bai, C., Dallasega, P., Orzes, G. and Sarkis, J., 2020. Industry 4.0 technologies assessment: A sustainability perspective. International journal of production economics, 229, p.107776.

Beg, S., Swain, S., Rahman, M., Hasnain, M.S. and Imam, S.S., 2019. Application of design of experiments (DoE) in pharmaceutical product and process optimization. In Pharmaceutical quality by design (pp. 43-64). Academic Press.

Berrueco, C., Mastral, F.J., Esperanza, E. and Ceamanos, J., 2002. Production of waxes and tars from the continuous pyrolysis of high density polyethylene. Influence of operation variables. Energy & fuels, 16(5), pp.1148-1153.

Bhat, M.A., Gedik, K. and Gaga, E.O., 2022. Atmospheric micro (nano) plastics: future growing concerns for human health. Air Quality, Atmosphere & Health, pp.1-30.

Bhattacharya, P., Steele, P.H., Hassan, E.B.M., Mitchell, B., Ingram, L. and Pittman, C.U. 2009. Wood/plastic copyrolysis in an auger reactor: Chemical and physical analysis of the products. Fuel. 88(7):1251–1260. DOI: 10.1016/j.fuel.2009.01.009.

Birch, B., Buttsworth, D. and Zander, F., 2020. Measurements of freestream density fluctuations in a hypersonic wind tunnel. Experiments in Fluids, 61(7), pp.1-13.

Boumanchar, I., Chhiti, Y., Alaoui, F.E.M.H., Elkhouakhi, M., Sahibed-Dine, A., Bentiss, F., Jama, C. and Bensitel, M., 2019. Investigation of (co)-combustion kinetics of biomass, coal and municipal solid wastes. Waste Management, 97, pp.10-18.

Budsaereechai, S., Hunt, A.J. and Ngernyen, Y., 2019. Catalytic pyrolysis of plastic waste for the production of liquid fuels for engines. RSC advances, 9(10), pp.5844-5857.

Busca. G., 2020. Silica-alumina catalytic materials: A critical review. *Catalysis Today*. *357*. pp.621-629.

Çepelioğullar, Ö. and Pütün, A.E., 2013. Utilization of two different types of plastic wastes from daily and industrial life. Journal of Selcuk University Natural and Applied Science, 2(2), pp.694-706.

Chai, Y., Wang, M., Gao, N., Duan, Y. and Li, J., 2020. Experimental study on pyrolysis/gasification of biomass and plastics for H2 production under new dual-support catalyst. Chemical Engineering Journal, 396, p.125260.

Chen, H., Wan, K., Zhang, Y. and Wang, Y., 2021. Waste to wealth: chemical recycling and chemical upcycling of waste plastics for a great future. ChemSusChem, 14(19), pp.4123-4136.

Chen, H.L., Nath, T.K., Chong, S., Foo, V., Gibbins, C. and Lechner, A.M., 2021. The plastic waste problem in Malaysia: management, recycling and disposal of local and global plastic waste. SN Applied Sciences, 3(4), pp.1-15.

Cheng, Y., Song, W., Tian, H., Zhang, K., Li, B., Du, Z., Zhang, W., Wang, J., Wang, J. and Zhu, L., 2021. The effects of high-density polyethylene and polypropylene microplastics on the soil and earthworm Metaphire guillelmi gut microbiota. Chemosphere, 267, p.129219.

Chunfeng, W., Jiansheng, L.I., Xia, S.U.N., Lianjun, W.A.N.G. and Xiuyun, S.U.N., 2009. Evaluation of zeolites synthesized from fly ash as potential adsorbents for wastewater containing heavy metals. Journal of environmental sciences, 21(1), pp.127-136.

Ciliz, N.K., Ekinci, E. and Snape, C.E., 2004. Pyrolysis of virgin and waste polypropylene and its mixtures with waste polyethylene and polystyrene. Waste management, 24(2), pp.173-181.

d'Ambrières, W., 2019. Plastics recycling worldwide: current overview and desirable changes. Field Actions Science Reports. The journal of field actions, (Special Issue 19), pp.12-21.

Dabros, T.M., Stummann, M.Z., Høj, M., Jensen, P.A., Grunwaldt, J.D., Gabrielsen, J., Mortensen, P.M. and Jensen, A.D., 2018. Transportation fuels from biomass fast pyrolysis, catalytic hydrodeoxygenation, and catalytic fast hydropyrolysis. Progress in Energy and Combustion Science, 68, pp.268-309.

Dai, L., Zhou, N., Lv, Y., Cheng, Y., Wang, Y., Liu, Y., Cobb, K., Chen, P., Lei, H. and Ruan, R., 2022. Pyrolysis technology for plastic waste recycling: A state-of-the-art review. Progress in Energy and Combustion Science, 93, p.101021.

de Silveira, G., Forsberg, P. and Conners, T.E., 2020. Scanning electron microscopy: A tool for the analysis of wood pulp fibers and paper. In Surface analysis of paper (pp. 41-71). CRC Press.

De Stefanis, A., Cafarelli, P., Gallese, F., Borsella, E., Nana, A. and Perez, G., 2013. Catalytic pyrolysis of polyethylene: A comparison between pillared and restructured clays. Journal of Analytical and Applied Pyrolysis, 104, pp.479-484.

Demirbaş, A. 2002. Gaseous products from biomass by pyrolysis and gasification: Effects of catalyst on hydrogen yield. Energy Conversion and Management. 43(7):897–909. DOI: 10.1016/S0196-8904(01)00080-2.

Demirbas, A. 2004. Pyrolysis of municipal plastic wastes for recovery of gasoline-range hydrocarbons. Journal of Analytical and Applied Pyrolysis. 72(1):97–102. DOI: 10.1016/j.jaap.2004.03.001.

Dewangga, P.B. and Purnomo, C.W., 2020. Styrene Recovery from the Pyrolysis of Polystyrene Waste Using Bentonite and Natural Zeolite Catalyst. In Key Engineering Materials (Vol. 849, pp. 84-89). Trans Tech Publications Ltd.

Ding, K., Liu, S., Huang, Y., Liu, S., Zhou, N., Peng, P., Wang, Y., Chen, P. and Ruan, R., 2019. Catalytic microwave-assisted pyrolysis of plastic waste over NiO and HY for gasoline-range hydrocarbons production. Energy Conversion and Management, 196, pp.1316-1325.

Dogu, O., Pelucchi, M., Van de Vijver, R., Van Steenberge, P.H., D'hooge, D.R., Cuoci, A., Mehl, M., Frassoldati, A., Faravelli, T. and Van Geem, K.M., 2021. The chemistry of chemical recycling of solid plastic waste via pyrolysis and gasification: State-of-the-art, challenges, and future directions. Progress in Energy and Combustion Science, 84, p.100901.

Du, S., Valla, J.A., Parnas, R.S. and Bollas, G.M., 2016. Conversion of polyethylene terephthalate based waste carpet to benzene-rich oils through thermal, catalytic, and catalytic steam pyrolysis. ACS Sustainable Chemistry & Engineering, 4(5), pp.2852-2860.

Dwivedi, P., Mishra, P.K., Mondal, M.K. and Srivastava, N., 2019. Non-biodegradable polymeric waste pyrolysis for energy recovery. Heliyon, 5(8), p.e02198.

Ellis, L.D., Rorrer, N.A., Sullivan, K.P., Otto, M., McGeehan, J.E., Román-Leshkov, Y., Wierckx, N. and Beckham, G.T., 2021. Chemical and biological catalysis for plastics recycling and upcycling. Nature Catalysis, 4(7), pp.539-556.

Elordi, G., Olazar, M., Castaño, P., Artetxe, M. and Bilbao, J. 2012. Polyethylene cracking on a spent FCC catalyst in a conical spouted bed. Industrial and Engineering Chemistry Research. 51(43):14008–14017. DOI: 10.1021/ie3018274.

Escola, J.M., Aguado, J., Serrano, D.P., García, A., Peral, A., Briones, L., Calvo, R. and Fernandez, E., 2011. Catalytic hydroreforming of the polyethylene thermal cracking oil over Ni supported hierarchical zeolites and mesostructured aluminosilicates. Applied Catalysis B: Environmental, 106(3-4), pp.405-415.

Evode, N., Qamar, S.A., Bilal, M., Barceló, D. and Iqbal, H.M., 2021. Plastic waste and its management strategies for environmental sustainability. Case Studies in Chemical and Environmental Engineering, 4, p.100-142.

Fakhrhoseini, S.M. and Dastanian, M. 2013. Predicting pyrolysis products of PE, PP, and PET using NRTL activity coefficient model. Journal of Chemistry. 2013. DOI: 10.1155/2013/487676.

Fang, K., Liu, M.Q., Qin, H. and Zhou, Y.D., 2018. Theory and application of uniform experimental designs (Vol. 221). Singapore: Springer.

Faraca, G. and Astrup, T., 2019. Plastic waste from recycling centres: Characterisation and evaluation of plastic recyclability. Waste Management, 95, pp.388-398.

Forfás, I., 2007. Waste Management in Ireland: Benchmarking Analysis and Policy Priorities. Update 2010. Forfás.

Fortman, D.J., Brutman, J.P., De Hoe, G.X., Snyder, R.L., Dichtel, W.R. and Hillmyer, M.A., 2018. Approaches to sustainable and continually recyclable cross-linked polymers. ACS Sustainable Chemistry & Engineering, 6(9), pp.11145-11159.

Gebre, S.H., Sendeku, M.G. and Bahri, M., 2021. Recent Trends in the Pyrolysis of Non-Degradable Waste Plastics. ChemistryOpen, 10(12), pp.1202-1226.

Goh, B.H.H., Chong, C.T., Ong, H.C., Seljak, T., Katrašnik, T., Józsa, V., Ng, J.H., Tian, B., Karmarkar, S. and Ashokkumar, V., 2022. Recent advancements in catalytic conversion pathways for synthetic jet fuel produced from bioresources. Energy Conversion and Management, 251, p.114974.

Grause, G., Handa, T., Kameda, T., Mizoguchi, T. and Yoshioka, T., 2011. Effect of temperature management on the hydrolytic degradation of PET in a calcium oxide filled tube reactor. Chemical engineering journal, 166(2), pp.523-528.

Hahladakis. J.N. and Iacovidou. E., 2018. Closing the loop on plastic packaging materials: What is quality and how does it affect their circularity? *Science of the Total Environment*. *630*. pp.1394-1400.

Hakeem, I.G., Aberuagba, F. and Musa, U. 2018. Catalytic pyrolysis of waste polypropylene using Ahoko kaolin from Nigeria. Applied Petrochemical Research. 8(4):203–210. DOI: 10.1007/s13203-018-0207-8.

Harussani. M.M., Sapuan. S.M., Nadeem. G., Rafin. T. and Kirubaanand. W., 2022. Recent applications of carbon-based composites in defence industry: A review. *Defence Technology*.

Heikkinen, J.M., Hordijk, J.C., De Jong, W. and Spliethoff, H. 2004. Thermogravimetry as a tool to classify waste components to be used for energy generation. Journal of Analytical and Applied Pyrolysis. 71(2):883–900. DOI: 10.1016/j.jaap.2003.12.001.

Heracleous, E., Pachatouridou, E., Hernández-Giménez, A.M., Hernando, H., Fakin, T., Paioni, A.L., Baldus, M., Serrano, D.P., Bruijnincx, P.C.A., Weckhuysen, B.M. and Lappas, A.A., 2019. Characterization of deactivated and regenerated zeolite ZSM-5-based catalyst extrudates used in catalytic pyrolysis of biomass. Journal of Catalysis, 380, pp.108-122.

Horodytska, O., Cabanes, A. and Fullana, A., 2019. Plastic waste management: current status and weaknesses. In Plastics in the Aquatic Environment-Part I (pp. 289-306). Springer, Cham.

Hou, Q., Zhen, M., Qian, H., Nie, Y., Bai, X., Xia, T., Rehman, M.L.U., Li, Q. and Ju, M., 2021. Upcycling and catalytic degradation of plastic wastes. Cell Reports Physical Science, 2(8), p.100514.

Hradil, D. and Hostomský, J., 2002. Effect of composition and physical properties of natural kaolinitic clays on their strong acid weathering rates. Catena, 49(1-2), pp.171-181.

Hu, Y., Yu, W., Wibowo, H., Xia, Y., Lu, Y. and Yan, M. 2019. Effect of catalysts on distribution of polycyclic-aromatic hydrocarbon (PAHs) in bio-oils from the pyrolysis of dewatered sewage sludge at high and low temperatures. Science of the Total Environment. 667:263–270. DOI: 10.1016/j.scitotenv.2019.02.320.

Huang. J., Veksha. A., Chan. W.P., Giannis. A. and Lisak. G., 2022. Chemical recycling of plastic waste for sustainable material management: A prospective review on catalysts and processes. *Renewable and Sustainable Energy Reviews*. *154*. p.111866.

Idumah, C.I. and Nwuzor, I.C., 2019. Novel trends in plastic waste management. SN Applied Sciences, 1(11), pp.1-14.

Idumah. C.I., 2022. Recent advancements in thermolysis of plastic solid wastes to liquid fuel. *Journal of Thermal Analysis and Calorimetry*. *147*(5). pp.3495-3508.

Jambeck, J., Hardesty, B.D., Brooks, A.L., Friend, T., Teleki, K., Fabres, J., Beaudoin, Y., Bamba, A., Francis, J., Ribbink, A.J. and Baleta, T., 2018. Challenges and emerging solutions to the land-based plastic waste issue in Africa. Marine Policy, 96, pp.256-263.

Janssen, R., Turhollow, A.F., Rutz, D. and Mergner, R. 2013. Production facilities for second-generation biofuels in the USA and the EU - current status and future perspectives. Biofuels, Bioproducts and Biorefining. 7(6):647–665. DOI: 10.1002/bbb.1451.

Jonscher, C., Seifert, M., Kretzschmar, N., Marschall, M.S., Le Anh, M., Doert, T., Busse, O. and Weigand, J.J., 2022. Origin of Morphology Change and Effect of Crystallization Time and Si/Al Ratio during Synthesis of Zeolite ZSM-5. ChemCatChem, 14(3), p.e 202101248.

Jung, S.H., Cho, M.H., Kang, B.S. and Kim, J.S., 2010. Pyrolysis of a fraction of waste polypropylene and polyethylene for the recovery of BTX aromatics using a fluidized bed reactor. Fuel processing technology, 91(3), pp.277-284.

Kalem, M.S., 2022. Effect of fractional distillation pretreatment on fuel quality of plastic waste pyrolytic oils. Separation and Purification Technology, 300, p.121859.

Karimi, S., Feizy, J., Mehrjo, F. and Farrokhnia, M. 2016. Detection and quantification of food colorant adulteration in saffron sample using chemometric analysis of FT-IR spectra. RSC Advances. 6(27):23085–23093. DOI: 10.1039/c5ra25983e.

Karnjanakom, S., Bayu, A., Xiaoketi, P., Hao, X., Kongparakul, S., Samart, C., Abudula, A. and Guan, G., 2016. Selective production of aromatic hydrocarbons from catalytic pyrolysis of biomass over Cu or Fe loaded mesoporous rod-like alumina. Rsc Advances, 6(56), pp.50618-50629.

Kazemimoghadam, M. and Mohammadi, T., 2011. Preparation of nano pore hydroxysodalite zeolite membranes using of kaolin clay and chemical sources. Desalination, 278(1-3), pp.438-442.

Ke, H., Li-Hua, T., Zi-Bin, Z. and Cheng-fang, Z., 2005. Reaction mechanism of styrene monomer recovery from waste polystyrene by supercritical solvents. Polymer degradation and stability, 89(2), pp.312-316.

Khan, A.H., Sharholy, M., Alam, P., Al-Mansour, A.I., Ahmad, K., Kamal, M.A., Alam, S., Pervez, M.N. and Naddeo, V., 2022. Evaluation of cost benefit analysis of municipal solid waste management systems. Journal of King Saud University-Science, 34(4), p.101997.

Khan, M.I., Lubner, S.D., Ogletree, D.F. and Dames, C., 2018. Temperature dependence of secondary electron emission: A new route to nanoscale temperature measurement using scanning electron microscopy. Journal of Applied Physics, 124(19), p.195104.

Khan, S., Anjum, R., Raza, S.T., Bazai, N.A. and Ihtisham, M., 2022. Technologies for municipal solid waste management: Current status, challenges, and future perspectives. Chemosphere, 288, p.132403.

Kiran, N., Ekinci, E. and Snape, C.E., 2000. Recyling of plastic wastes via pyrolysis. Resources, Conservation and Recycling, 29(4), pp.273-283.

Kremer, I., Tomić, T., Katančić, Z., Erceg, M., Papuga, S., Parlov Vuković, J. and Schneider, D.R., 2022. Catalytic pyrolysis and kinetic study of real-world waste plastics: multi-layered and mixed resin types of plastics. Clean Technologies and Environmental Policy, 24(2), pp.677-693.

Król. M., 2020. Natural vs. synthetic zeolites. *Crystals*. *10*(7). p.622.

Kumagai, S., Morohoshi, Y., Grause, G., Kameda, T. and Yoshioka, T., 2015. Pyrolysis versus hydrolysis behavior during steam decomposition of polyesters using 18 O-labeled steam. RSC advances, 5(76), pp.61828-61837.

Kumagai, S., Yamasaki, R., Kameda, T., Saito, Y., Watanabe, A., Watanabe, C., Teramae, N. and Yoshioka, T., 2020. Catalytic Pyrolysis of Poly (ethylene terephthalate) in the Presence of Metal Oxides for Aromatic Hydrocarbon Recovery Using Tandem μ-Reactor-GC/MS. Energy & Fuels, 34(2), pp.2492-2500.

Kumagai, S., Yamasaki, R., Kameda, T., Saito, Y., Watanabe, A., Watanabe, C., Teramae, N. and Yoshioka, T., 2018. Aromatic hydrocarbon selectivity as a function of CaO basicity and aging during CaO-catalyzed PET pyrolysis using tandem μ-reactor-GC/MS. Chemical Engineering Journal, 332, pp.169-173.

Kumar Mishra, R. and Mohanty, K. 2020. Effect of low-cost catalysts on yield and properties of fuel from waste biomass for hydrocarbon-rich oil production. Materials Science for Energy Technologies. 3:526–535. DOI: 10.1016/j.mset.2020.05.007.

Kumar, S., Panda, A.K. and Singh, R.K., 2011. A review on tertiary recycling of high-density polyethylene to fuel. Resources, Conservation and Recycling, 55(11), pp.893-910.

Law, K.L. and Narayan, R., 2022. Reducing environmental plastic pollution by designing polymer materials for managed end-of-life. Nature Reviews Materials, 7(2), pp.104-116.

Leatherdale, S.T., 2019. Natural experiment methodology for research: a review of how different methods can support real-world research. International Journal of Social Research Methodology, 22(1), pp.19-35.

Lebreton. L. and Andrady. A., 2019. Future scenarios of global plastic waste generation and disposal. *Palgrave Communications*. *5*(1). pp.1-11.

Lee, K.H., 2012. Effects of the types of zeolites on catalytic upgrading of pyrolysis wax oil. Journal of Analytical and Applied Pyrolysis, 94, pp.209-214.

Lee. W.T., van Muyden. A., Bobbink. F.D., Mensi. M.D., Carullo. J.R. and Dyson. P.J., 2022. Mechanistic classification and benchmarking of polyolefin depolymerization over silica-alumina-based catalysts. *Nature Communications*. *13*(1). pp.1-13.

Li, W., Wang, D., Zhu, Y., Chen, J., Lu, Y., Li, S., Zheng, Y. and Zheng, Z., 2020. Efficient ex-situ catalytic upgrading of biomass pyrolysis vapors to produce methylfurans and phenol over bio-based activated carbon. Biomass and Bioenergy, 142, p.105794.

Li, Z., Jia, X., Jin, H., Ma, L., Xu, C. and Wei, H., 2021. Determining optimal municipal solid waste management scenario based on best-worst method. Journal of Environmental Engineering and Landscape Management, 29(2), pp.150-161.

Lin, X., Lei, H., Huo, E., Qian, M., Mateo, W., Zhang, Q., Zhao, Y., Wang, C. and Villota, E., 2020. Enhancing jet fuel range hydrocarbons production from catalytic co-pyrolysis of Douglas fir and low-density polyethylene over bifunctional activated carbon catalysts. Energy Conversion and Management, 211, p.112757.

Liu, J., Wang, S., Peng, Y., Zhu, J., Zhao, W. and Liu, X., 2021. Advances in sustainable thermosetting resins: From renewable feedstock to high performance and recyclability. Progress in Polymer Science, 113, p.101-353.

Liu, R., Rahman, M.M., Sarker, M., Chai, M., Li, C. and Cai, J., 2020. A review on the catalytic pyrolysis of biomass for the bio-oil production with ZSM-5: Focus on structure. Fuel Processing Technology, 199, p.106301.

López, A., de Marco, I., Caballero, B.M., Adrados, A. and Laresgoiti, M.F. 2011. Deactivation and regeneration of ZSM-5 zeolite in catalytic pyrolysis of plastic wastes. Waste Management. 31(8):1852–1858. DOI: 10.1016/j.wasman.2011.04.004.

Luyt, A.S. and Malik, S.S., 2019. Can biodegradable plastics solve plastic solid waste accumulation? In Plastics to energy (pp. 403-423). William Andrew Publishing.

Maafa, I.M., 2021. Pyrolysis of polystyrene waste: A review. Polymers, 13(2), p.225.

Maisarah, M., Bong, C.P.C., Ho, W.S., Lim, J.S., Ab Muis, Z., Hashim, H., Elagroudy, S., Teck, G.L.H. and Ho, C.S., 2018. Review on the suitability of waste for appropriate waste-to-energy technology. Chemical Engineering Transactions, 63, pp.187-192.

Mangesh, V.L., Padmanabhan, S., Tamizhdurai, P. and Ramesh, A. 2020. Experimental investigation to identify the type of waste plastic pyrolysis oil suitable for conversion to diesel engine fuel. Journal of Cleaner Production. 246:119066. DOI: 10.1016/j.jclepro.2019.119066.

Marcilla, A., Beltrán, M.I. and Navarro, R. 2008. Evolution of products generated during the dynamic pyrolysis of LDPE and HDPE over HZSM5. Energy and Fuels. 22(5):2917–2924. DOI: 10.1021/ef800229d.

Marcilla, A., García-Quesada, J.C., Sánchez, S. and Ruiz, R., 2005. Study of the catalytic pyrolysis behaviour of polyethylene–polypropylene mixtures. Journal of Analytical and Applied Pyrolysis, 74(1-2), pp.387-392.

Mariappan, M., Panithasan, M.S. and Venkadesan, G. 2021. Pyrolysis plastic oil production and optimisation followed by maximum possible replacement of diesel with bio-oil/methanol blends in a CRDI engine. Journal of Cleaner Production. 312:127687. DOI: 10.1016/j.jclepro.2021.127687.

Mastral, F.J., Esperanza, E., Garcıa, P. and Juste, M., 2002. Pyrolysis of high-density polyethylene in a fluidised bed reactor. Influence of the temperature and residence time. Journal of Analytical and Applied Pyrolysis, 63(1), pp.1-15.

Mawson, T., Nakamura, A., Petersen, T.C., Shibata, N., Sasaki, H., Paganin, D.M., Morgan, M.J. and Findlay, S.D., 2020. Suppressing dynamical diffraction artefacts in differential phase contrast scanning transmission electron microscopy of long-range electromagnetic fields via precession. Ultramicroscopy, 219, p.113097.

Melaningtyas, G.S.A., Krisnandi, Y.K. and Ekananda, R., 2019, March. Synthesis and characterization of NaY zeolite from Bayat natural zeolite: effect of pH on synthesis. In IOP Conference Series: Materials Science and Engineering (Vol. 496, No. 1, p. 012042). IOP Publishing.

Mgbemere, H., Ekpe, I. and Lawal, G., 2017. Zeolite synthesis, characterization and application areas: a review.

Mhaske, S.T., Mestry, S.U. and Patil, D.A., 2022. Cross-linking of polymers by various radiations: Mechanisms and parameters. In Radiation Technologies and Applications in Materials Science (pp. 1-28). CRC Press.

Miandad, R., Barakat, M.A., Aburiazaiza, A.S., Rehan, M. and Nizami, A.S. 2016. Catalytic pyrolysis of plastic waste: A review. Process Safety and Environmental Protection. 102:822–838. DOI: 10.1016/j.psep.2016.06.022.

Miandad, R., Barakat, M.A., Aburiazaiza, A.S., Rehan, M., Ismail, I.M.I. and Nizami, A.S., 2017. Effect of plastic waste types on pyrolysis liquid oil. International biodeterioration & biodegradation, 119, pp.239-252.

Miandad, R., Nizami, A.S., Rehan, M., Barakat, M.A., Khan, M.I., Mustafa, A., Ismail, I.M.I. and Murphy, J.D. 2016. Influence of temperature and reaction time on the conversion of polystyrene waste to pyrolysis liquid oil. Waste Management. 58:250–259. DOI: 10.1016/j.wasman.2016.09.023.

Miandad, R., Rehan, M., Barakat, M. A., Aburiazaiza, A. S., Khan, H., Ismail, I. M. I., Dhavamani, J., Gardy, J., Hassanpour, A., Nizami, A.S., 2019. Catalytic Pyrolysis of Plastic Waste: Moving Toward Pyrolysis Based Biorefineries. Front. Energy Res., 7, 27.

Miller, M.P., Pagan, D.C., Beaudoin, A.J., Nygren, K.E. and Shadle, D.J., 2020. Understanding micromechanical material behavior using synchrotron X-rays and in situ loading. Metallurgical and materials transactions A, 51(9), pp.4360-4376.

Millet. H., Vangheluwe. P., Block. C., Sevenster. A., Garcia. L. and Antonopoulos. R., 2018. The nature of plastics and their societal usage.

Miskolczi, N., 2006. Kinetic model of the chemical and catalytic recycling of waste polyethylene into fuels. Feedstock Recycling and Pyrolysis of Waste Plastics: Converting Waste Plastics into Diesel and Other Fuels, pp.225-247.

Miskolczi, N., Bartha, L. and Deák, G. 2006. Thermal degradation of polyethylene and polystyrene from the packaging industry over different catalysts into fuel-like feed stocks. In Polymer Degradation and Stability. V. 91. Elsevier. 517–526. DOI: 10.1016/j.polymdegradstab.2005.01.056.

Mohamed, B.A., Ellis, N., Kim, C.S. and Bi, X. 2019. Microwave-assisted catalytic biomass pyrolysis: Effects of catalyst mixtures. Applied Catalysis B: Environmental. 253:226–234. DOI: 10.1016/j.apcatb.2019.04.058.

Moshoeshoe, M., Nadiye-Tabbiruka, M.S. and Obuseng, V., 2017. A review of the chemistry, structure, properties and applications of zeolites. Am. J. Mater. Sci, 7(5), pp.196-221.

Murray, H.H., Pozo, M. and Galán, E., 2011. An introduction to palygorskite and sepiolite deposits—location, geology and uses. In Developments in clay science (Vol. 3, pp. 85-99). Elsevier.

Nanda. S., and Berruti. F., 2021. A technical review of bioenergy and resource recovery from municipal solid waste. *Journal of hazardous materials*. *403*. p.123970.

Napper. I.E. and Thompson. R.C., 2020. Plastic debris in the marine environment: history and future challenges. *Global Challenges*. *4*(6). p.1900081.

Nasution, F., Husin, H., Abnisa, F., Yani, F.T. and Maulinda, L., 2022. Conversion of pyrolysis vapors derived from non-biodegradable waste plastics (PET) into valuable fuels using nickel-impregnated HZSM5-70 catalysts. Energy Conversion and Management, 273, p.116440.

Nemani, S.K., Annavarapu, R.K., Mohammadian, B., Raiyan, A., Heil, J., Haque, M.A., Abdelaal, A. and Sojoudi, H., 2018. Surface modification of polymers: methods and applications. Advanced Materials Interfaces, 5(24), p.1801247.

Nyankson, E., Efavi, J.K., Yaya, A., Manu, G., Asare, K., Daafuor, J. and Abrokwah, R.Y., 2018. Synthesis and characterisation of zeolite-A and Zn-exchanged zeolite-A based on natural aluminosilicates and their potential applications. Cogent Engineering, 5(1), p.1440480.

Oballim, T., 2021. Determination of the characteristics of solid fuel developed from a mixture of thermoplastic wastes and clay materials (Doctoral dissertation, Kyambogo University (Unpublished work)).

Olagunju, O.A. and Kiambi, S.L. 2021. Catalytic Pyrolysis of Municipal Solid Waste: Effect of South African synthesized zeolite on Polyethylene plastic waste. Proceedings of the South African Chemical Engineering Congress 2021. South Africa, 20 – 22 September 2021. ISBN 978-1-991213-99-0.

Olivera, M., Musso, M., De León, A., Volonterio, E., Amaya, A., Tancredi, N. and Bussi, J., 2020. Catalytic assessment of solid materials for the pyrolytic conversion of low-density polyethylene into fuels. Heliyon, 6(9), p.e05080.

Ong, H.C., Chen, W.H., Farooq, A., Gan, Y.Y., Lee, K.T. and Ashokkumar, V., 2019. Catalytic thermochemical conversion of biomass for biofuel production: A comprehensive review. Renewable and Sustainable Energy Reviews, 113, p.109266.

Onwudili, J.A., Insura, N. and Williams, P.T., 2009. Composition of products from the pyrolysis of polyethylene and polystyrene in a closed batch reactor: Effects of temperature and residence time. Journal of Analytical and Applied Pyrolysis, 86(2), pp.293-303.

Orjioke, M.N., Uchechukwu, O., Igwe, C.N. and Ajah, U., 2016. Synthesis and characterization of zeolite and its application in adsorption of nickel from aqueous solution. Journal Pharmaceutical and Chemical Biological Science, 4, pp.592-600.

Orzolek, M. ed., 2017. A guide to the manufacture, performance, and potential of plastics in agriculture. Elsevier.

Pan, T., Wu, Z. and Yip, A.C., 2019. Advances in the green synthesis of microporous and hierarchical zeolites: a short review. Catalysts, 9(3), p.274.

Panda, A.K. 2018. Thermo-catalytic degradation of different plastics to drop in liquid fuel using calcium bentonite catalyst. International Journal of Industrial Chemistry. 9(2):167–176. DOI: 10.1007/s40090-018-0147-2.

Papari, S., Bamdad, H. and Berruti, F., 2021. Pyrolytic conversion of plastic waste to value-added products and fuels: A review. Materials, 14(10), p.2586.

Park, J.J., Park, K., Kim, J.S., Maken, S., Song, H., Shin, H., Park, J.W. and Choi, M.J., 2003. Characterization of styrene recovery from the pyrolysis of waste expandable polystyrene. Energy & fuels, 17(6), pp.1576-1582.

Patel, K., Chikkali, S.H. and Sivaram, S., 2020. Ultrahigh molecular weight polyethylene: Catalysis, structure, properties, processing and applications. Progress in Polymer Science, 109, p.101290.

Patel. A.D., Zabeti. M., Seshan. K. and Patel. M.K., 2020. Comparative technical process and product assessment of catalytic and thermal pyrolysis of lignocellulosic biomass. *Processes*. *8*(12). p.1600.

Peng. Y., Wang. Y., Ke. L., Dai. L., Wu. Q., Cobb. K., Zeng. Y., Zou. R., Liu. Y. and Ruan. R., 2022. A review on catalytic pyrolysis of plastic wastes to high-value products. *Energy Conversion and Management*. *254*. p.115243.

Pezzatti, J., Boccard, J., Codesido, S., Gagnebin, Y., Joshi, A., Picard, D., González-Ruiz, V. and Rudaz, S., 2020. Implementation of liquid chromatography–high resolution mass spectrometry methods for untargeted metabolomic analyses of biological samples: A tutorial. Analytica Chimica Acta, 1105, pp.28-44.

Phanisankar, B.S.S., Rao, N.V. and Manikanta, J.E., 2020. Conversion of waste plastic to fuel products. Materials Today: Proceedings, 33, pp.5190-5195.

Prasetyoko, D., Santoso, M., Qoniah, I., Leaw, W.L., Firda, P.B. and Nur, H., 2020. A review on synthesis of kaolin-based zeolite and the effect of impurities. *Journal of the Chinese Chemical Society*, *67*(6), pp.911-936.

Pütün, E. 2010. Catalytic pyrolysis of biomass: Effects of pyrolysis temperature, sweeping gas flow rate and MgO catalyst. Energy. 35(7):2761–2766. DOI: 10.1016/j.energy.2010.02.024.

Qian, M., Lei, H., Villota, E., Zhao, Y., Huo, E., Wang, C., Mateo, W. and Zou, R. 2021. Enhanced production of renewable aromatic hydrocarbons for jet-fuel from softwood biomass and plastic waste using hierarchical ZSM-5 modified with lignin-assisted re-assembly. Energy Conversion and Management. 236:114020. DOI: 10.1016/j.enconman.2021.114020.

Rajendran, K. M., Chintala, V., Sharma, A., Pal, S., Pandey, J. K., Ghodke, P., 2020 Review of catalyst materials in achieving the liquid hydrocarbon fuels from municipal mixed plastic waste (MMPW). Material Today Communication., 24, 100982.

Rajmohan, K.V.S., Ramya, C., Viswanathan, M.R. and Varjani, S., 2019. Plastic pollutants: effective waste management for pollution control and abatement. Current Opinion in Environmental Science & Health, 12, pp.72-84.

Ratnasari, D.K., Nahil, M.A. and Williams, P.T. 2017. Catalytic pyrolysis of waste plastics using staged catalysis for production of gasoline range hydrocarbon oils. Journal of Analytical and Applied Pyrolysis. 124:631–637. DOI: 10.1016/j.jaap.2016.12.027.

Rehan, M., Miandad, R., Barakat, M.A., Ismail, I.M.I., Almeelbi, T., Gardy, J., Hassanpour, A., Khan, M.Z., Demirbas, A. and Nizami, A.S., 2017. Effect of zeolite catalysts on pyrolysis liquid oil. International Biodeterioration & Biodegradation, 119, pp.162-175.

Ruíz-Baltazar, A., Esparza, R., Gonzalez, M., Rosas, G. and Pérez, R., 2015. Preparation and characterization of natural zeolite modified with iron nanoparticles. Journal of Nanomaterials, 2015.

Sadeghpour, P. and Haghighi, M., 2022. Three-step short-time temperature-programmed hydrothermal synthesis of ZSM-5 with high durability for conversion of methanol to propylene. Korean Journal of Chemical Engineering, 39(5), pp.1194-1206.

Sakata, Y., Uddin, M.A. and Muto, A. 1999. Degradation of polyethylene and polypropylene into fuel oil by using solid acid and non-acid catalysts. Journal of Analytical and Applied Pyrolysis. 51(1):135–155. DOI: 10.1016/S0165-2370(99)00013-3.

Sarker, M., Liu, R., Rahman, M.M., Li, C., Chai, M., Nishu and He, Y. 2020. Impact of acid-modified ZSM-5 on hydrocarbon yield of catalytic co-pyrolysis of poplar wood sawdust and high-density polyethylene by Py-GC/MS analysis. Journal of the Energy Institute. 93(6):2435–2443. DOI: 10.1016/j.joei.2020.08.001.

Sebestyén, Z., Barta-Rajnai, E., Bozi, J., Blazsó, M., Jakab, E., Miskolczi, N., Sója, J. and Czégény, Z. 2017. Thermo-catalytic pyrolysis of biomass and plastic mixtures using HZSM-5. Applied Energy. 207:114–122. DOI: 10.1016/j.apenergy.2017.06.032.

Sekar, M., Ponnusamy, V.K., Pugazhendhi, A., Nižetić, S. and Praveenkumar, T.R. 2022. Production and utilization of pyrolysis oil from solidplastic wastes: A review on pyrolysis process and influence of reactors design. Journal of Environmental Management. 302:114046. DOI: 10.1016/j.jenvman.2021.114046.

Serrano, D.P., Aguado, J. and Escola, J.M. 2012. Developing advanced catalysts for the conversion of polyolefinic waste plastics into fuels and chemicals. ACS Catalysis. 2(9):1924–1941. DOI: 10.1021/cs3003403.

Serrano, D.P., Aguado, J., Escola, J.M., Rodríguez, J.M. and San Miguel, G., 2005. An investigation into the catalytic cracking of LDPE using Py–GC/MS. Journal of analytical and applied pyrolysis, 74(1-2), pp.370-378.

Shah, J. and Jan, M.R., 2014. Conversion of waste polystyrene through catalytic degradation into valuable products. Korean Journal of Chemical Engineering, 31(8), pp.1389-1398.

Sharuddin, S.A.D., Abnisa, F., Wan Daud, W.M.A. and Aroua, M.K. 2016. A review on pyrolysis of plastic wastes. Energy Conversion and Management. 115:308–326. DOI: 10.1016/j.enconman.2016.02.037.

Shen, W., Zhang, Y., Zhao, B., Chang, D., Lyu, J. and Zhang, H., 2019. Experimental and modelling studies on pyrolysis and its main light gas products for typical C8 hydrocarbons. Journal of Analytical and Applied Pyrolysis, 142, p.104622.

Shrivastava, A., 2018. Introduction to plastics engineering. William Andrew.

Siddiqui, M.N. and Redhwi, H.H. 2009. Pyrolysis of mixed plastics for the recovery of useful products. Fuel Processing Technology. 90(4):545–552. DOI: 10.1016/j.fuproc.2009.01.003.

Suresh, A., Alagusundaram, A., Kumar, P.S., Vo, D.V.N., Christopher, F.C., Balaji, B., Viswanathan, V. and Sankar, S., 2021. Microwave pyrolysis of coal, biomass and plastic waste: A review. Environmental Chemistry Letters, 19(5), pp.3609-3629.

Tejaswini, M.S.S.R., Pathak, P., Ramkrishna, S. and Ganesh, S.P., 2022. A comprehensive review on integrative approach for sustainable management of plastic waste and its associated externalities. Science of The Total Environment, pp.153-973.

Thahir, R., Irwan, M., Alwathan, A. and Ramli, R. 2021. Effect of temperature on the pyrolysis of plastic waste using zeolite ZSM-5 using a refinery distillation bubble cap plate column. Results in Engineering. 11:100231. DOI: 10.1016/j.rineng.2021.100231.

Toninelli, C., Gerhardt, I., Clark, A.S., Reserbat-Plantey, A., Götzinger, S., Ristanović, Z., Colautti, M., Lombardi, P., Major, K.D., Deperasińska, I. and Pernice, W.H., 2021. Single organic molecules for photonic quantum technologies. Nature Materials, 20(12), pp.1615-1628.

Ukei, H., Hirose, T., Horikawa, S., Takai, Y., Taka, M., Azuma, N. and Ueno, A., 2000. Catalytic degradation of polystyrene into styrene and a design of recyclable polystyrene with dispersed catalysts. Catalysis today, 62(1), pp.67-75.

Umarov, S.K., Gasanov, N.Z. and Khozhiev, T.S., 2021. Temperature dependence of the parameters of the crystalline lattice of a single crystal TlGaSe 2. Global Science and Innovations: Central Asia (см. в книгах), 7(1), pp.39-44.

Ünsal, M., Işık-Gülsaç, I., Üresin, E., Budak, M.S., Özgür-Büyüksakallı, K., Sayar, A., Aksoy, P., Ünlü, N., Okur, O., Şahin, H. and Karadaş, M., 2020. Optimisation of biomass catalytic depolymerisation conditions by using response surface methodology. Waste Management & Research, 38(3), pp.322-331.

Velvizhi. G., Shanthakumar. S., Das. B., Pugazhendhi. A., Priya. T.S., Ashok. B., Nanthagopal. K., Vignesh. R. and Karthick. C., 2020. Biodegradable and non-biodegradable fraction of municipal solid waste for multifaceted applications through a closed loop integrated refinery platform: Paving a path towards circular economy. *Science of the Total Environment*. *731*. p.138049.

Verdoliva, V., Saviano, M. and De Luca, S., 2019. Zeolites as acid/basic solid catalysts: recent synthetic developments. Catalysts, 9(3), p.248.

Wang, K., Zhang, J., Shanks, B.H. and Brown, R.C., 2015. Catalytic conversion of carbohydrate-derived oxygenates over HZSM-5 in a tandem micro-reactor system. Green Chemistry, 17(1), pp.557-564.

Wang, X., You, Y., Han, X. and Jiang, X., 2022. Product distribution and coke formation during catalytic pyrolysis of oil shale with zeolites. Journal of Thermal Analysis and Calorimetry, 147(15), pp.8535-8549.

Wojnowska-Baryła, I., Kulikowska, D. and Bernat, K., 2020. Effect of bio-based products on waste management. Sustainability, 12(5), p.2088.

World Economic Forum The New Plastics Economy - Rethinking the Future of Plastics; Ellen MacArthur Foundation and McKinsey & Company, 2016.

Wu, Y., Wang, H., Li, H., Han, X., Zhang, M., Sun, Y., Fan, X., Tu, R., Zeng, Y., Xu, C.C. and Xu, X., 2022. Applications of catalysts in thermochemical conversion of biomass (pyrolysis, hydrothermal liquefaction and gasification): A critical review. Renewable Energy.

Xiang, Z., Liang, J., Morgan, H.M., Liu, Y., Mao, H. and Bu, Q. 2018. Thermal behavior and kinetic study for co-pyrolysis of lignocellulosic biomass with polyethylene over Cobalt modified ZSM-5 catalyst by thermogravimetric analysis. Bioresource Technology. 247:804–811. DOI: 10.1016/j.biortech.2017.09.178.

Yan, G., Jing, X., Wen, H. and Xiang, S., 2015. Thermal cracking of virgin and waste plastics of PP and LDPE in a semibatch reactor under atmospheric pressure. Energy & Fuels, 29(4), pp.2289-2298.

Yang, H., Coolman, R., Karanjkar, P., Wang, H., Dornath, P., Chen, H., Fan, W., Conner, W.C., et al. 2017. The effects of contact time and coking on the catalytic fast pyrolysis of cellulose. Green Chemistry. 19(1):286–297. DOI: 10.1039/c6gc02239a.

Yaya, A., Tiburu, E.K., Vickers, M.E., Efavi, J.K., Onwona-Agyeman, B. and Knowles, K.M., 2017. Characterisation and identification of local kaolin clay from Ghana: A potential material for electroporcelain insulator fabrication. Applied Clay Science, 150, pp.125-130.

Youssef, H., Ibrahim, D., and Komarneni, S. 2018. Microwave-assisted versus conventional synthesis of zeolite A from metakaolinite. Microporous Mesoporous Material, 115: 527-534.

Zannikos, F., Kalligeros, S., Anastopoulos, G. and Lois, E. 2013. Converting Biomass and Waste Plastic to Solid Fuel Briquettes. Journal of Renewable Energy. 2013:1–9. DOI: 10.1155/2013/360368.

Zeng, Y., Wang, Y., Liu, Y., Dai, L., Wu, Q., Xia, M., Zhang, S., Ke, L., Zou, R. and Ruan, R., 2022. Microwave catalytic co-pyrolysis of waste cooking oil and low-density polyethylene to produce monocyclic aromatic hydrocarbons: Effect of different catalysts and pyrolysis parameters. Science of The Total Environment, 809, p.152182.

Zhang, X., Lei, H., Yadavalli, G., Zhu, L., Wei, Y. and Liu, Y. 2015. Gasoline-range hydrocarbons produced from microwave-induced pyrolysis of low-density polyethylene over ZSM-5. Fuel. 144:33–42. DOI: 10.1016/j.fuel.2014.12.013.

Zhao, L., Wang, Z.H., Chen, D.Z., Ma, X.B. and Luan, J., 2012. Influence of impurities on waste plastics pyrolysis: products and emissions. Huan Jing ke Xue= Huanjing Kexue, 33(1), pp.329-336.

Zhou, J., Zhao, J., Zhang, J., Zhang, T., Ye, M. and Liu, Z., 2020. Regeneration of catalysts deactivated by coke deposition: A review. Chinese Journal of Catalysis, 41(7), pp.1048-1061.

Zhou, N., Dai, L., Lyu, Y., Wang, Y., Li, H., Cobb, K., Chen, P., Lei, H., 2022. A structured catalyst of ZSM-5/SiC foam for chemical recycling of waste plastics via catalytic pyrolysis. Chemical Engineering Journal. 440:135836. DOI: 10.1016/j.cej.2022.135836.

Zhou. N., Dai. L., Lv. Y., Li. H., Deng. W., Guo. F., Chen. P., Lei. H. and Ruan. R., 2021. Catalytic pyrolysis of plastic wastes in a continuous microwave assisted pyrolysis system for fuel production. *Chemical Engineering Journal*. *418*. p.129412.

Zhu, X., Gao, Y., Wang, X., Haribal, V., Liu, J., Neal, L.M., Bao, Z., Wu, Z., Wang, H. and Li, F., 2021. A tailored multi-functional catalyst for ultra-efficient styrene production under a cyclic redox scheme. Nature communications, 12(1), pp.1-11.

Zhu. S., Chen. H., Wang. M., Guo. X., Lei. Y. and Jin. G., 2019. Plastic solid waste identification system based on near infrared spectroscopy in combination with support vector machine. *Advanced Industrial and Engineering Polymer Research*. *2*(2). pp.77-81.